The Synthesis and use of Cobalt Complexes in Catalytic Chain Transfer Polymerisation

Jennifer Louise Waterson

A Thesis Submitted for the Degree of Doctor of Philosophy

Department of Chemistry,
University of Warwick,
Coventry, CV4 7AL.

April 2000

A. ***Contents.*** ***Page***

B. Table of Tables

Chapter 2

Chapter 3

Chapter 4

Chapter 5

Chapter 6

C. *Table of Figures*

Chapter 1

Chapter 2

Chapter 3

Chapter 4

D. Acknowledgements

Firstly I would like to thank my supervisors Prof. D. M. Haddleton and Dr S. N. Richards for all their guidance and support over the three years. Secondly I would like to thank members of the chemistry department who have helped with the analysis of compounds: Dr. A.P. Jarvis, Dr. D. J. Duncalf and Dr. A Clarke. I would also like to take this opportunity to thank Dr R Harrison and Dr ir S.A.F. Bon for all their help. Thanks must also go to past and present members of the polymer group who have helped and supported me during my three years.

I would also like to take this opportunity to thank my parents for all their love, support and encouragement throughout my life, I am eternally grateful to them.

Finally I would like to thank and dedicate this thesis to my husband Carl for all his love encouragement and support over the last seven years.

E. Declaration

All experimental work contained in this thesis is original research that was carried out by the author in the Department of Chemistry, University of Warwick, between October 1996 and October 1999. No material contained herein has been submitted for any other degree to this, or any other, institution. Results from other authors are referenced in the usual manner throughout the text.

Signed Date

F. Summary

Work in this thesis examines the structural properties of various catalytic chain transfer agents (CCTA's) and their effect and implications on catalytic chain transfer polymerisation (CCTP). CCTP is an effective polymerisation technique for producing low molecular weight methacrylate and styrene polymers that contain terminal vinyl functionalities. CCTP has also been shown to be effective in both emulsion and bulk polymerisation techniques using catalytic quantities of the CCTA. The products of CCTP (macromonomers) can also be used to produce copolymers.

The work contained here has examined the effect of increasing equatorial carbons in low spin cobalt (II) complexes, whilst both the effects of equatorial and axial ligands has been examined for cobalt (III) analogues in both MMA and Styrene bulk polymerisations. Results have shown that the activity (C_s values) for cobalt (II) complexes is affected by varying the equatorial carbons, increasing the number of carbons leads to a decrease in C_s. Cobalt (III) complexes have shown that a strong axial base ligand (pyridine) combined with increased equatorial carbons leads to a further decrease in catalytic activity whilst the introduction of a weak base (water), combined with increased equatorial carbons increases activity when compared to the pyridine analogues. It has been shown that it is possible to control the partitioning properties of these complexes by varying the equatorial and/or axial ligands. Results indicate that the complexes would depending on their partitioning results be effective to a lesser or greater degree in emulsion polymerisation.

G. Abbreviations

MMA	*Methyl Methacrylate*
STY	*Styrene*
THF	*Tetrahydrofuran*
GPC	*Gel Permeation Chromatography*
MS	*Mass Spectrometry*
M_w	*Weight Average Molecular Weight*
M_n	*Number Average Molecular Weight*
mL	*Milliliters*
FTIR	*Fourier Transform Infrared Spectroscopy*
NMR	*Nuclear Magnetic Resonance*
UV	*Ultraviolet*
Bpt.	*Boiling Point*
ppm	*parts per million*
PDi	*Polydispersity*
CCTP	*Catalytic Chain Transfer Polymerisation*
CCTA	*Catalytic Chain Transfer Agent*
Cs	*Chain Transfer Coefficient*
CLD	*Chain Length Distribution*
$E_{transfer}$	*Activation Energy of Transfer*
E_{prop}	*Activation Energy of Propagation*

Chapter 1

Introduction

1.0. Introduction

1.1. Addition Polymerisation [1,2,3,4,5]

Two general types of chemical processes are responsible for the incorporation of monomers into a polymeric chain, referred to as *step growth* and *addition* mechanisms. In free radical addition or chain growth polymerisation each polymer molecule is formed in a short period of time and then is usually excluded from further participation in the reaction.

The most often applied addition polymerisations are those of vinyl monomers, see fig 1.1.

Figure 1.1 Polymerisation of vinyl monomers.

Important polymers from this class of monomers are poly(ethylene) (X=H), poly(propylene) (X=CH_3), poly(styrene) (X=phenyl) and poly(vinylchloride) (X=Cl). In addition, some vinyl monomers are polymerised on a large scale; an example of this is methyl methacrylate 1, see figure 1.2.

Figure 1.2. Structure of Methyl Methacrylate (MMA)

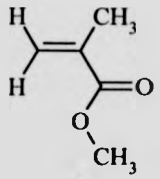

1

Depending on the nature of the substituent X, the addition polymerisation can be carried out by different techniques and mechanisms, one of these being radical polymerisation.

1.2. Free radical polymerisation.

This can be described by a sequence of three steps:

1. Initiation
2. Propagation
3. Termination

1.2.1 Initiation.

The initiation step consists of two separate reactions. The first is the production of free radicals by any one of a number of reactions. The usual case is the homolytic dissociation of an initiator (I) to yield a pair of radicals R ·.

$$I \xrightarrow{k_d} 2\,R\cdot \qquad (1.1)$$

Where k_i is the rate constant for the initiator dissociation.

$$R\cdot + M \xrightarrow{k_i} M_1\cdot \qquad (1.2)$$

Where k_i is the rate constant for the initiation.

The second part of the initiation involves the addition of this radical to the first monomer molecule to produce the chain initiating species M_1 ·. Where M represents a monomer molecule and k_i is the rate constant for the initiation step.

1.2.1.1 Modes of generating primary radicals.

There are several ways of generating radicals from the dissociation of initiator these include *thermal decomposition*, *photo-dissociation* and *redox* reactions, the former method will be discussed.

1.2.1.1.1 Thermal decomposition.

The most common initiators in this class usually contain weak bonds, which decompose at significant rates at moderate temperatures to yield free radicals. The usual kinetic requirement of such a thermal initiator is that it should decompose with a first-order rate constant. The thermally unstable bonds concerned are peroxide (-O-O-) or azo (-N=N-).

α.α'-Azobisisobutyronitrile (AIBN) is often used as a thermal initiator in radical addition polymerisation systems. Its effective decomposition process is shown below, see fig 1.3.

Figure 1.3. Decomposition of AIBN.

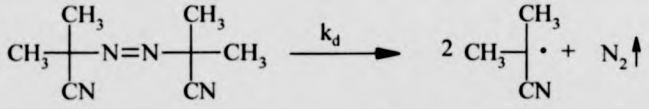

(1.3)

During the decomposition nitrogen gas is evolved and cyanopropyl radicals are generated, which subsequently add onto a monomer molecule to commence the growth of the chain, i.e. propagation.

AIBN is usually employed as a thermal initiator at temperatures in the range of 315-335 K. Not every act of decomposition of an AIBN molecule leads to a pair of free radicals, which are able to react with the monomer concerned. Some of the radicals fail to escape from the surrounding solvent cage before they undergo other deactivating processes, thus an efficiency factor (f) is defined. This is a measure of the fraction of initiator fragments, which actually initiate chain growth. The actual initiation rate (R_i) of polymerisation can be expressed by the rate of decomposition of the initiator molecules modified by f and the number of radicals generated per molecule decomposed.

The rate of initiation R_i will be given by

$$R_i = 2f\, k_d[I] \qquad (1.4)$$

Where [I] = concentration of initiator.

Figure 1.4. Initiation of methylmethacrylate.

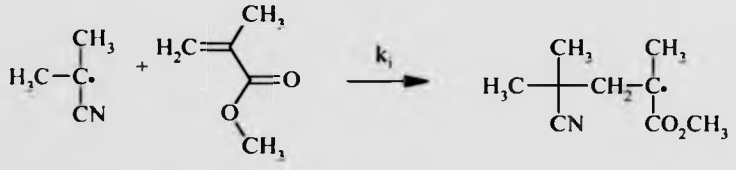

AIBN MMA

1.2.2 Propagation

Propagation consists of the growth of M_1 • by successive additions of monomer molecules. Each addition creates a new radical, which has a similar identity to the one previously, except that it is larger by one monomer unit. The successive additions may be presented in general terms by:

$$Mn^{\bullet} + M \xrightarrow{k_p} Mn+1^{\bullet}$$

(1.5)

Where k_p is the rate constant for propagation. Propagation with growth of the chain to high polymer proportions takes place very rapidly.

Figure 1.5. Propagation of MMA.

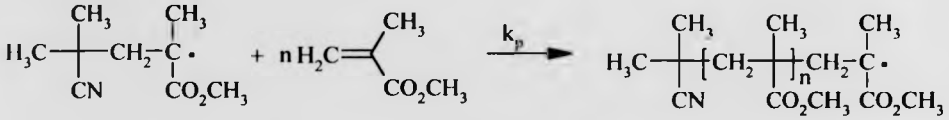

Growing Polymer Chain

1.2.3 Termination

At some point in the reaction the propagating polymer chain stops propagating and terminates. Termination with the annihilation of the radical center occurs by bimolecular reaction between two radicals. This occurs by one of two competing ways, *combination* and *disproportionation*.

1.2.3.1. Combination

Two radicals react with each other by combination (coupling) to form 'head to head' linkage within the polymer chain, simplified as:

$$Mn^{\bullet} + Mm^{\bullet} \xrightarrow{k_{tc}} Mn + m$$

(1.6)

Figure 1.6. Combination of PMMA.

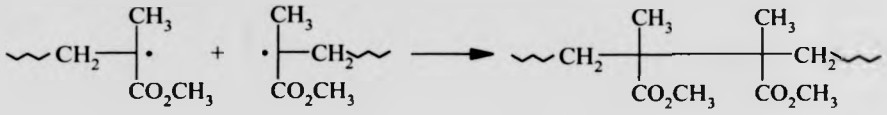

Where k_{tc} is the rate constant for termination by combination. The formation of a head to head linkage will cause an irregularity or 'weak link' in the polymer chain. This in turn will lead to a reduction in the thermal stability of the corresponding polymer product, especially in the case of PMMA [6].

1.2.3.2 Disproportionation.

This is where a hydrogen radical that is β to one radical center is transferred to a second radical center. This results in the formation of two polymer molecules, one saturated and one unsaturated, simplified as:

$$Mn\cdot + Mm\cdot \xrightarrow{k_{td}} Mn + Mm \qquad (1.7)$$

Where k_{td} is the rate constant for termination via disproportionation.

Figure 1.7. Termination of PMMA by disproportionation.

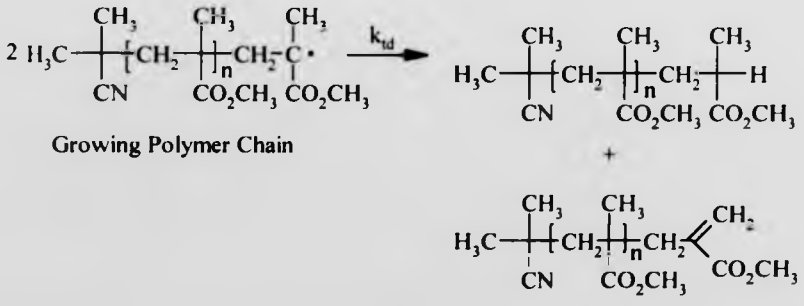

Growing Polymer Chain

It has previously been shown [5] that for oligomeric alkyl methacrylate radicals, disproportionation will favour the abstraction of a hydrogen atom from the α-methyl group to give terminal unsaturation rather than from a methylene unit which would form an internal double bond. It is easier to abstract the hydrogen at the α-methyl group. Both combination and disproportionation can, and do occur simultaneously for a given polymer system. The relative proportion of each will depend on the reactants used and the polymerisation conditions being employed. The ratio of disproportionation to combination for MMA (the ratio of k_{td}/k_{tc}) varies widely from 0.6 to greater than 1.8 [5]. Styrene and acrylates terminate predominantly via combination with less than 10% of termination arising from disproportionation [1].

1.2.3.3 Chain transfer

The overall process involves a propagating chain Mn reacting with a transfer agent (T) to terminate one polymer chain and produce a radical (T·), which initiates a new chain (M). The transfer agent may be a deliberate additive or it may be the initiator, monomer, polymer, solvent or any other species present in the reaction medium.

Chain transfer:

$$Mn\cdot + T \xrightarrow{k_{tr}} Mn + T\cdot \qquad (1.8)$$

Where k_{tr} is the rate constant for transfer

Reinitiation:

$$T\cdot + M \xrightarrow{k_s} Mn\cdot \qquad (1.9)$$

Where k_s is the rate constant for reinitiation.

In kinetic analysis an assumption is made which postulates that the total concentration of radicals in the system will reach a constant (steady state) value. At this 'steady state' it follows that the rate of termination will be equal to the rate of initiation, this is not always a valid assumption. In free radical polymerisations such as bulk systems it is sometimes found that as higher conversions are reached there is a sudden increase in the overall rate of polymerisation. This arises since the increased viscosity of the system at higher polymer concentration will lead to a decrease in the rate of termination compared to the rate of propagation. This is known as the *Gel* or *Trommsdorff effect*.[7]

The kinetic chain length ν of a radical polymerisation is defined as the average number of monomer molecules consumed per radical.[1] This is given by the ratio of the overall rate of polymerisation, R_p, to the rate of initiation, R_i or to the rate of termination, R_t, i.e.

$$\nu = \frac{R_p}{R_i} = \frac{R_p}{R_t} \qquad (1.10)$$

Substitution of individual rates into the above expression leads to the kinetic chain length being inversely proportional to the square root of the initiator concentration. This means that any increase in the initiator concentration in an attempt to increase the polymerisation rate will lead to shorter polymer molecules being formed.

1.3.Methods of controlling molecular weight in free radical polymerisations system.[1,8]

Usually, in most free radical systems, the molecular weight of the polymer produced is very high and can often be too high for some practical purposes, indeed in certain

instances very low molecular weight polymers (oligomers) are required which thus necessitates the need for molecular weight control to be employed. In the past, one, or both, of the following methods have achieved this control:

1.3.1. Use of high initiator concentrations.

By altering the ratio of initiator to monomer in the polymerisation system some control over the molecular weight of the polymer can be achieved. With more initiator being present there will be a higher radical concentration for a given amount of monomer, thus producing lower molecular weight polymer.

1.3.2. Addition of chain transfer agents.

Chain transfer agents are added to the polymerisation system where a reduction in molecular weight is required. The transfer reaction competes with the propagation step: the radical formed by the transfer agent can then go on to reinitiate monomer, which may then proceed to propagate. Common chain transfer agents used are alkyl mercaptans, carbon tetrahalides and tertiary amines, all of which provide a decrease in the molecular weight of selected polymers without significantly altering the rate of polymerisation.

1.4. Polymerisation systems.[4,9,10]

When starting the production of a polymer, one has to consider which polymerisation system and which polymerisation reactor is most appropriate. This choice is determined by a number of factors, which are specific for polymer systems:

- The chemical composition of all chains should be the same.
- Successive product charges should possess the same desired molar mass distribution.
- The viscosity of the reaction medium may increase enormously during polymerisation.
- Purification of the polymer after its production is unattractive.

1.4.1. Bulk polymerisation.

This system is essentially composed of only monomer/polymer. This technique is most commonly used for polymerisations which proceed through functional groups in a stepwise manner and then the method merely involves heating the straight monomer or monomer mixture (sometimes with addition of a small amount of a catalyst to increase the reaction rate). The system is maintained in a fluid state by keeping the temperature sufficiently high. In this type of reaction there is a progressive increase in molecular weight and the high viscosity of the resultant polymer melt can lead to handling difficulties. When the technique of bulk polymerisation is applied to polymerisations, which involve chain reactions, the monomer is heated with a small amount of appropriate initiator. Again there is a substantial rise in viscosity as the concentration of polymer (which is soluble in the monomer) increases and this can lead to difficulty in dissipating the high exothermic heat of reaction which is usually a feature of such polymerisations. As there is a possibility of localised overheating leading to degradation and discoloration of the polymer, bulk polymerisation is seldom practiced with large batches. Bulk polymerisation results in a relatively pure polymer.

1.4.2 Solution polymerisation

Here the monomer is dissolved in a solvent prior to polymerisation. This technique is commonly employed for the ionic polymerisation of gaseous vinyl monomers. The solvent facilitates contact of monomer and initiator (which may or may not be soluble in the solvent) and assists dissipation of exothermic heat of reaction. A limitation of this technique is the possibility of chain transfer to the solvent with consequent formation of low molecular weight polymer. An added disadvantage is the need to remove the solvent in order to isolate the solid polymer. In this respect it is common practice to use a solvent in which the monomer the resulting polymer are soluble.

1.4.3 Suspension polymerisation

The monomer is dispersed in water in small droplets maintained by vigorous stirring. This technique is extensively used for free radical polymerisation of vinyl monomers. An initiator soluble in monomer is added and polymerisation occurs within each droplet. Besides facilitating the removal of exothermic heat of reaction, suspension polymerisation has the advantage that the polymer is obtained in the form of small beads, which are easily collected and dried. The polymer is relatively free from contaminants and there are no solvent recovery considerations.

1.4.4 Emulsion polymerisation.

Here the monomer is dispersed in water containing a soap to form an emulsion, such dispersion is stable and its existence is not dependant on continued agitation. This technique is extensively used for the free radical polymerisation of diene monomers in the preparation of synthetic rubbers. In this case a water-soluble initiator is used and the

course of the polymerisation is considerably different from that followed in the systems described previously. At the start of an emulsion polymerisation three components are present:

1. Relatively large droplets of monomer, stabilised by soap molecules around the periphery.
2. Aggregates (micelles) of 50-100 soap molecules swollen with monomer.
3. The aqueous phase containing a few monomer molecules and the initiator which gives rise to free radicals.

The monomer droplets and the micelles swollen with monomer compete for the free radicals generated in the aqueous phase, but since there are many more micelles than droplets in the system most of the free radicals enter micelles resulting in polymerisation within individual micelles. The monomer consumed during the resulting polymerisation is replenished by diffusion of new monomer molecules from the aqueous phase, which in turn, is kept saturated with monomer from the droplets of monomer. Polymerisation continues within a given micelle until a second free radical enters the micelle in which case termination quickly occurs because of the small volume of the reaction locus. The particle then remains inactive until a subsequent free radical enters the particle resulting in larger particles of polymer swollen with monomer which are stabilised by soap molecules around the periphery. Monomer continues to diffuse into these particles and polymerisation is maintained therein until the monomer supply is exhausted.

The final product is a stable dispersion (latex) of polymer particles. The polymer is isolated by 'breaking' the latex, usually by the addition of acid which converts the soap to fatty acid. In some instances, the latex is used directly without coagulation, such is the

case in, for example, the preparation of poly(vinylacetate) latex paints. An attractive feature of emulsion polymerisation is that it is possible to prepare very high molecular weight material at high rates of conversion.

1.5. Polymer molecular weight averages.

Polymers are generally polydisperse, meaning that in a sample the individual molecules are not all the same size and there is a range of molecular masses accordingly. Thus only average values of relative molecular masses can be specified usually for a bulk polymer. Immediately there is complexity because there are several types of average which of these averages is measured depends on which method is used to determine it.

1.5.1 Number average molecular weight ($\overline{M_n}$).

This is the simplest average and is denoted as $\overline{M_n}$. It is defined by the following expression :

$$\overline{M_n} = \frac{\sum N_i M_i}{\sum N_i} \qquad (1.11)$$

Where N_i is the number of molecules in each separate fraction, M_i number of molecules of just one relative molecular mass within the fraction, ΣN_i, the total number of molecules in the original sample. The relative mass of N_i molecules of relative molecular mass M_i is the product N_iM_i, so that ΣN_iM_i is the mass of the original sample. $\overline{M_n}$ is the total mass divided by the toal number of molecules. $\overline{M_n}$ is given by molecular weight

methods that depend upon end-group analysis or colligative properties (e.g. by osmotic pressure etc.) i.e. where the number of molecules are analysed.

1.5.2 Weight average molecular weight.

The weight average molecular weight ($\overline{M_w}$) of a polymer arises from analysis of the weight fraction of each species present (as opposed to number fraction for $\overline{M_n}$). The weight average molecular weight is calculated as follows:

$$\overline{M_w} = \frac{\sum W_i M_i}{\sum W_i} = \frac{\sum N_i M_i^2}{\sum N_i M_i} \qquad (1.12)$$

Methods of measurement include light scattering and ultracentrifugation methods that depend on the mass of the species present.

1.5.3 Polydispersity Index.

The value of $\overline{M_w}$ of any polymer is always greater than that of $\overline{M_n}$ since a distribution of molecular weight is invariably observed. The width of this distribution is quantified in terms of the polydispersity index (PDi) where:

$$PDi = \frac{\overline{M_w}}{\overline{M_n}} \qquad (1.13)$$

1.6. GPC analysis.

GPC analysis has been utilised throughout this work for the characterisation of products. Gel permeation chromatography, more correctly termed size exclusion chromatography, is a separation method for polymers, similar to but advanced in practice over gel filtration. The separation takes place in a chromatographic column filled with beads of a rigid porous gel, highly crosslinked porous polystyrene and porous glass are preferred column packing materials. The pores in these gels are of the same size as the dimensions of polymer molecules. A sample of a dilute polymer solution is introduced into a solvent stream flowing through the column. As the dissolved polymer molecules flow past the porous beads they can diffuse into the thermal pore structure of the gel to an extent depending on their size and the pore size distribution of the gel. Larger molecules can enter only a small fraction of the internal portion of the gel, or are completely excluded, smaller polymer molecules penetrate a larger fraction of the interior of the gel. The larger the molecule, therefore, the less time it spends inside the gel, and the sooner it flows through the column. The different molecular species are eluted from the column in order of their molecular size as distinguished from the molecular weight, the largest emerging first. Subsequent to elution the polymer solution passes through a detector. There are various types of detectors, the one utilised in this work is the refractive index detector (DRI).

1.7. Catalytic chain transfer polymerisation (CCTP).

1.7.1 Introduction

In 1975 the phenomenon known as 'catalytic chain transfer' emerged [11]. Catalytic chain transfer differs from conventional chain transfer as the catalyst is regenerated and as such small quantities of the transfer agent are required to effectively reduce molecular weight. A combination of both points leads to the advantage that little colour, toxicity or odour properties are incorporated in the product. In comparison, conventional chain transfer where for example, when thiol containing agents were used then odour is a problem. CCTP also offers a further advantage in that it introduces an end functionality in the form of a double bond which can subsequently be modified [12].

CCTP utilises cobalt containing complexes as chain transfer agents. Initial CCT research/polymerisations were carried out in bulk.[11,13-16] However, the development of the process in emulsion polymerisation has allowed its use and applications to be extended to the paints, adhesives and coatings industries. This has enabled the industries to become more environmentally friendly, which today is a much sought after commodity with respect to the environment legislation requiring the use of low levels of organic solvents.

Free radical polymerisation has been widely adopted in the synthesis of plastics and coatings for over fifty years owing to its versatility of the reaction with high tolerance to impurities, water, functional groups and additives. However, a disadvantage with this method of polymerisation is that free radicals tend to be highly reactive non-selective intermediates and it is difficult to isolate 'clean' products. This leads to broad

molecular weight distributions and random stereochemical configuration of units along the macromolecular chain.

Conversely CCTP on the other hand produces low molecular weight polymers/oligomers, which would otherwise require the use of high concentrations of initiator and/or mercaptan chain transfer agents. In addition cobalt complexes have been utilsed to produce narrow polydispersity polymers via the pseudo-living free radical polymerisations of acrylates [17-20].

1.7.2 Mechanism of CCTP.

CCTP has its origins in biochemistry where coenzyme B_{12} is utilised in many 'free radical' reactions. Coenzyme B_{12} catalyses three different reactions in biochemistry- i). intramolecular rearrangements, ii). methylations, iii). reduction of ribonucleotides to deoxyribonucleotides. Intramolecular rearrangements are exchanges of two groups on adjacent carbon atoms. The first step involves cleavage of the cobalt carbon bond to form cobalt (II) d^7 with an unpaired electron and a homolytic cleavage reaction. The key to the effectiveness of coenzyme B_{12} is the facile nature of the homolytic bond cleavage.

The first work on polymerisations utilizing analogues of B_{12} was carried out by Smirnov and coworkers [11,15,16], they discovered that it was possible to catalytically regulate the molecular weight of a polymer. Catalytic restriction of the molecular weight was discovered in the case of the polymerisation of methylmethacrylate initiated by AIBN in the presence of the cobalt complex of tetramethylester of hematoporphyrin. Results showed that less than ten percent of the catalyst was consumed, therefore the potential number of times each catalyst molecule could be used reached a value in the

order of 10^{6}. It was also assumed on the basis of spectrophotometric data that during the polymerisation the bulk of the catalyst existed in the reaction medium in the form of the original porphyrin. The catalytic nature of the reaction derived from the regeneration of the cobalt porphyrin complex was proved by isolation at the end of the polymerisation [11]. This paper also reported that the kinetic laws observed for methacrylic monomers were similar to those for methylmethacrylate but that a more complicated law was observed for the polymerisation of styrene and acrylic monomers [11].

In a proceeding paper the authors [16] discussed the possibility that chain transfer catalysts affected the transport of a hydrogen atom by some route or other as it was concluded that although the catalyst reduced the molecular weight of the polymer it had no influence on the rates of other elementary stages, it was not consumed during the process and did not appear in the composition of the product. The catalytic nature of CCT is shown in the following reaction sequences [13]:

$$MMA + Co - Por \Leftrightarrow [MMACo - Por]$$

$$[MMACo - Por] + R_n\cdot \rightarrow P_n\cdot + HCo - Por + R_1\cdot \qquad (1)$$

$$R_n\cdot + Co - Por \rightarrow P_n + HCo - Por$$

$$HCo - Por + MMA \rightarrow R_1\cdot + Co - Por \qquad (2)$$

The first sequence suggests the activation of monomer by Michaelis-Menton catalyst with subsequent chain transfer to the activated monomer. Whilst in the second sequence the growing radical disproportionates the catalyst with formation of cobalt hydride which then reinitiates a new chain. The second sequence was also suggested by O'Driscoll [21].

Chain transfer constants given for the porphyrin complexes are three to four orders of magnitude above those quoted for mercaptan derivatives. The importance of the cobalt (III) hydride as an intermediate has been verified by the trapping and synthesis of the unstable compounds which have been shown to act as initiators [19,22]. O'Driscoll found that temperature and chain length affected CCTP and that some retardation on the rate of polymerisation was seen when a CCT agent was added [21,23]. The author stated that this retardation was not associated with chemical control but was solely determined by the chain length of the growing macroradicals. Smirnov [23] used a variety of cobalt based CCT agents and argued that if the explanation given by O'Driscoll was correct then the retardation should be independent of catalyst and solely determined by chain length. Their results appeared to show that there was both a catalyst effect and a chain length effect. A point of interest with CCTP is whether the polymerisation progresses entirely via a free radical route or whether the cobalt complex coordinates to the chain end and is thus central to the propagation itself. Davis et al after studying the results from other workers suggested that experimental evidence pointed to the involvement of monomer in the catalytic transfer process [24]. They believe that the straightforward mechanism of hydrogen abstraction and initiation of a new monomer with a hydrogen atom could be discounted. In support of their claim they suggested that the addition of a hydrogen atom to monomer is not likely to be 100% regiospecific and some measurable amount of head

to head addition would occur. They claim that the regiospecific addition of the hydrogen is unlikely in a free transfer event and therefore coordination of the monomer with the cobalt complex allowing insertion of hydrogen to start a new growing chain is more likely. They proposed an alternative mechanism for the production of oligomers by cobalt coordination compounds, a catalytic cycle, Figure 1.8. The cycle conforms to the generated reaction model presented by Scheffold for cobalt carbon bond formation and cleavage [25]. Davis et al [26] then attempted to build a mechanism for CCTP using a simulation based on the Daikh + Finke model as a starting point [27]. Daikh and Finke modeled a rearrangement of a cobalt complex via free radical intermediates and showed that in certain cases the radical reaction can be controlled very specifically. The aim behind the work of Davis was to show that significant changes in the mechanistic route can occur through very subtle variations in the processes. Most of the cobalt species exists in complexed forms, less as free radicals and even less as caged radicals. Radical termination is suppressed although not entirely stopped by a build up of the cobalt (II) free radical species relative to alkyl radical. For the propagation step when monomer is included there are two possible sites where propagation can occur: (i) The alkyl free radical can act as an initiator resulting in chain growth with time. This growing radical can also exist in equilibrium with the cobalt complex in the same way that the initial alkyl radical does.(ii) Insertion of monomer into the caged radical species - it is not known whether this can occur- if propagation occurred like this then the transition state for radical addition would be unchanged unless coordination occurred, there is no data to prove this. Davis [26] shows by a simulation that the majority of chain growth originates from the free radical species as opposed to the caged radical because the concentration of

free radicals are higher than the concentration of caged radicals. This also suggests that the drawing of the cobalt species as central to the propagating centre is misleading [28,29] suggesting a cobalt group transfer polymerisation mechanism. Also if coordination polymerisation was occurring simultaneously with the free radical process then its contribution is likely to be negligible. CCTP is a radical - radical process and is therefore very fast and diffusion controlled, therefore it is unlikely to be rate determining. The reinitiation of chains occurs via an insertion reaction, this step may be partially responsible for the retardation of the rate observed. As the transfer process is extremely efficient this reaction step will become important relative to the propagation event, i.e.: if $k_i<k_p$ a difference in overall rate of polymerisation will become observable. This would explain Smirnovs' observation that the nature of the cobalt complex determines to some extent the change in the rate of retardation [23]. The influence of an external source of radicals was also discussed. Davis refined Hawthornes'[30,31] observation that the rate of reaction in the absence of an external initiator is very slow. Hawthorne implied that an external source was required to replace radicals that were lost from the system. Although Davis stated that this is true, he further demonstrated that the loss of radicals with time was not substantial, and therefore the effect of increasing the concentration of radicals was to increase the rate simply because there are more growing chains hence increase the rate of termination. In the specific case where a cobalt (II) compound was used in conjunction with a free radical initiator (as described by O'Driscoll et al [21]) then the initiator fragment can either initiate polymerisation directly or it can react with cobalt (II) to form a cobalt (III) complex which in turn will initiate the polymerisation. The relative importance of these initiation routes will depend on the specific ratios of the rate

constants and the concentrations of the components in the system. Haddleton et al have shown that the majority of the oligomers formed by CCT do not have initiator ends [32,33].

1.7.3 Proposed catalytic cycle for CCTP.

In catalytic chain transfer polymerisation, initiation, propagation, and termination are thought to occur by a free-radical process. The chain transfer reaction is thought to involve a growing polymer chain, encountering a cobalt (II) complex, resulting in hydrogen abstraction, producing a dead polymer chain, with an unsaturated end group and a cobalt (III) hydride species. Monomer can then react with Co(III) hydride to produce a monomeric radical – reinitiation, (which then propagates to form another chain) and the original cobalt(II) catalyst. A mechanism is illustrated in figure 1.8.

Figure 1.8. Proposed catalytic cycle for CCTP by Davis and co-workers.

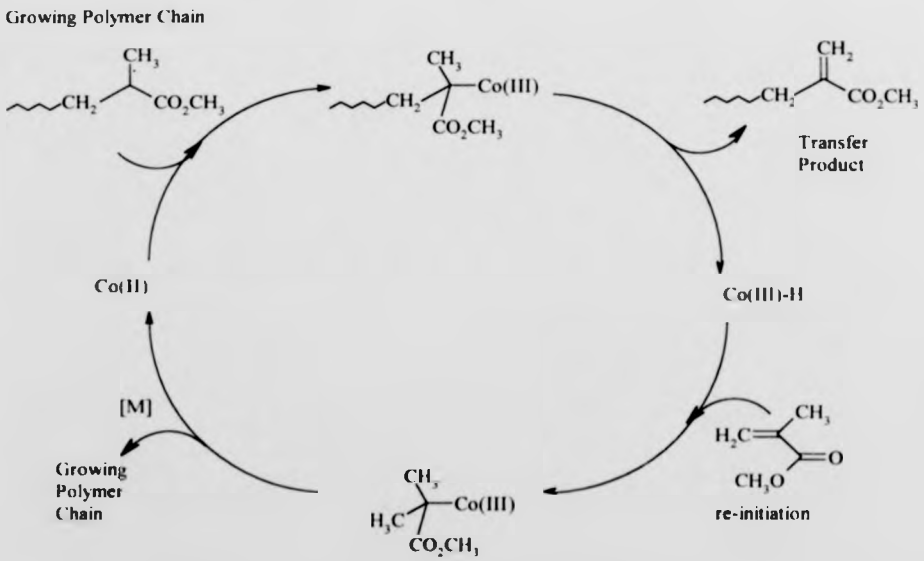

The aim of the following sections is to discuss some of the points and products in the cycle.

1.7.3.1 The use of cobalt (II) and cobalt (III) complexes in CCTP.

As stated previously CCTP has its origins in biochemistry where coenzyme B_{12} is used. Coenzyme B_{12} consists of a corrin ring (not completely delocalised) with a central cobalt atom that can have a +1, +2 or +3 oxidation state. The development of chain transfer agents over the years has led to the use of certain low spin cobalt (II) and cobalt (III) complexes which are today regarded as highly efficient chain transfer agents.

The application of cobalt mediated free radical reactions to polymerisations was first reported by Takahashi [34] who noted that vinyl monomers could be polymerised by a cobalt cyanide complex in the presence of hydrogen. Pentacyano cobalt (II) and (III) derivatives were later found to be active as free radical initiators [35].

This work was followed by Smirnov and Enikolopyan [11,13] who discovered that cobalt reagents catalysed chain transfer in free radical polymerisations. Cobalt porphyrins (Co-Por) of the type in Figure 1.9, (tetramethyl ether of cobalt hematoporphyrin) were found to induce catalytic chain transfer in methylmethacrylate polymerisations, they also noted that porphyrin complexes of other metals such as Rh, Pd, Fe, Cu and Zn and the unmetallated porphyrins were also catalytically inactive in addition to cobalt compounds such as the acetate, stearate, and acetylacetonate. A range of other cobalt porphyrin complexes have also been investigated with varying degrees of success [11,15,36,37].

Figure 1.9. Structure of the porphyrin complex first used in CCTP by Smirnov.

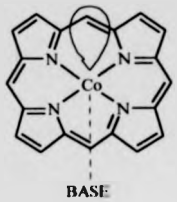

Gridnev et al [36] investigated the structural aspects necessary for a complex to be a good CCTA. The following general features were outlined:

(i) The complex should have cobalt in its low spin state,

(ii) There should be not less than three donor N-atoms

(iii) There should be a 'semi-ring' system of π - conjugation i.e. not fully conjugated

(iv) The ligand should carry one or two delocalised negative charges.

In 1984 O'Driscoll used cobaloximes for the first time [21,22]. This involved replacement of the porphyrin with a cobalt (II) dimethyl glyoxime (Co-DMG) , Figure 1.10. It was found that this complex was extremely oxygen sensitive and that in the presence of oxygen it underwent oxidative addition of O_2 to its metal center and formed a stable complex of cobalt (III) which was no longer active. In order to improve the oxygen stability of the cobaloxime O'Driscoll used triphenylphosphine as a base ligand which stablised the cobaloxime and enabled them to handle the complex.

Trans to the base ligand is the sixth coordination position in the cobaloxime, which can be considered as a phantom ligand. This lobe of electron density is the site of the cobalt (II) complexes catalytic activity.

Figure 1.10. Structure of cobaloxime first used by O'Driscoll.

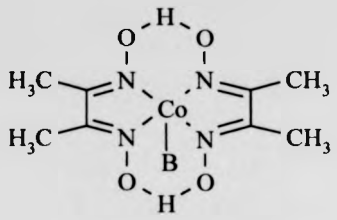

Where B = Base ligand

Two patents were filed utilising the cobaloxime [38,39]. Carlson patented the cobaloxime with pyridine and phosphines as base ligands. The claimed advantages were that the pyridine dioxime complex of cobalt (II) provided an excellent chain transfer mechanism for controlling molecular weight of the polymers. The polymers had improved colour over the porphyrin based complexes and were extremely easy to synthesise.

Sanayei et al [22,40] reported the use of BF_2 bridged derivative of cobaloxime (CoBF) as a CCTA whilst the Du Pont group patented its use [41], see Figure 1.11. It is reported to be more tolerant to oxidation and hydrolysis.

Figure 1.11. Structure of bis(dimethylglyoximate) Cobalt Boron Fluoride (CoBF).

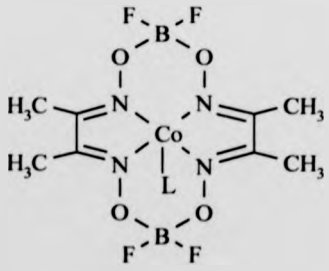

Several publications describe the use of CoBF [22,26,30,40,42-48] for emulsion and bulk polymerisations. The DuPont series of patents covers its use in solution terpolymerisation [49], suspension [50] and emulsion polymerisation [51]. The results demonstrate the versatility of the structure and its tolerance to solvents and reaction conditions. The synthesis of this compound has been described by Bakac and Espenson [52].

All of the original catalysts were based on cobalt (II). Hawthorne [30,31] has developed a series of cobalt (III) catalysts which are directly analogues to the cobalt (II) structures, see Figure 1.12, porphyrins, cobaloxime, pentacyano and CoBF except for the presence of an alkyl ligand. The cobalt (III) catalysts are reported to be superior to the cobalt (II) catalysts in emulsion polymerisation [53].

Figure 1.12. Structure of the cobalt (III) complex used by Hawthorne and Moad.

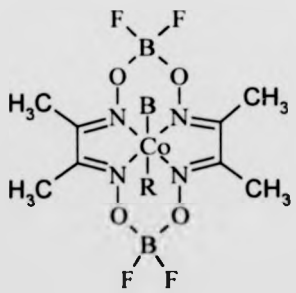

Where R = Alkyl, Halogen

B= Base ligand

1.7.3.1.1.The use of axial ligands in cobalt (II) and cobalt (III) complexes.

The nature of the axial ligands have been shown to be vital in controlling the efficiency of chain transfer.

1.7.3.1.1.1.The use of axial ligands in cobalt (II) complexes in CCTP.

Square planar cobalt (II) complexes feature ligands in the axial positions coordinated to the central metal. The nature of these ligands will depend on the synthetic route taken to the cobalt (II) complex. For example, if the product is obtained by recrystallisation from methanol then the axial ligands will be methanol. Similarly, if synthesis is carried out in the presence of coordination bases such as pyridine, then the axial positions will be occupied by the pyridine molecules.

1.7.3.1.1.2. The use of axial ligands in cobalt (III) complexes in CCTP:

These compounds are slightly more complex as it is normal to have one base ligand and one alkyl ligand as shown previously in Figure 1.12. For cobalt (III) complexes to become effective chain transfer agents they must be reduced to cobalt (II). The tendency towards reduction depends on the nature of the ligands which determines the degree of oxidation of the cobalt atom. Clearly the nature of the axial ligands has an effect on the bond dissociation energy. Several workers have observed that the chain transfer coefficient (C_s) and rate of polymerisation can be affected by using different ligands. Gridnev et al investigated this effect on cobaloximes [54] stating that if the ligand R is NO_2 ,CN , or a primary alkyl then the reduction of Co(III) to Co(II) is blocked. If however R is an acid group such as a halogen or CNS group then the reduction proceeds. Gridnev

termed ligands of type R as unique switches for catalysis of chain transfer. It is reported that the effect of ligands B of the Lewis base type increase the catalytic activity of the cobaloxime in proportion to an increase in their own trans effect.

Halpern postulated that the dissociation of the cobalt carbon bond involves reduction of the cobalt, i.e., a decrease in the formal oxidation state of cobalt. Thus more basic ligands are expected to stabilise the parent cobalt(III)-alkyl relative to the cobalt (II) dissociation product and hence increase the bond dissociation energy. Moad states that the effectiveness of cobalt (III) complexes of the CoBF type is reduced when strong basic ligands are used [53].

1.7.3.2 The use of monomers in CCTP.

CCT is known to be an effective method for regulating molecular weight in methyl methacrylate. However, its application and effectiveness in styrene polymerisations is greatly reduced although still effective, whilst CCTP for acrylates is complicated.

As stated the mechanism for CCTP involves a transfer step. This involves abstraction of a hydrogen atom from the end of a growing polymer chain to yield a cobalt (III) hydride and an unsaturated chain end. This process will occur readily for monomers which possess an α-methyl group such as in methacrylates, leading to the formation of a double bond. Monomers without such a group such as acrylates and styrene will not undergo the chain transfer step as readily as the formation of an internal double bond would occur. The reduction in chain transfer activity for styrene when compared to MMA was noted by Smirnov [11,55] when a bulk polymerisation with cobalt porphyrins was carried out. When they investigated the bulk polymerisation of the afore mentioned

monomers and also acrylates it was seen by UV spectroscopy that the spectrum, and hence coordination of the cobalt porphyrins with MMA and styrene did not change throughout the reaction whilst, that of the acrylate monomer did, indicating that the cobalt complex was coordinating with the acrylate forming the stable cobalt (III) alkyl complex and that the dissociation of the complex was irreversible. This observation was also seen by Gridnev under the same conditions [54]. It was also noted by this author in another publication [37] that when MMA undergoes CCTP a tertiary radical is produced resulting in the formation a tertiary C-Co bond which is labile [56]. Styrene forms secondary radicals and possesses an easily polarizable π electron system [57], it can therefore participate in complex formation as an additional axial ligand of the catalyst, thus completing the conjugation system of the porphyrin macrocycle. In this case no activation of the monomer takes place but in the polymerisation mixture the catalyst appears in two forms: (i) in the free state and (ii) as the complex with the monomer. These forms differ in reactivity with a radical. This in turn can be the reason for the appearance of two modes in the weight molecular mass distribution. The rate of polymerisation for styrene in the presence of the cobalt porphyrin is reduced more markedly than for MMA [55]. Bimodal peaks for styrene were also observed here. Haddleton and Davis [24,47] have stated that the CCT of MMA is diffusion controlled whilst that for styrene is not, they too think that the monomer complexes with the catalyst. Acrylate monomers although they do not participate in CCTP can be used in pseudo-living polymerisations [17]. The mechanism of polymerisation involves photolytic cleavage of the cobalt carbon bond, insertion of the monomer units and rapid cage recombination in a repetitive process.

1.7.3.3 Products of CCTP- proof of structure, reactivity and use of.

The predominant mode of termination for methacrylates in CCTP is chain transfer to give a methacrylate polymer with an unsaturated end group, termed a macromonomer, Figure 1.15. Interestingly this structure is identical to the chain end structure generated when a PMMA radical terminates by self disproportionation.

Figure 1.13. Structure of macromer product from CCTP

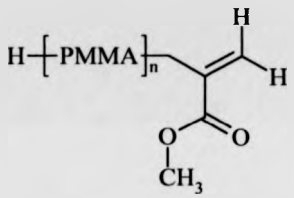

Work [58] utilising ^{1}H and ^{13}C NMR to quantify the number of vinylidene groups per chain has concluded that in CCTP >82% of polymer chains are vinyl terminated by abstraction indicating that radical-radical disproportionation events are suppressed and that the primary mode of chain termination is via CCTP transfer process. Matrix Assisted Laser Desorption Ionisation Time of Flight Mass Spectrometry (MALDI TOF MS) has also been used as a method of characterising the polymer chain ends [33,59,60]. Results [33] have shown that the vast majority of polymer molecules are initiated by a hydrogen atom.

Suddaby et al [61] reported a continuous process for the production of kilogram quantities of PMMA macromers. These macromers were synthesised in a tubular reactor and isolated from unreacted monomer using a twin screw extruder. For polymerisations at high CCTA concentrations these end groups will be almost exclusive and the

molecular weight of the polymer formed will be low. These short chain terminally unsaturated species are found under certain circumstances to be reactive at the double bond. Abbey et al [62] isolated the dimeric product of MMA by distillation following a CCT polymerisation and carried out a number of copolymerisation experiments to assess the reactivity of the terminal unsaturation. Similar studies conducted by Caciolli [63] who copolymerised PMMA macromer with ethyl acrylate, styrene, MMA, acrylonitrile and vinyl acetate. Some limited copolymerisation was observed but the reaction was retarded. This retardation originates from facile β-scission of the macromer chain end, resulting in termination. In this way the macromer is acting as a conventional chain transfer agent- terminating one growing chain and reinitiating another.

In fact MMA macromers are themselves found to be effective chain transfer agents in the polymerisation of MMA [40,44]. Haddleton et al [44] have used macromer chain transfer agents in CCTP to produce α-ω-telechelic PMMA and found the dimer to be an effective CCTA. Moad et al [56] have investigated the transfer activity of MMA macromers. It was found that the dimer was substantially less effective as a CCTA than the trimer or the higher macromers. Davis et al [46,64] have copolymerised styrene with MMA and styrene with α-methylstyrene. The aim of the latter was to investigate whether the C_s of α-methylstyrene was as high as that of MMA.

Davis et al [65] have devised a novel route for the preparation of aldehyde end functionalised macromers via CCTP. The aim being to introduce a different end functionality without the need for a post polymerisation modification.

1.7.3.4 Cobalt (III) hydride-proof of existence.

Smirnov [15] examined the structure of the macromers formed by CCT using NMR. It was concluded that from all the possible structures the one which was in strong agreement with the data was that of a hydrogen transfer mechanism. He confirmed this in a later publication by using deuterated MMA [16].

The kinetic studies also showed that the interaction between the cobalt porphyrin and polymer radicals was the limiting step and that the catalyst regeneration stage was so short that the transient intermediate eluded detection. It was postulated that the hydride cobalt complex was the active intermediate in the catalysis of chain transfer to monomer.

In 1981 Smirnov et al [55] studied the radical polymerisation of styrene with hematoporphyrin tetramethyl ester at 60 °C. It was found that CCT of the monomer occurred but was weaker than that of MMA and was complicated by secondary processes. Based on infra red analysis concerning the structure of oligomer end groups it was concluded that styrene in the same way as MMA underwent hydrogen atom transfer from the radical to the monomer molecule.

Sanayei [22] polymerised MMA in bulk without using a conventional initiator but in the presence of a CTA under a hydrogen atmosphere. The cobalt (III) hydride complex was formed.

Later Gridnev and his group of workers investigated the concept of hydrogen transfer in CCT [18,19]. Before this set of work the intermediacy of the cobalt (III) hydride had not been directly observed in cobalt (II) chain transfer in radical polymerisation but kinetic and mechanistic studies were fully compatible with a cycle involving hydrogen transfer. Theory behind the research was that cobalt (II) porphyrins in the presence of

dialkyl cyanomethyl radicals function as a convenient source for cobalt (III) hydrides that react with alkenes and alkynes to form alkyl and β-hydroxyalkyl complexes. They found that this was the case and concluded that the results proved the evidence for the intermediacy of the cobalt (III) hydride species. Gridnev et al [66] then carried out an isotopic investigation which involved carrying out two identical bulk polymerisations, one with protio-MMA-H_8 monomer whilst the other used deuterio MMA. It was found that the molecular weight of the deuterated polymer oligomers (macromers) was significantly higher than that for the corresponding undeuterated monomer. This, they reported indicated a clear kinetic isotopic effect which indicated that hydrogen atom transfer was involved in the rate determining step of the chain transfer process and the existence of cobalt (III) hydride.

1.7.3.5. Measurement of chain transfer constants (C_s).

The efficiency of a chain transfer agent is determined by comparing the molecular weight of a polymer produced with and without the presence of a chain transfer agent under identical polymerisation conditions. The value obtained is termed the chain transfer coefficient-C_s.

There are several methods for determining this coefficient although they all rely on molecular weight data obtained from GPC. The three commonly used methods are the Mayo method [67], $2/D_{pw}$ and the chain length distribution method [68]. The advantages of each and examples of results obtained from all three methods can be found in chapter 3. The higher the C_s value the more effective the chain transfer agent is at reducing molecular weight.

CoBF typically exhibits a value of around 35000 in bulk polymerisations of MMA [33,45] whilst mercaptans exhibit a value of approximately 1. The efficiency of these catalysts based on cobalt porphyrins [11,15,16], cobaloximes [21] and the BF_2 bridged set [22,40] are affected by the nature of axial ligand [53,54], equatorial ligands [45], monomer[47], temperature [45,47], solvents [45] and polymerisation system [42]. Each property will be discussed in more detail in the subsequent chapters.

1.7.3.6 Summary of CCTP.

1. CCTP, is a free radical mechanism involving a catalytic reduction oxidation cycle between cobalt (II) and cobalt (III).
2. The system is catalytic with respect to the cobalt complex - regeneration following the transfer step.
3. Owing to this regeneration no catalyst is incorporated in the polymer chain.
4. The transfer step involves abstraction of a hydrogen atom from the end of a growing polymer chain to yield a cobalt (III) hydride and an unsaturated chain end product-macromer. This step occurs readily for monomers possessing an α-methyl group, such as methylmethacrylate, but does not occur as readily for monomers such as styrene or acrylates.
5. A continual supply of radicals is required for effective CCTP – constant radical feed, otherwise the rate of polymerisation would decrease and cessation of the cycle could occur.

6. Effective CCTA's are those based on low spin cobalt (II) complexes. Cobalt (III) complexes can be used as a source of cobalt (II) generation. Cobalt (III) must reduce to cobalt (II) to allow effective chain transfer.
7. The nature of the equatorial and axial ligands has been shown to have an effect on the rate of polymerisation.

1.7.4 Applications of CCTP.

CCT polymerisation finds its use in applications requiring products of high solid content together with a low concentration of volatile organic compounds. The use of a range of cobalt complexes has been the subject of several patents [38,41,49]. It has been shown that CCTP is not just limited to solution systems but has been successfully extended to suspension and emulsion systems [41,69]. The products of CCTP show reactivity due to their terminal unsaturation. This has been used by companies and several patents have been filed utilizing macromers in cross linkable products [70,71], star polymers [72] and graft copolymers [73]. The macromers themselves can also be used as CCTA 's.

1.8. References

1) Odian, G. *Principles of Polymerisation*; 3 ed.; John Wiley & Sons:, 1991.

2) Campbell, I. M. *Introduction to Synthetic Polymers*; 1st ed.; Oxford University Press:, 1994.

3) Challa, G. *Polymer Chemistry An Introduction*; 1st ed.; Ellis Horwood:, 1993.

4) Saunders, K. J. *Organic polymer chemistry*; 2 ed.; Blackie Academic & Professional, Chapman & Hall:, 1994.

5) Moad, G.; Soloman, D. H. *The chemistry of free radical polymerisation*; Pergamon Press:, 1995.

6) Cacioli, P.; Moad, G.; Rizzardo, E.; Serelis, A. K.; Soloman, D. H. ; *Polym. Bull.*, **1984**, *11*, 325.

7) Allcock, H. E.; Lampe, F. W. *Contemporary Polymer Chemistry*; 1st ed.; Prentice Hall:, 1981.

8) Stevens, M. P. *Polymer Chemistry An Introduction*; 2 ed.; Oxford University Press:, 1990.

9) Young, R. J.; Lovell, P. A. *Introduction to polymers*; Chapman & Hall:, 1991.

10) Billmeyer, F. W. *Textbook of Polymer Science*; 2 ed.; Wiley Interscience:, 1962.

11) Smirnov, B. S.; Begovskii, I. M.; Ponamov, G. V.; Enikolopyan, N. S. ; *Doklady Akademii Nauk SSSR*, **1980**, *254*, 127.

12) Davis, T. P.; Kukulj, D.; Haddleton, D. M.; Maloney, D. R. ; *Trends in Polymer Science*, **1995**, *3*, 365.

13) Enikolopyan, N. S.; Smirnov, B. R.; Ponomarev, G. V.; Belgovskii, I. M. ; *J. Pol. Sci, Pol.Chem.Ed*, **1981**, *19*, 879.

14) Enikolopyan, N. S.; Pashchenko, D. I.; Vinogradora, E. K. ; *Doklady Akademii Nauk SSSR*, **1982**, *265*, 889.

15) Smirnov, B. R.; Morozova, I. S.; Pushchaeva, L. M.; Marchenko, A. P.; Enikolopian, N. S. ; *Doklady Akademii Nauk SSSR*, **1980**, *255*, 609.

16) Smirnov, R. R.; Morozova, I. S.; Marchenko, A. P. ; *Doklady Akademii Nauk SSSR*, **1980**, *253*, 891.

17) Arvanitopoulos, L. D.; Greuel, M. P.; Harwood, H. J. ; *J. Am. Chem. Soc. Polym.Prepr.*, **1991**, *32*, 545.

18) Gridnev, A. A.; Ittel, S. D.; Fryd, M.; Wayland, B. B. ; *J. Chem. Soc. Chem. Comm.*, **1993**, *12*, 1010.

19) Gridnev, A. A.; Ittel, S. D.; Fryd, M.; Wayland, B. B. ; *Organometallics*, **1993**, *12*, 4871.

20) Gridnev, A. A.; Ittel, S. D.; Fryd, M.; Wayland, B. B. ; *Abs. of Am. Chem. Soc.*, **1993**, *206*, 323.

21) Burczyk, A. F.; O'Driscoll, K. F.; Rempel, G. L. ; *J. Polym. Sci. Part A Polym. Chem.*, **1984**, *22*, 3255.

22) Sanayei, R. A. ; Ph.D. Thesis, Synthesis and properties of oligomers of methyl methacrylate , University of Waterloo, Waterloo, Canada, **(1989)**.

23) Smirnov, B. R.; Pushchaeyeva, I. M.; Plotnikov, V. D. ; *Polym. Sci. USSR.*, **1989**, *31*, 2607.

24) Davis, T. P.; Haddleton, D. M.; Richards, S. N. ; *J. Macromol. Sci.,Rev. Macromol. Chem. Phys.*, **1994**, *C34*, 243.

25) Scheffold, R.; Rytz, G.; Walder, L. *Modern synthetic methods*; R. Schefford, Ed. ed.; Wiley:; Vol. 3.

26) Davis, T. P.; Kukujl, D.; Maxwell, I. A. ; *Macromol.Theory Simul.*, **1995**, *4*, 195.

27) Daikh, B. E.; Finke, R. G. ; *J. Am. Chem. Soc.*, **1992**, *114*, 2938.

28) Bhandal, H.; Howell, A. R.; Patel, V. F.; Pattenden, G. J. ; *J. Chem. Soc., Perkin Trans.*, **1990**, *1*, 2703.

29) Bandaranayake, W. M.; Pattenden, G. ; *J. Chem. Soc., Chem. Comm.*, **1988**, , 1179.

30) Hawthorne, D. G. ; World Patent 87/03605, (**1987**).

31) Hawthorne, D. G. ; European Patent 0249614 A1, (**1992**).

32) Haddleton, D. M.; Suddaby, K. G.; Maloney, D. R. ; *Proc.Am.Chem.Soc., Div. Polym. Mater. Sci. Eng.*, **1995**, *73*, 420.

33) Maloney, D. R.; Haddleton, D. M. ; *J. Chem. Soc., Chem. Commun.*, **1995**, , 561.

34) Takahashi, M. ; *Bull. Chem. Soc. Jpn.*, **1963**, *36*, 622.

35) Aoki, S.; Shirafuji, C.; Otsu, T. ; *Makromol. Chem.*, **1969**, *126*, 1.

36) Gridnev, A. A.; Lampeka, Y. D.; Smirnov, B. R. ; *Teor. Eks. Khim.*, **1987**, *23*, 317.

37) Gridnev, A. A.; Gonocharov, A. V.; Lampeka, Y. D.; Gavrish, S. P. ; *Teor. Eks. Khim.*, **1989**, *25*, 698.

38) Carlson, G. M.; Abbey, K. J. ; United States Patent 4526945, (**1985**).

39) Enikolopyan, N. S. ; Russian Patent SU940487, (**1980**).

40) Sanayei, R. A.; O'Driscoll, K. F. ; *J. Macromol. Sci.-Chem.*, **1989**, *A26*, 1137.

41) Janowicz, A. H. ; United States Patent 4 694 054, (**1987**).

42) Suddaby, K. G.; Haddleton, D. M.; Hastings, J. J.; Richards, S. N.; O'Donnell, J. P. ; *Macromolecules*, **1996**, *29*, 8083.

43) Suddaby, K. G.; Maloney, D. R.; Haddleton, D. M. ; *Macromolecules*, **1997**, *30*, 702.

44) Haddleton, D. M.; Topping, C.; Hastings, J. J.; Suddaby, K. G. ; *Macromol. Chem. Phys.*, **1996**, *197*, 3027.

45) Haddleton, D. M.; Maloney, D. R.; Suddaby, K. G.; Muir, A. V. G.; Richards, S. N. ; *Macromol. Symp.*, **1996**, *111*, 37.

46) Kukulj, D.; Heuts, J. P. A.; Davis, T. P. ; *Macromolecules*, **1998**, *31*, 6034.

47) Heuts, J. P. A.; Forster, D. J.; Davis, T. P. ; *Macromolecules*, **1999**, *32*, 5514.

48) Suddaby, K. G.; O'Driscoll, K. F.; Rudin, A. ; *J. Polym. Sci., Part A Polym. Chem.*, **1992**, *30*, 643.

49) Janowicz, A. H.; Melby, R. L. ; United States Patent 4 680 352, (**1987**).

50) Melby, L. R.; Janowicz, A. H.; Ittel, S. D. ; European Patent 0199436 A1, (**1986**).

51) Janowicz, A. H. ; United States Patent 5 028 677, (**1991**).

52) Bakac, A.; Brynildson, M. E.; Espenson, J. H. ; *Inorg. Chem.*, **1986**, *25*, 4108.

53) Moad, G.; Moad, C. L.; Krstina, J.; Rizzardo, E.; Thang, S.; Fryd, M. ; World Patent 96/15158, (**1996**).

54) Gridnev, A. ; *Pol.Sci.,USSR.*, **1989**, *31*, 2369.

55) Smirnov, B. R.; Plotnikov, V. D.; Ozenkovskii, B. V. ; *Vysokomol.Soyed.*, **1981**, *A23*, 2588.

56) Moad, C. L.; Moad, G.; Rizzardo, E.; Thang, S. H. ; *Macromolecules*, **1996**, *29*, 7717.

57) Plotnikov, V. D. ; *Vysokomolekulyarnye Soedineniya Seriya A & Seriya B*, **1997**, *39*, 406.

58) McCord, E. F.; Anton, W. L.; Wiczek, L.; Ittel, S. D.; Lissa, N. T.; Raffell, K. D. ; *Makromol.Chem., Macromol.Symp.*, **1994**, *86*, 47.

59) Creel, H. S. ; *Trends Polym. Sci.*, **1993**, *1*, 336.

60) Campana, J. E.; Long-Sheng, S.; Shew, S. L.; Winger, B. E. ; *Trends Anal. Chem.*, **1994**, *13*, 239.

61) Suddaby, K. G.; Sanayei, R. A.; Rudin, A.; O'Driscoll, K. F. ; *J. App. Polym. Sci.*, **1991**, *43*, 1565.

62) Abbey, K. J.; Carlson, G. M.; Masola, M. J.; Trumbo, D. ; *Proc. Am. Chem. Soc., Div. Polym. Mater. Sci. Eng.*, **1986**, *55*, 235.

63) Cacioli, P.; Hawthorne, D. G.; Laslett, R. L.; Rizzardo, E.; Solomon, D. H. ; *J. Macromol. Sci. Chem.*, **1986**, *A23*, 839.

64) Heuts, J. P. A.; Kukulj, D.; Forster, D. J.; Davis, T. P. ; *Macromolecules*, **1998**, *31*, 2894.

65) Davis, T. P.; Zammit, M. D.; Heuts, J. P. A.; Moody, K. ; *J. Chem. Soc. Chem. Commun.*, **1998**, , 2383.

66) Gridnev, A. A.; Ittel, S. D.; Wayland, B. B.; Fryd, M. ; *Organometallics*, **1996**, *15*, 5116.

67) Mayo, F. R. ; *J. Am. Chem. Soc*, **1943**, *65*, 2324.

68) Gilbert, R. G.; Clay, P. A. ; *Macromolecules*, **1995**, *28*, 552.

69) Lin, J.; Abbey, K. J. ; United States Patent 4 680 354, (**1987**).

70) Kerr, S. R. ; European patent 0 187 045, (**1986**).

71) Berge, C. T.; Darmon, M. J.; Antonelli, J. A. ; United States Patent 5 371 151, (**1994**).

72) Antonelli, J. A.; Scopazzi, C. ; United States Patent 5 310 807, (**1994**).

73) Devlin, B. P.; Antonelli, J. A.; Scopazzi, C. ; World Patent 93/03081, (**1992**).

Chapter 2

Characterisation of cobalt (II) and cobalt (III) boron fluoride bridged complexes.

2.0 The characterisation of cobalt (II) and cobalt (III) complexes.

2.1. Aim.

The aim of this work was to synthesise a range of cobalt (II) and cobalt (III) complexes with a range of hydrophobicity. This was achieved by altering the axial and equatorial ligands. The effects of which will be discussed in this and other chapters.

2.2. Introduction

Effective catalytic chain transfer agents have been shown to be based on low spin cobalt (II) complexes [1-4] although cobalt (III) can also be used as a source of cobalt (II). The most effective being the BF_2 bridged set [5,6]. It has been shown by various workers that altering catalyst structure can have a profound effect on molecular weight reduction [7]. It has also been shown that cobalt (III) must reduce to cobalt (II) to become an effective CCTA [8,9]. The rate of this reduction and hence effectiveness as a cobalt (II) species can be controlled by using different axial base ligands. Characterisation of these CCTA's is dependable on whether the species are low spin cobalt (II) or cobalt (III). Cobalt (II) CCTA's are paramagnetic therefore analysis by NMR spectroscopy is not possible. An excellent technique to assure low spin confirmation for cobalt (II) is by calculation of its magnetic moment [10]. Cobalt (III) species are diamagnetic and it is therefore possible to acquire useful interpretational NMR spectra [11-13]. Methods of characterisation which are useful for both cobalt (II) and (III) CCTA's are infrared spectroscopy [12,14-17], FAB MS, and CHN analysis, however the latter is not always interpretably useful owing to the boron and fluorine groups present. It is therefore the purpose of this chapter to introduce the CCTA's

which have been used in investigations throughout this thesis and discuss characterisation where necessary.

2.3. The structure of cobalt (II) complexes utilised in this work.

Table 2.1 shows which catalysts have been synthesised corresponding to the general structure outlined in Figure 2.1. Table 2.1 indicates the nature of the axial and equatorial ligands, as stated previously the ligands in cobalt (II) complexes are generally occupied by solvents which are used in the purification of the complex.

Figure 2.1. Structure of cobalt (II) complexes.

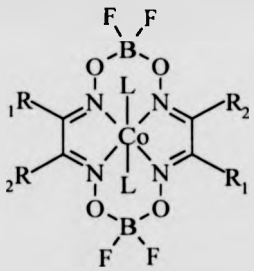

Where L= CH_3OH (I-IV), Ethyl acetate (V-VI), H_2O (VII).

The aim of this work was to ascertain what role the equatorial groups (R_1 + R_2) played on the chain transfer activity of the complexes in bulk polymerisations using MMA and styrene. It was also interesting to see how the structure of the complex affected its partitioning properties when used with MMA and water. It would also be interesting to compare the cobalt (II) complexes with both the cobalt (III) analogues utilising pyridine and water as the axial ligands (L). It was also interesting to see what effect isomerisation had on complex III activity.

Table 2.1. Nature of catalysts synthesised for cobalt (II) complexes.

Complex number	Abbreviated name	R_1	R_2
I	CoH_4BF	H	H
II	CoBF	CH_3	CH_3
III	$CoEt_2Me_2BF$	CH_3	CH_2CH_3
IV	$CoEt_4BF$	CH_2CH_3	CH_2CH_3
V	$Co(Me_2Prop_2)BF$	CH_3	$CH_2CH_2CH_3$
VI	$Co(Me_2But_2)BF$	CH_3	$CH_2CH_2CH_2CH_3$
VII	$Co(C_5H_5\text{-}CH_3)BF$	$(C_5H_5)CH_3$	$(C_5H_5)CH_3$

2.4. The use of cobalt (III) complexes utilising pyridine as one of the axial ligands.

The following catalysts were synthesised corresponding to the general structure outlined in Figure 2.2, containing ethyl (R) and pyridine (B) axial ligands, table 2.2.

Figure 2.2. Structure of cobalt (III) complexes with pyridine as axial ligands.

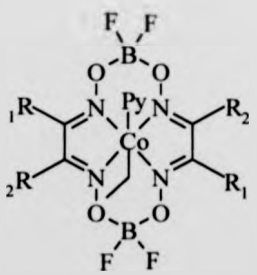

The aim here was to see what effect using a strong base as one of the axial ligands had on the chain transfer activity of the complex. The results from these complexes in both MMA and styrene bulk polymerisations would be compared with both its cobalt

(II) and cobalt (III) - water analogues. The effect of the ligand would also be investigated in the partitioning experiments again using MMA and water.

Again the effect of isomerisation on catalytic activity could also be important for complex IX.

Table 2.2. Nature of cobalt (III) complexes with pyridine as an axial ligand.

Complex number	Abbreviated name	R_1	R_2
VIII	Co(III)BF/PyEt	CH_3	CH_3
IX	Co(III)Et_2Me_2BF/PyEt	CH_3	CH_2CH_3
X	Co(III)Et_4BF/PyEt	CH_2CH_3	CH_2CH_3

2.5. The use of cobalt (III) complexes utilising water as an axial base ligand.

The following catalysts were synthesised corresponding to the general structure outlined in Figure 2.3, containing ethyl (R) and water (B) axial ligands, table 2.3.

Figure 2.3. Structure of cobalt (III) complexes with water as axial ligands.

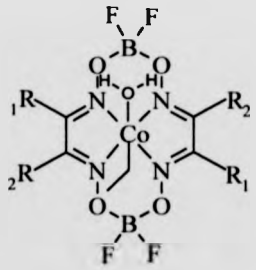

The aim here was to compare the results obtained for the chain transfer activity of the complex in both MMA and styrene bulk polymerisations with those of the cobalt (II) and cobalt (III) pyridine analogues. The effect of the weak base ligand was also investigated in the partitioning experiments using MMA and water and again

compared with its cobalt (II) and cobalt (III) pyridine analogues. The effect of cis/trans isomers for complex XII could also play a role in catalytic activity.

Table 2.3. Nature of cobalt (III) complexes with water as one of the axial ligands.

Complex number	Abbreviated name	R_1	R_2
XI	Co(III)BF/H_2OEt	CH_3	CH_3
XII	Co(III)Et_2Me_2BF/H_2OEt	CH_3	CH_2CH_3
XIII	Co(III)Et_4BF/H_2OEt	CH_2CH_3	CH_2CH_3

2.6. The characterisation of the cobalt (II) and cobalt (III) complexes.

2.6.1. Magnetic moment measurements.

Cobalt (II) complexes are d^7 which exist in one of two electronic states either high or low spin (Figure 2.4).

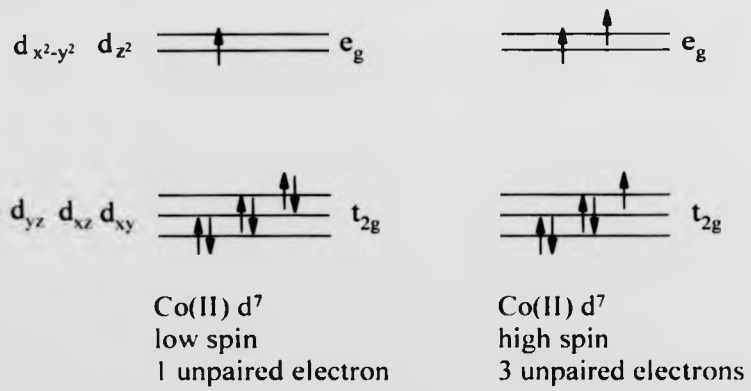

Figure 2.4. The possible electronic states of cobalt (II).

Electrons in an incompletely filled shell will give rise to a magnetic moment which is dependent on the number of unpaired electrons. It is therefore possible to relate the

number of unpaired electrons (n) to the effective magnetic moment (e), in an expression known as the "Spin Only Formula".

$$\mu_e = (n(n + 2)$$

The magnetic moments of the synthesised cobalt complexes have been measured and are presented in table 2.4.

2.6.1.1. Magnetic moment values for cobalt (II) complexes.

Illustrated below, table 2.4. are the magnetic moment values for the cobalt (II) complexes II – VII.

Table 2.4. Magnetic moment data for cobalt (II) complexes.

Complex number	Catalyst	Stereo-chemistry	Hybrid Orbitals	n	μ_e (B.M) Spin only	Expt
II	CoBF	oct	spd^3	1	1.73	1.71
III	$Co(Me_2Et_2)BF$	oct	spd^2	1	1.73	2.33
IV	$Co(Et_4)BF$	oct	spd^2	1	1.73	1.44
V	$Co(Me_2Prop_2)$ BF	oct	spd^2	1	1.73	1.85
VI	$Co(Me_2Bu_2)BF$	oct	spd^2	1	1.73	2.07
VII	$Co(Pent_2)BF$	oct	spd^2	1	1.73	1.80

The values in table 2.4 show that all the cobalt complexes synthesised using the Co(II) pathway are low spin which according to previous workers observations [10] would suggest that all seven complexes in theory should be effective as CCTA's.

2.6.2. Infra red analysis of cobalt (II) and cobalt (III) complexes.

2.6.2.1. Infra red analysis of cobalt (II) complexes.

The infrared analysis of complexes I-VII are shown in table 2.5 along with C-H and axial ligand stretching frequencies in table 2.6.

Table 2.5. Infrared stretching frequencies (cm^{-1}) for cobalt (II) complexes.

Complex	C=N	B-O	N-O	N-O	B-F	B-O	Co-N	C=N-O
I	1633		1150	1000	900	840	510	755
II	1618	1210	1161	1088	950	803	504	730
III	1610	1253	1195	1097	992	901	506	714
IV	1607	1235	1167	1045	1010	832	508	762
V	1613	1247	1227	1047	993	813	509	764
VI	1614	1245	1213	1045	1000	821	507	734
VII	1634						506	718

An increase in C-H stretching band (typically 2960 cm^{-1}), increases when the number of skeletal carbons increases, see table 2.6. The infrared results not only show that the complexes have been successfully synthesised but that the catalyst structure seems to affect certain band stretching frequencies [14]. For instance with the cobalt (II) species I - IV the C=N stretching frequency decreases whilst the first set of N-O bands increases and the second decreases. This is thought to be attributable to an increase in the number of carbons on the skeleton as the axial ligands in this case are either the same or very similar. In complexes V-VI the carbon chain length of the equatorial group increases and the axial ligands are also different to those of I-IV. The C=N stretching frequency increases here whilst for the N-O stretching frequency there is no effect seen. The effects are most likely due to the electron withdrawing nature of the

C=O group on the ethyl acetate, and its interaction with the cobalt atom and respective back donation and interaction with C=N and N-O groups.

The data in table 2.6 shows that the axial ligands have successfully complexed to the central cobalt. The strength of the C-H intensity increases with an increase in carbons although the frequency values do not appear to be affected. It should be noted that there were peaks observed for the C-H stretching for complexes I and VII. It should also be noted that some of the stretching frequencies were not observed for complex VII in table 2.5

Table 2.6. Infrared stretching frequencies for C-H bands and axial ligand frequencies (cm^{-1}) for cobalt (II) complexes.

Complex	C-H	L
I		3244 O-H, bonded (w)
II	2927Asym CH_3 (w)	3593 + 3525 O-H, non-bonded (wm)
III	2983 Asym CH_3 (m) 2943 Asym CH_2 (m)	3198.1 O-H, bonded (b,m)
IV	2985 Asym CH_3 (m) 2947 Asym CH_2 (m)	3591 + 3513 O-H, non – bonded, (m)

Table 2.6. Continued.

Complex	C-H	L
V	2969 Asym CH_3 (m) 2937 Asym CH_2 (m) 2877 Sym CH_3 (ms)	1714 C=O (s) 1278 + 1188 C-O (m)
VI	2959 Asym CH_3 (s) 2932 Asym CH_2 (s) 2871 Sym CH_3 (s)	1732 C=O (s) 1282 + 1185 C-O (m)
VII		3198 O-H bonded

2.6.2.2. Infrared analysis of cobalt (III) complexes utilising pyridine as an axial ligand.

The infrared analysis of complexes VIII-X are shown in table 2.7 along with C-H and axial ligand stretching frequencies in table 2.8.

Table 2.7. Infra red stretching frequencies (cm^{-1}) for cobalt (III) complexes containing pyridine axial ligands.

Complex	C=N	B-O	N-O	N-O	B-F	B-O	Co-N	C=N-O
VIII	1622	1226	1199	1092	950	827	508	744
IX	1609	1254	1207	1067	982	900	509	743
X	1609	1254	1174	1067	1024	833	510	743

The axial ligands for cobalt (III) species have a profound effect on the stretching frequencies. For instance if we consider C=N, the pyridine group decreases the stretching frequency. This is due to pyridine being a strong base, owing to its strength

the electron density around the cobalt center increases, this facilitates in back donation from cobalt to the nitrogen resulting in an increased electron density in the C=N bond and a lower frequency shift. The B-F and Co-N stretching frequencies also increase, again this is attributable to the strong base.

Table 2.8. C-H strength and axial ligand stretching frequencies (cm^{-1}).

Complex	Axial R= Ethyl	Axial B = Pyridine
VIII	2943 Asym CH_3 1149 C - H stretch	3200 + 1489 C - H stretch 1539 C=N stretch 1290 + 1252 C - N stretch
IX	2358 Asym CH_3 1173 C-H stretch	3147 + 3118, 1489 C - H stretch 1538 C=N stretch 1290 C-N stretch
X	2360 Asym CH_3 1174 C - H stretch	3147 + 3118, 1488 C - H stretch 1538 C=N stretch 1290 C – N stretch

Again the results in table 2.8 show the presence of the axial ligands. The CH_3 and C-H stretching frequencies increase with an increase in carbons.

2.6.2.3. Infra red analysis of cobalt (III) complexes utilising water as an axial ligand.

The infrared analysis of complexes XI - XIII are shown in table 2.9 along with C-H and axial ligand stretching frequencies in table 2.10.

Table 2.9. Infra red stretching frequencies (cm^{-1}) for cobalt (III) complexes containing water as an axial ligand.

Complex	C=N	B-O	N-O	N-O	B-F	B-O	Co-N	C=N-O
XI	1622	1226	1200	1093	1030	827	504	736
XII	1615	1250	1232	1104	1006	910	514	760
XIII	1606	1220	1164	1050	1020	835	509	720

From table 2.9 it can be seen that water increases the C=N stretching frequency which is the reverse effect of the pyridine group. Water is a weak base as opposed to a strong base. The trans effect from water is not as profound as that of pyridine and gives little cis effect to the equatorial ligand therefore increasing the C=N stretching frequency.

Table 2.10. C-H strength and axial ligand stretching frequencies (cm^{-1}).

Complex	Axial R = Ethyl	Axial R = Water
XI	2942 Asym CH_3 1150 C - H stretch	3565 + 3484 O - H non bonded
XII	2358 Asym CH_3 1191 C - H stretch	3524 + 3176 O - H bonded
XIII	2358 Asym CH_3 1205 C - H stretch	3551 + 3463 O - H non bonded

Table 2.10 shows the presence of the axial ligands and shows that the C-H stretching frequency increases with an increase in carbons, the CH_3 stretching frequency does not appear to be affected.

2.6.3. ^1H and ^{13}C NMR analysis of cobalt (III) complexes.

2.6.3.1 ^1H NMR.

2.6.3.1.1 ^1H NMR analysis of cobalt (III) complexes containing pyridine as an axial ligand.

By using NMR spectroscopy it was possible to further consolidate the proof of the cobalt (III) complexes containing pyridine as an axial ligand therefore confirming successful synthesis of these complexes. Table 2.11. gives NMR data for complexes VIII-X. It is not possible to analyse cobalt (II) complexes by this method owing to their paramagnetic properties.

Table 2.11. ^1H NMR (300 MHz) frequencies for cobalt (III) complexes containing pyridine as axial ligand.

Complex	R_1 (ppm)	R_2 (ppm)	B (ppm)	R (ppm)
VIII	2.40(s, 12H)	2.40(s, 12H)	9.12(m, 2H) 8.89(m, 1H) 8.34(m, 2H)	2.09(m, 2H) 0.10(m, 3H)
IX	2.42(s, 6H)	2.87(m, 4H) 1.15(m, 6H)	9.14(m, 2H) 8.91(m, 1H) 8.35(m, 2H)	1.23(q, *J* 9.2 Hz,2H) 0.02(t, *J* 9.3 Hz, 3H)
X	2.94(q, *J* 7.6 Hz,4H) 1.27(t, *J* 7.3 Hz,6H)	2.94(q, *J* 7.6 Hz,4H) 1.27(t, *J* 7.3 Hz,6H)	9.14(m, 2H) 8.91(m, 1H) 8.36(m, 2H)	1.97(q, *J* 7.3 Hz,2H) 0.14(t, *J* 7.5 Hz,3H)

Table 2.11 shows the characteristic signals for the axial and equatorial ligands of the cobalt (III) complexes containing pyridine. Where the nature of the groups are identical, i.e. CH_3 the signal from complex to complex does not change.

2.6.3.1.2. The characterisation of cobalt (III) complexes containing H_2O as an axial ligand.

Table 2.12 below gives information for complexes XI-XIII containing water as an axial ligand.

Table 2.12. ^{1}H NMR (300 MHz) frequencies for cobalt (III) complexes containing water as the axial ligand.

Complex	R_1 (ppm)	R_2 (ppm)	B (ppm)	R (ppm)
XI	2.36(s, 12H)	2.36(s, 12H)	2.70(s, 2H)	1.89(q, *J* 6.3 Hz, 2H) 0.02(t, *J* 6.1 Hz, 3H)
XII	2.45(s, 12H)	2.94(m, 4H) 1.20(m, 6H)	3.66(s, 2H)	1.99(m, 2H) 0.07(m, 3H)
XIII	2.90(m, 10H) 1.25(m, 12H)	2.90(m, 10H) 1.25(m, 12H)	-	1.97(m, 2H) 0.12(m, 3H)

From table 2.12 the presence of all the relevant signals for each group in each complex is shown proving that the abstraction of the pyridine molecule and replacement with water has been successful. However complex XIII fails to show the presence of the water ligand, although it should be noted that the presence of a pyridine molecule was not observed after abstraction in the NMR spectrum.

2.6.3.2 The characterisation of cobalt (III) complexes using ^{13}C NMR spectroscopy.

2.6.3.2.1 The characterisation of cobalt (III) complexes containing pyridine as an axial ligand.

Table 2.13 gives ^{13}C NMR frequencies for complexes VIII-X containing pyridine as one of the axial ligands.

Table 2.13. ^{13}C NMR (75.0 MHz) frequencies for cobalt (III) complexes containing pyridine as the axial ligand.

Complex	R_1 (ppm)	R_2 (ppm)	B (ppm)	R (ppm)	C=N
VIII	13.56	13.56	160.00 (C2) 148.00 (C4) 129.00 (C3)	16.93 9.0	-
IX	20.86 11.00	14.00	172.00 164.00	-	-
X	20.90 11.00	20.90 11.00	-	17.00	-

Table 2.13 shows the presence of both equatorial ligands although the C=N frequency from the complex is not observed owing to the small size of the peaks on the NMR spectra.

2.6.3.2.2. ^{13}C NMR characterisation of cobalt (III) complexes containing H_2O as an axial ligand.

Table 2.14 gives NMR frequencies for cobalt (III) complexes XI-XIII containing water as an axial ligand.

Table 2.14. ^{13}C NMR (75.0 MHz) frequencies for cobalt (III) complexes containing water as the axial ligand.

Complex	R_1	R_2	R	C=N
XI	14.00	14.00		164.28
XII	20.84 11.00	14.00	21.95 16.00	
XIII	20.89 11.00	20.89 11.00	17.00	164.43

Table 2.14 shows the characteristic frequencies for the axial and equatorial ligands. It also confirms the absence of pyridine as an axial ligand and therefore the successful exchange of a pyridine molecule for a water molecule. It should be noted here that some peak information is not present (R complex XI and C=N complex XII), this is due to the size of the peaks on the NMR spectra making it impossible to correctly assign.

2.6.4. X-ray crystallography [10,18-24]

2.6.4.1. X-ray crystal structure of $CoEt_4BF$ (complex III).

Figure 2.5. X-ray crystal structure of $CoEt_4BF$.

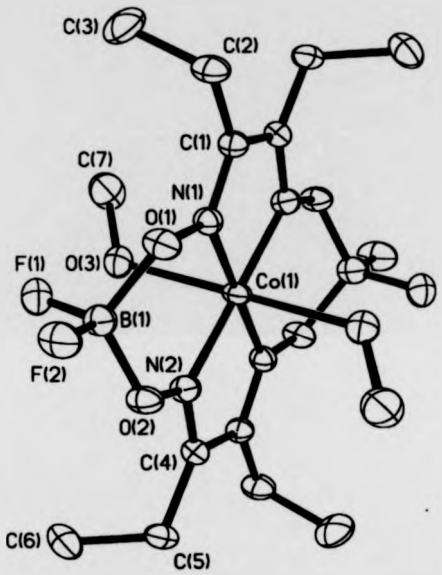

The ligands around the metal centre are arranged in a pseudo octahedral geometry. The cobalt atom is attached to two 3,4-hexanedioxime ligands with nitrogen bond distance given as 1.879(2) Å, with methanol ligands taking the trans positions, bond distance 2.279(2) Å.

2.6.4.2. X-ray crystal structure of $CoEt_4H_2O$/PyEt.

Figure 2.6. X-ray crystal structure of $CoEt_4H_2O$/PyEt.

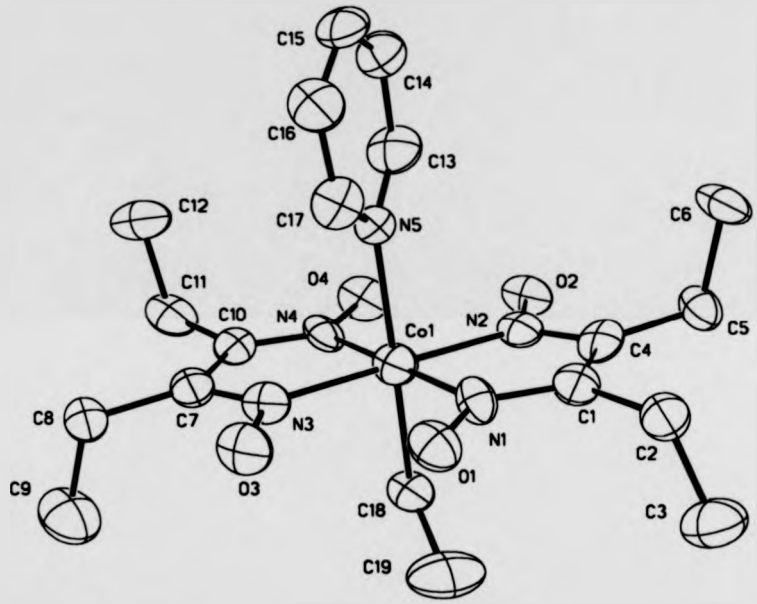

The ligands around the metal centre are arranged in a pseudo octahedral geometry. The cobalt atom is attached to two 3,4-hexanedioxime ligands with nitrogen bond distance given as 1.886(10)Å, with one pyridine and one ethyl ligand taking the trans positions, bond distance 2.076(9)Å and 2.032(11)Å respectively.

2.6.4.3. X-ray crystal structure of $CoMe_2Et_2BF/H_2OEt$ (complex XII).

Figure 2.7. X-ray crystal structure of $CoMe_2Et_2BF/H_2OEt$.

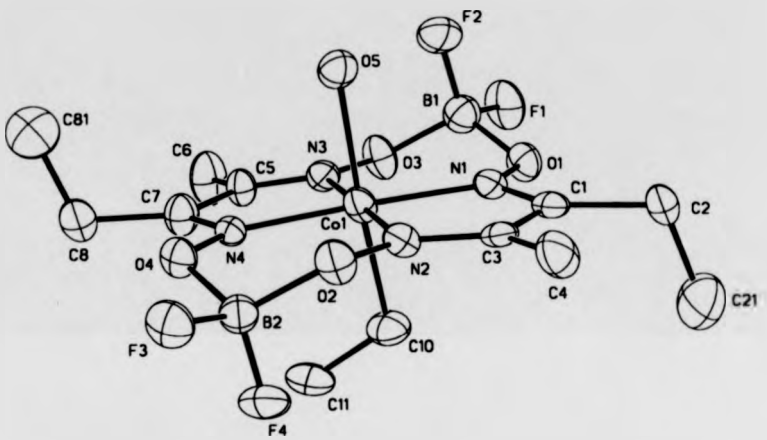

The ligands around the metal centre are arranged in a pseudo octahedral geometry. The cobalt atom is attached to two 3,4-hexanedioxime ligands giving nitrogen bond distance as 1.873(4)Å, with one water and ethyl ligand taking respectively the trans positions, bond distances 2.123(4)Å and 2.072(5)Å respectively.

2.7. Conclusions.

The magnetic moments of complexes I - VII prove that they are low spin cobalt (II) species [10].

The Infra-red results not only show that the complexes have been successfully synthesised but that the catalyst structure seems to affect certain band stretching frequencies [14]. For instance with the cobalt (II) species I - IV the C=N stretching

frequency decreases whilst the first set of N-O bands increases and the second decreases. This is thought to be attributable to an increase in the number of carbons on the skeleton as the axial ligands in this case are either the same or very similar. In complexes V-VI the carbon chain length of the equatorial group increases and the axial ligands are also different to those of I-IV. The C=N stretching frequency increases here whilst for the N-O stretching frequency there is no effect seen. The effects are most likely due to the electron withdrawing nature of the C=O group on the ethyl acetate, and its interaction with the cobalt atom and respective back donation and interaction with C=N and N-O groups.

The axial ligands for cobalt (III) species have a profound effect on the stretching frequencies. For instance if we consider C=N, the pyridine group decreases the stretching frequency whilst a water group increases it. Pyridine is a strong base and therefore increases electron density around the cobalt centre by donation of electrons. This facilitates in back donation from cobalt to the nitrogen resulting in an increased electron density in C=N which results in and a lower frequency shift. Water on the other hand gives an increase in electron density, its trans effect is not as profound and gives little cis effect to the equatorial ligand therefore C=N stretching frequency increases as is the situation for cobalt (II) species.

The NMR results also prove that the cobalt (III) catalysts have been successfully synthesised and that pyridine can be successfully replaced by water if necessary. The ^{13}C NMR spectra also show C=N frequencies which are present in the complex directly and also in pyridine where necessary.

The X-ray crystal structures show that there is little difference with regard to bond distances between the central metal atom and the hexanedione ligands when there is water or methanol attached as one of the central axial ligands but there is a

decrease in this value when pyridine is used as an axial ligand. The bond lengths of the cobalt (III) ligands are shorter than those of the cobalt (II) complexes. It should be noted that there are two analogues, one being cobalt (II) and the other a cobalt (III) both containing 3,4-hexanedioxime ligands as the equatorial ligands. The axial and equatorial ligand bond lengths are shorter for the cobalt (III) analogues.

It should also be noted that there are two possible isomers for complexes III,IX and XII, namely the cis and trans isomers. It was however not possible to separate the isomers for the potential identification of catalytic effectiveness and partitioning properties. It is possible that each isomer could demonstrate different catalytic activity.

2.8. References.

1) Burczyk, A. F.; O'Driscoll, K. F.; Rempel, G. L. ; *J. Polym. Sci. Part A Polym. Chem.*, **1984**, *22*, 3255.

2) Smirnov, B. R.; Morozova, I. S.; Pushchaeva, L. M.; Marchenko, A. P.; Enikolopian, N. S. ; *Doklady Akademii Nauk SSSR*, **1980**, *255*, 609.

3) Smirnov, B. S.; Begovskii, I. M.; Ponamov, G. V.; Enikolopyan, N. S. ; *Doklady Akademii Nauk SSSR*, **1980**, *254*, 127.

4) Smirnov, R. R.; Morozova, I. S.; Marchenko, A. P. ; *Doklady Akademii Nauk SSSR*, **1980**, *253*, 891.

5) Sanayei, R. A.; O'Driscoll, K. F. ; *J. Macromol. Sci.-Chem.*, **1989**, *A26*, 1137.

6) Sanayei, R. A. ; Ph.D. Thesis, Synthesis and properties of oligomers of methyl methacrylate , University of Waterloo, Waterloo, Canada, (**1989**).

7) Haddleton, D. M.; Maloney, D. R.; Suddaby, K. G.; Muir, A. V. G.; Richards, S. N. ; *Macromol. Symp.*, **1996**, *111*, 37.

8) Davis, T. P.; Haddleton, D. M.; Richards, S. N. ; *J. Macromol. Sci.,Rev. Macromol. Chem. Phys.*, **1994**, *C34*, 243.

9) Davis, T. P.; Kukulj, D.; Haddleton, D. M.; Maloney, D. R. ; *Trends in Polymer Science*, **1995**, *3*, 365.

10) Bakac, A.; Brynildson, M. E.; Espenson, J. H. ; *Inorg. Chem.*, **1986**, *25*, 4108.

11) Brown, T. L.; Ludwick, L. M.; Stewart, R. S. ; *J. Am. Chem. Soc.*, **1972**, *94*, 384.

12) Gillard, R. D.; Wilkinson, G. ; *J. Chem. Soc.*, **1963**, *5*, 6041.

13) Schrauzer, G. N.; Windgassen, R. J. ; *J. Am. Chem. Soc*, **1966**, *88*, 3738.

14) Yamazaki, N.; Hohokabe, Y. ; *Bull. Chem. Soc. Jpn.*, **1971**, *44*, 63.

15) Burger, K.; Ruff, I.; Ruff, F. ; *J. Inorg. Nucl. Chem.*, **1965**, *27*, 179.

16) Nakahara, A.; Fujita, J.; Tsuchida, R. ; *Bull. Chem. Soc. Japan.*, **1956**, *29*, 296.

17) Blinc, R.; Hadzi, D. ; *J. Chem. Soc*, **1958**, *5*, 4536.

18) Lance, K. A.; Lin, W. K.; Busch, D. H.; Alcock, N. W. ; *Acta. Cryst.*, **1991**, *47*, 1401.

19) Lenhert, P. G. ; *J. Chem Soc.,Chem.Comm.*, **1967**, , 980.

20) McFadden, D. L.; McPhail, A. T. ; *J. Chem. Soc., Dalton Trans.*, **1974**, , 363.

21) Giannotti, G.; Fontaine, C.; Chiaroni, A.; Riche, C. ; *J. Organomet. Chem.*, **1976**, *113*, 57.

22) Ohashi, Y.; Sasada, Y. ; *Bull. Chem. Soc. Japan*, **1977**, *11*, 2863.

23) Ohashi, Y.; Sasada, Y. ; *Bull. Chem. Soc. Japan*, **1977**, *50*, 1710.

24) Randaccio, L.; Pahor, N. B.; Zangrando, E. ; *Chem. Soc. Rev*, **1989**, *18*, 225.

Chapter 3

Investigation into the effect of catalyst structure and initiator concentration on chain transfer constants in MMA polymerisation. Comparison of the different methods used to obtain their value.

3.0 An investigation into the effect of catalyst structure and initiator concentration on chain transfer constants in MMA polymerisations and a comparison of the different methods used to obtain their value.

3.1 Aim.

The aim of this chapter was to investigate what effect if any, the structure of the catalysts synthesised in chapter 2 had on the chain transfer constant value (C_s) in MMA bulk polymerisations and to compare the values obtained by using different methods for obtaining C_s. It was also interesting to see what effect initiator concentration had on the chain transfer constant value.

3.2. Introduction.

As stated previously it is known that the structure of a catalyst plays an important role on its effectiveness at reducing molecular weight. Both Davis [1] and Haddleton [2] have noted this independently for the BF_2 bridged derivatives. Gridnev in the 1980's stated that small changes in catalyst structure could affect C_s [3].

Davis et al [4,5] have stated that CCT is reliant on a constant radical feed, it will therefore be interesting to see what effect if any is seen with a variation in initiator concentration under identical reaction conditions. The methods for determining C_s all rely on GPC information, however it is which set of data used which distinguishes each method from the other [6-8]. It should be noted that the larger the value for C_s the more efficient the catalyst is at reducing molecular weight.

It should also be noted that isomerisation could play an important role on catalytic activity. However it was not possible to isolate the cis and trans isomers for complexes II,IX and XII therefore their effects can only be speculated.

3.2.1. The Mayo method.

In 1943 the Mayo equation was devised [7], which allowed C_s to be calculated, equation 1.

$$\frac{1}{DP_n} = \frac{1}{DP_n}_0 + Cs \frac{[S]}{[M]} \qquad (1)$$

Where DP_n is the number average degree of polymerisation (M_n / M_w), DP_n^0 is the number average degree of polymerisation for polymer produced under the same conditions in the absence of added chain transfer agent, [S] and [M] are the concentrations of added chain transfer agent and monomer respectively and C_s is the chain transfer constant. The experimental procedure for obtaining C_s can be found in Chapter 6, but to summarise a total of five solutions are made up with differing quantities of chain transfer agent one with none added (the control), with constant initiator concentration, which, are polymerised under identical conditions and from GPC data a plot of 1/DP vs. [S]/[M] is drawn, C_s is equivalent to the slope of the graph, whilst intercept equals $1/DP_n^0$. The Mayo method, as it is known, is an established method for determining C_s.

3.2.2. Half weight average degree of polymerisation- the $2/DP_w$ method.

This is a modified method of the Mayo procedure and relies on M_w information [9,10] rather than M_n which can be subject to a large uncertainty due to baseline subtraction errors, M_w

on the other hand is not. Here the weight average degree of polymerisation (DP_w) is used instead of DP_n. In a chain transfer dominated system $DP_w/DP_n = 2$ and hence $1/DP_n = 2/DP_w$.

Again the same general experimental procedure is followed, however from the GPC information M_w information is used. A plot of $2/DP_w$ vs [S]/[M] gives slope (C_s) and intercept $2/DP_w^0$.

3.2.3.The Chain Length Distribution method (CLD) [6].

This is also known as the Gilbert method [8,11], which has recently emerged as an effective method for calculation of C_s. It involves manipulation of the data obtained from GPC. The number distribution (N(M)) i.e. number of chains of molecular weight M is calculated, the natural logarithm of these values are then plotted against DP to give a slope (Λ). The chain transfer constant (C_s) is determined by plotting Λ for a series of experiments (as stated previously, with different catalyst concentrations), against [S]/[M], yielding a slope equal to C_s.

Recently a discussion has started in the literature with regard to which molecular weight region Λ should be determined [6,12,13] i.e., whether the slope should be determined in the high molecular weight region (Λ_{HIGH}), which is the correct theoretical limit [8] or in the region of the peak molecular weight (Λ_{PEAK}), which suffers from less experimental uncertainties [6]. Davis [12] found that Λ_{PEAK} results compared most favorably with the $2/DP_w$ results, the 2/DPw seems to be the preferred method of determination followed by the CLD procedure. The values are taken from numerous sets of data/repeat runs for each complex.

3.3. Chain transfer constants for cobalt (II) and cobalt (III) complexes in bulk MMA polymerisations at 60 °C.

The chain transfer constants for complexes I-XIII were evaluated for polymerisations of bulk MMA using AIBN as the thermal initiator at 60°C. Polymerisations were terminated after a period of 15 minutes in order to achieve low conversions of approximately 5%. Experimental conditions and molecular weight/conversion data are summarised in tables 3.1-3.6. The values are taken from numerous sets of data/repeat runs for each complex. Conversion data were obtained by drying a known mass of reaction mixture to constant weight in a vacuum oven.

3.3.1 The use of cobalt (II) complexes in bulk polymerisations with MMA at 60 °C.

The primary aim of this work was to investigate what effect the equatorial groups on the cobalt (II) complexes had on the chain transfer activity of the complexes [2]. It was also the intention to compare these values with the cobalt (III) analogues containing either pyridine or water as one axial ligand. Figure 3.1 gives the structure of the complexes used indicating the position of the axial ligands and their nature.

Figure 3.1. Structure of Cobalt (II) complexes.

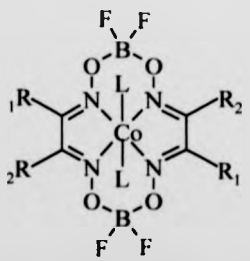

Where L = CH_3OH (I – IV), Ethyl acetate (V – VI), H_2O (VII)

Tables 3.1 and 3.2 give GPC and chain transfer values for complexes II-VII, the procedure used can be found in chapter 6, no data was obtained for complex I as it would not dissolve in monomer, water or any other solvent tried. Two different concentrations of CCTA/Monomer were used for complex III and two different purities of complex IV were used (crude and pure).

Table 3.1. Experimental and GPC information, for complexes II – VII.

Complex	[CCTA]/ [MMA] x 10^{-7} molar ratio	AIBN (moles) x 10^{-4}	*Mn*	*Mw*	Pdi	% Conv
II	0.0	1.52	194900	394400	2.02	5.94
	1.32	1.52	20360	42340	2.08	4.53
	2.65	1.52	11300	42020	3.71	4.62
	3.97	1.52	7700	37040	4.83	4.55
III	0.0	1.52	104400	255450	2.44	5.65
Conc^{n} set	0.654	1.52	99550	196830	1.97	5.65
1	1.31	1.52	61840	132600	2.14	5.63
	2.62	1.52	22530	63500	2.02	5.11
	5.23	1.52	16090	43620	2.71	4.87
III	0.0	1.52	178420	347100	1.94	5.66
Conc^{n} set	1.39	1.52	29340	68370	2.33	4.83
2	2.77	1.52	22970	56540	2.46	5.13
	4.16	1.52	17170	38370	2.23	4.86
	5.55	1.52	127410	25350	1.99	4.78
IV	0.0	1.53	115200	212360	1.84	5.09
Pure	0.558	1.53	27330	58650	2.14	4.21
	1.17	1.53	20920	44860	2.13	4.51
	2.35	1.53	11380	27210	2.39	3.63
	4.70	1.53	6400	22280	3.48	4.06

Table 3.1. Continued.

Complex	[CCTA]/ [MMA] x 10^{-7} molar ratio	AIBN (moles) x 10^{-4}	*Mn*	*Mw*	Pdi	% Conv
IV	0.00	1.55	135570	250050	1.84	7.17
Crude	0.748	1.55	55160	78600	1.42	6.36
	1.5	1.55	23700	56200	2.37	6.51
	2.99	1.55	21480	54300	2.52	5.76
	5.98	1.55	10950	27780	2.53	5.21
V	0.0	1.61	160900	292250	1.81	5.25
	0.891	1.61	109340	215650	1.97	4.98
	1.78	1.61	91960	178160	1.93	4.95
	2.67	1.61	85130	169160	1.97	4.94
	3.57	1.61	70300	146190	2.08	5.02
VI	0.0	1.62	204440	401550	1.96	5.54
	0.937	1.62	176390	342400	1.94	4.53
	1.87	1.62	114410	220820	1.93	5.02
	2.81	1.62	82580	155720	1.88	5.20
	3.75	1.62	60570	117140	1.93	4.98
VII	0.0	1.61	171750	361200	2.10	4.92
	0.69	1.61	143470	316080	2.20	4.83
	1.38	1.61	155160	292030	1.88	4.74
	2.76	1.61	137940	246560	1.78	5.56
	5.52	1.61	143980	383510	2.66	5.21

Table 3.1 shows that as the concentration of the chosen complex increases the molecular weight decreases, this is profound when comparing the control which contains no

complex with the second solution which in comparison to the other proceeding three contains the least.

Table 3.2 shows that the nature of the equatorial groups play an important role in the activity of the complexes at reducing molecular weight and hence the value of C_s for each. It is apparent from the data in table 3.2 and graphically in figure 3.2 that the C_s values for all complexes have decreased with an increase in carbons on the main skeletal carbon backbone when compared with the value obtained for CoBF, complex II. It is of course possible that catalyst purity plays an important role as the purity of the other complexes when compared to that of CoBF could differ considerably and that this could be a reason for the decrease in activity. It is also important to consider the role of isomerisation on the activity of the complex. This is important when one considers complex III as it is quite possible that there are two isomers present. The cis and trans conformations. It is quite possible that one isomer is an effective CCTA whilst the other is not. It was however not possible in this work to isolate the isomers. When one considers complexes V and VI independently of the other complexes it appears that this trend is not followed, it is in fact the opposite, i.e. an increase in C_s with an increase in skeletal backbone is observed. This could possibly be due to catalyst purity or the effect of the axial ligands which in this case are ethyl acetate for both, this is known from FAB-MS information. It is plausible that the nature of the withdrawing groups on the C=O group of the ligand destabilises the normally stabilised complex, and allows the cobalt carbon bond to break, subsequently the forming and breaking of the cobalt (III) alkyl allowing the CCT cycle to continue. It should also be noted that other factors such as

purity, isomerisation and presence of axial ligands could also affect chain transfer activity.

It is thought that the effect of methanol and water as axial ligands is minimal when comparing the C_s values for complexes II – IV and VII. Complex IV was used in two forms, crystalline (pure) and powder (crude). From table 3.2 it can be seen that there is a definite increase in C_s when the crystals are used indicating that purity affects catalytic activity and hence supporting the explanation for differences in C_s for the other complexes.

The general overall decrease in C_s when compared to complex II is considered to be due to either an increase in cross sectional area or the strength of the cobalt – polymer bond. It is possible that the latter being largely responsible for the catalytic activity as this bond must break to allow continuation of the cycle, its mobility (diffusion effect) will decrease with an increase in steric bulk. Haddleton et al [2] observed a decrease in C_s by increasing the bulkiness on the equatorial ligand. They also favour a reduction in mobility as an explanation for decreased activity.

The results in table 3.2 gives the C_s values for complexes II-VII. It should be noted that for complex III two different concentrations of complex were used. For complex IV two different purities were used, the crude and pure forms. The C_s values for complex VII involves data from two different plots, one using four out of five points and the other all five points, the purpose of the latter was to see what difference removal of a rogue point had on the overall chain transfer activity.

Table 3.2. Chain transfer constants for complexes II-VII

Complex	Cs Mayo	Error +/-	Cs 2/DPw	Error +/-	Cs CLD	Error +/-
II	31390	460	11125	4980	41210	23260
III						
Conc^n 1	11100	1600	7720	750	11500	400
Conc^{n}2	12370	1200	12200	1370		
IV						
Pure	30800	1200	16260	3220	30960	1340
Crude	13490	1580	9590	1450	-	-
V	2090	212	1830	190	-	-
VI	3170	400	3330	400	-	-
VII						
4 pts	420	240	920	40	-	-
5 pts	150	120	70	300	-	-

The results in table 3.2 also show that each method of determining C_s give slightly different values for each complex although they are reasonably close.

Figure 3.2. Mayo plot overlay for complexes II – VII.

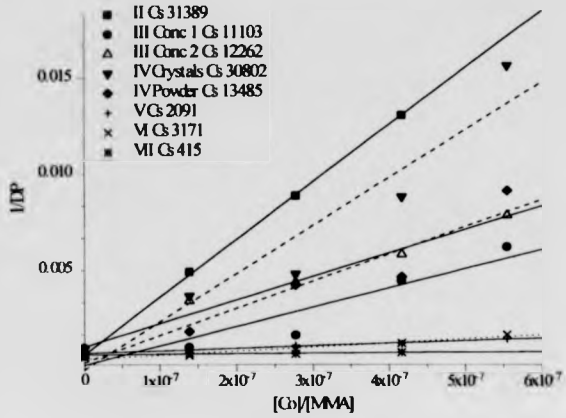

Figure 3.3. $2/DP_w$ overlay plot for complexes II – VII.

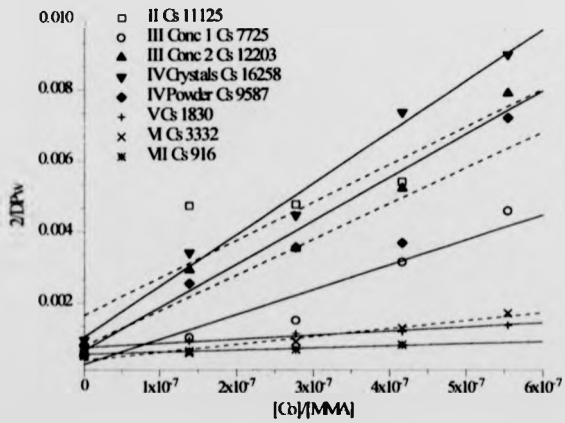

Figure 3.4. Plot of DP vs Ln(N(M)) for complex II.

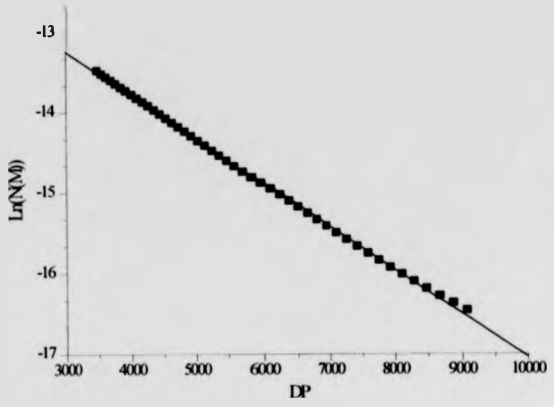

Figure 3.5. CLD plot for complex IV

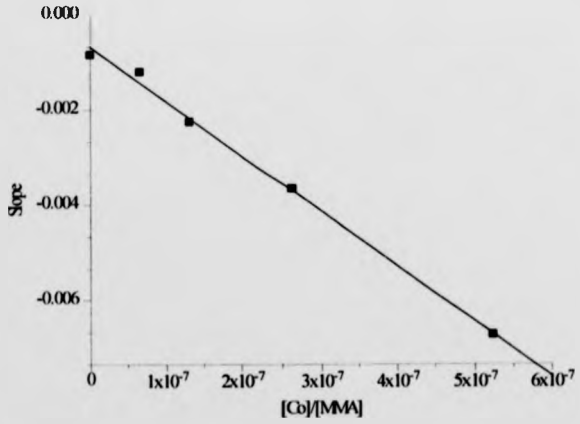

The plots in figures 3.2 – 3.4 shows linear behavior although some plots show more of a curve than linearity. They also highlight the differences of each method, although all three procedures utilise the concentration of complex/monomer as the x axis.

3.3.2. The use of cobalt (III) complexes in bulk polymerisations with MMA at 60 °C.

The aim here was to investigate what effect the axial base ligands had on the chain transfer constants obtained when two different axial base ligands are used, namely pyridine and water, see figure 3.6. This was of interest as it has been previously reported that different bases affect C_s [14]. The results obtained for these complexes would be compared to each other and also with the cobalt (II) analogues from 3.3.1.

Figure 3.6. Structure of cobalt (III) complexes.

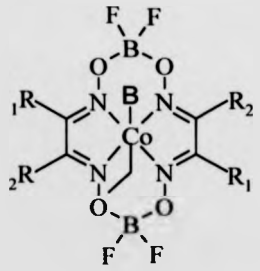

Where B= Pyridine or water

3.3.2.1. The use of cobalt (III) complexes utilising pyridine as one axial ligand in bulk polymerisations of MMA at 60 °C.

The aim here was to investigate what effect using a strong base, in this case pyridine, would have on the C_s activity of the cobalt complexes. The results obtained here would then be compared with those of both the cobalt (III) analogues containing water and also cobalt (II). For effective CCTP to occur the cobalt (III) complex must reduce to its cobalt (II) analogue. It is thought that a strong base hinders this. Table 3.3 gives GPC and experimental information for complexes VIII – X containing pyridine as the axial base ligand. The table shows that the complexes seem to be effective at reducing the molecular weights of the polymers formed if we again compare the control value with those of the solutions containing the complexes at increased concentrations.

Table 3.3. Experimental and GPC information for complexes VIII – X containing pyridine as an axial base ligand

Complex	[CCTA]/ [MMA] x 10^{-7} Molar ratio	AIBN (moles) x 10^{-4}	*Mn*	*Mw*	Pdi	% Conv
VIII	0.0	1.52	175630	283860	1.61	7.03
	1.08	1.52	32580	59530	1.83	6.07
	2.16	1.52	22630	40620	1.80	5.94
	3.24	1.52	20300	36960	1.82	4.01
	4.32	1.52	11360	20910	1.84	5.26

Table 3.3 continued.

Complex	[CCTA]/ [MMA] x 10^{-7} Molar ratio	AIBN (moles) x 10^{-4}	*Mn*	*Mw*	Pdi	% Conv
IX	0.0	1.52	191440	366460	1.91	5.27
	1.14	1.52	93210	177550	1.90	5.15
	2.28	1.52	69980	134710	1.92	5.02
	3.42	1.52	50700	99360	1.96	5.06
	4.57	1.52	41540	75410	1.81	5.03
X	0.0	1.52	262500	440160	1.67	5.33
	1.00	1.52	91170	177750	1.95	5.21
	2.01	1.52	47390	81890	1.72	4.79
	3.01	1.52	39890	68300	1.71	5.11
	4.01	1.52	26850	47900	1.78	4.75

From the results outlined in table 3.4 it can be seen that these values are considerably lower than those of the complexes cobalt (II) analogues. For cobalt (III) catalysts to be effective CCTA's they must be reduced to cobalt (II) at the beginning of the polymerisation process. This step involves cleavage of the cobalt–carbon bond from the ethyl group. It is thought that an increase in base strength leads to an increase in electron density around the cobalt center. This donation imparts a strengthening between the cobalt and the carbon on the ethyl group making this bond difficult to break, thus requiring more energy to break the bond [4,5]. This leads to a decrease in activity and therefore fewer re-initiation, propagation and termination steps are observed together with a reduction in C_s [14].

Table 3.4. Chain transfer constants for cobalt (III) complexes containing pyridine as one axial base ligand

Complex	Cs Mayo	Error +/-	Cs 2/DPw	Error +/-	Cs CLD	Error +/-
VIII	16970	2690	18310	2950	17360	2760
IX	4100	140	4470	230	4460	220
X	8090	620	9230	690	7490	740

Again the complex giving the highest C_s value in this section is the one containing the least number of carbons on the skeletal backbone (VIII), followed by the complex containing most carbons (X). All three methods of determination give similar values to each other for each complex and all give the highest value of C_s for complex VIII.

The plots in figures 3.7 – 3.8 illustrate graphically the values given in table 3.5, showing minimal error and linearity.

Isomerisation could be a possible explanation for the decrease in C_s for complex IX as there are 2 possible isomers cis and trans. It is plausible that one isomer is an effective CCTA whilst the other is not and that other factors such as purity could be influencing the C_s values obtained. During the CCTP process the substitution of the axial ligand by a new monomer molecule could also be limiting the complexes ability in performing CCT. Deviation from linearity was noted for some Mayo plots and this is indicative of some assumptions being broken which are made with respect to the way in which the Cs values are obtained. The deviations were also noted in other runs which utilised these complexes.

Figure 3.7. Overlay of complexes VIII – X, Mayo method.

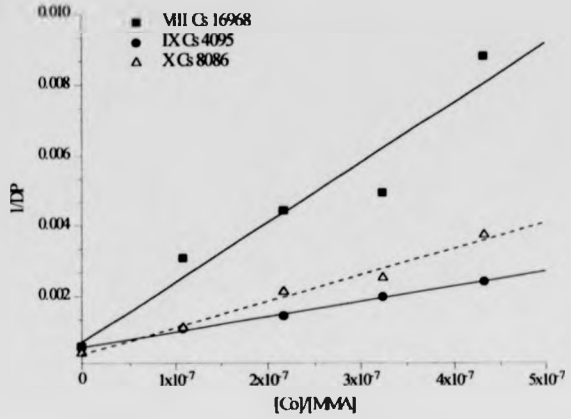

Figure 3.8. 2/DPw overlay plot for complexes VIII – X.

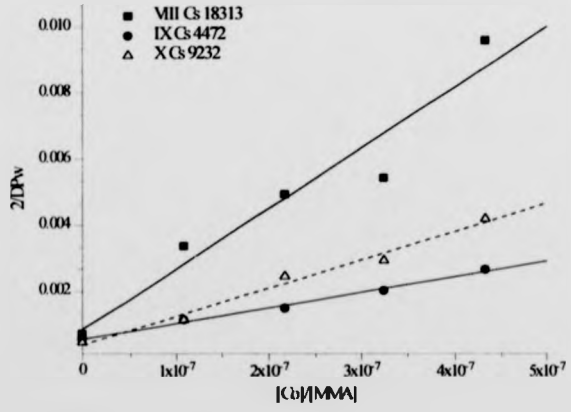

3.3.2.2. The use of cobalt (III) complexes containing water as an axial ligand in the bulk polymerisations with MMA at 60 °C.

The aim of this work was to evaluate what effect a weak base as an axial ligand had on the C_s values of the cobalt complexes. Again these were direct analogues of the pyridine containing systems with the exception that water was used instead of pyridine as one axial ligand. It was hoped that this ligand would give higher chain transfer activity than the cobalt–pyridine analogues and hence confirm that the nature of the axial ligand affects chain transfer activity and can therefore be used as a 'switch' to control CCTP. Table 3.5. gives GPC and experimental information for complexes XI – XIII containing water as the axial base ligand. The results in this table show that again reductions in molecular weight are observed when the cobalt complexes are used and that these reductions increase with an increase in cobalt concentration.

Table 3.5. Experimental and GPC information for complexes XI – XIII containing water as an axial ligand.

Complex	[CCTA]/ [MMA] x 10^{-7} Molar ratio	AIBN (moles) x 10^{-4}	*Mn*	*Mw*	Pdi	% Conv
XI	0.0	1.52	219030	490050	2.23	5.78
	1.38	1.52	23380	35740	1.52	5.10
	2.75	1.52	9520	16300	1.71	4.71
	4.13	1.52	8070	13100	1.62	4.63
	5.50	1.52	5520	9570	1.73	4.55

Table 3.5. Continued.

Complex	[CCTA]/ [MMA] x 10^{-7} Molar ratio	AIBN (moles) x 10^{-4}	*Mn*	*Mw*	Pdi	% Conv
XII	0.0	1.52	252030	384490	1.52	7.03
	1.29	1.52	52530	92130	1.75	6.19
	2.59	1.52	33880	57200	1.68	6.21
	3.88	1.52	19920	33220	1.66	5.44
	5.17	1.52	16290	26950	1.65	5.73
XIII	0.0	1.52	99170	208160	2.09	4.83
	1.22	1.52	23300	39490	1.69	4.59
	2.44	1.52	10390	18940	1.82	2.96
	3.66	1.52	6950	13250	1.90	4.27
	4.88	1.52	5270	10350	1.96	3.84

Table 3.6 gives the chain transfer constants for complexes XI – XIII. Again the complex containing the least number of equatorial carbons (XI) gives the highest C_s value followed by the one containing the most carbons (XIII). It is also interesting to note that the values obtained for all the cobalt (III) complexes containing water as the axial ligands give higher C_s values than those of the pyridine analogues. The water analogues also give very similar values to those obtained from the cobalt (II) complexes. This would therefore support the suggestion that the nature of the axial ligand can have a profound effect on its chain transfer activity. Water is a weak base and therefore imparts little if any effect on the cobalt-carbon bond. Again other factors to consider here for evalution

and conclusion of results for this set of CCTA's are purity isomerisation and the binding of monomer to the cobalt center.

Effective and non-effective isomers are a possible explanation for the lower values obtained for complex XII, one isomer (cis or trans) could be an effective CCTA whilst the other is not. Purity of the complex could be an important factor for the reason that any impurities which are present could hinder CCTA activity.

It should also be noted that the deviation from linearity for the Mayo plots are indicative of some assumptions being broken and hence the use of the line of best fit has been utilised where necessary. This deviation was also noted in the other repeat experiments for the complexes.

Table 3.6. Chain transfer constants for cobalt (III) complexes containing water as an axial base ligand.

Complex	Cs Mayo	Error +/-	Cs 2/DPw	Error +/-	Cs CLD	Error +/-
XI	31610	2450	36870	2130	38950	1350
XII	11300	630	13670	790	15600	380
XIII	37830	1440	38400	1000	45020	2070

The plots in figures 3.9 – 3.10 illustrate graphically the observations made from the table. Figure 3.11 illustrates an overlay of all the CLD values obtained for both the pyridine and water analogues and illustrates the differences in values between the pyridine and water analogues.

Figure 3.12 illustrates an example between the pyridine and water analogues for complexes IX and XII, again the water analogue gives the highest value and both behave linearly.

Figure 3.9. Mayo plot overlay for complexes XI – XIII.

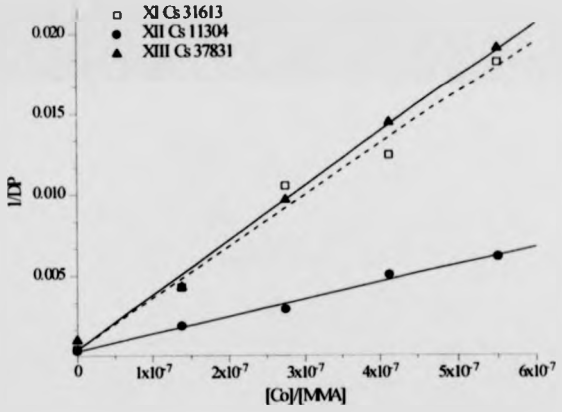

Figure 3.10. 2/DPw overlay for complexes XI – XIII.

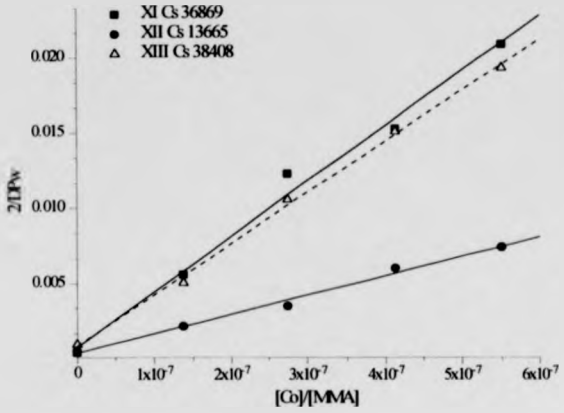

Figure 3.11. CLD plot overlay for complexes VIII - XIII.

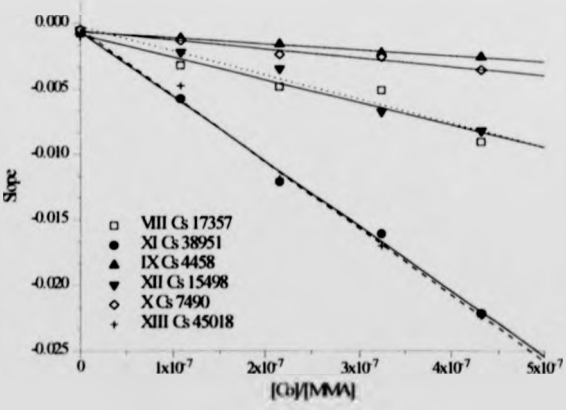

Figure 3.12. Mayo plot overlay for complexes IX (pyridine) and XII (water).

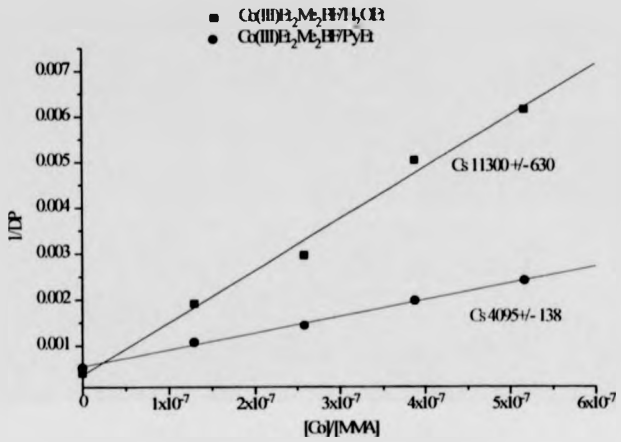

3.4. Effect of initiator concentration on chain transfer constants.

As stated earlier in this section it has been reported that CCT relies on a constant radical feed [4,5]. It was therefore interesting to observe the effect upon polymerisation when the initiator concentration was lowered from 5.2×10^{-4} to 10.1×10^{-6} moles.

Table 3.7 gives GPC and experimental data for complexes II – IV. The experimental procedure followed was that shown in Chapter 6. From table 3.7 it would appear that again a reduction in molecular weight is observed when the cobalt complexes are used, again an increase in molecular weight reduction is observed with an increase in cobalt concentration.

Table 3.7. GPC and experimental data for complexes II-IV with lower initiator concentrations.

Complex	[CCTA]/ [MMA] x 10^{-7} Molar ratio	AIBN (moles) x 10^{-4}	*Mn*	*Mw*	Pdi	% Conv
II	0.0	1.01	810790	1034600	1.27	1.77
	1.25	1.01	18040	34150	1.89	1.30
	2.50	1.01	14850	23110	1.55	1.19
	3.75	1.01	10210	15970	1.56	1.20
	5.0	1.01	8500	12160	1.43	1.32
III	0.0	1.02	1215570	805850	1.65	1.55
	1.66	1.02	20800	33920	1.63	1.19
	3.31	1.02	24220	41720	1.72	1.10
	4.97	1.02	20240	35980	1.77	1.20
	6.63	1.02	17520	30430	1.74	1.11
IV	0.0	0.97	717700	1332710	1.85	2.01
	1.02	0.97	87960	152680	1.73	1.73
	2.03	0.97	47250	78970	1.67	1.55
	3.05	0.97	38250	67600	1.76	1.57
	4.07	0.97	36760	54510	1.48	1.51

Table 3.8 gives the chain transfer values for complexes II – IV at reduced initiator concentration. It has previously been found that the rate of polymerisation in CCT is not dependant on the concentration of the CTA, but is dependant on initiator concentration, although an initial decrease in rate is observed on introduction of the CTA [15,16].

Hawthorne [17,18] reported that the rate of reaction in CCT in the absence of an external initiator source is very slow. This implies that an external source of free radicals is required to replenish the radicals lost from the CCT system. Davis et al [19] have also demonstrated Hawthorne's findings but have however found that this dependence is not substantial. When free radical initiators are introduced into a CCT system, they can directly initiate the polymer or they can react with the CTA to form a cobalt (III) alkyl, which then initiates the monomer.

The results shown here indicate that the value for C_s is decreased with a reduction in concentration of initiator and that the rate of reaction is also lowered. The latter is highlighted by comparison of the percentage conversions obtained for bulk polymerisations with low and high initiator concentrations, tables 3.7 and 3.1 respectively.

Table 3.8. Chain transfer constants for complexes II – IV at reduced initiator concentration.

Complex	Cs Mayo	Error +/-	Cs 2/DPw	Error +/-
II	22070	2910	31390	1860
III	6880	2880	7440	3540
IV	6530	1120	8560	920

Figure 3.13. Mayo plot overlay for low initiator concentration experiments II – IV.

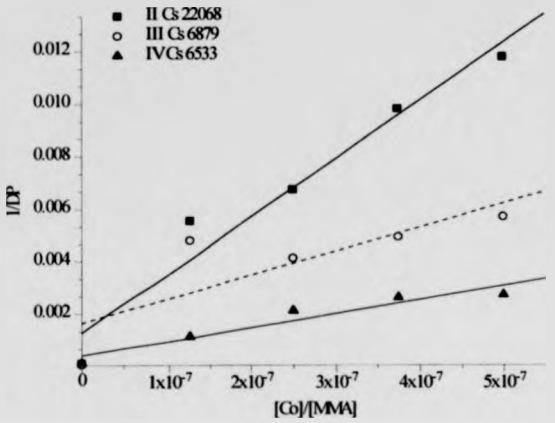

Figure 3.14. 2/DPw overlay for complexes II – IV with low initiator concentration.

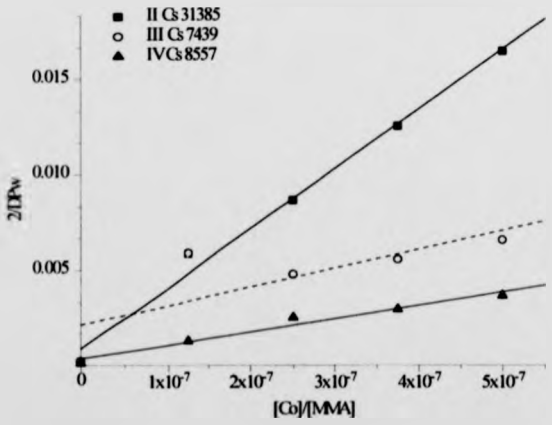

3.5. Conclusions.

From the results in this chapter it can be concluded that the structure of the complex plays an important role in its chain transfer activity. In particular from the results outlined in table 3.2 it is noted that the nature of the equatorial groups play an important role in the activity of the complexes at reducing molecular weight and hence the value of C_s for each. It is apparent from the data in table 3.2 that the C_s values for all complexes have decreased with an increase in carbons on the main skeletal carbon backbone when compared with the value obtained for CoBF, complex II. However, when one considers complexes V and VI independently of the others it appears that this trend is not followed. The general overall decrease in C_s when compared to complex II is considered to be due to either an increase in cross sectional area or the strength of the cobalt-polymer bond. The latter being largely responsible for the catalytic activity as this bond must break to allow continuation of the cycle, its mobility (diffusion effect) will decrease with an increase in steric bulk. Haddleton et al [2] observed a decrease in C_s by increasing the bulkiness on the equatorial ligand. They also favour a reduction in mobility as an explanation for decreased activity. It is also possible that the purity of the complexes are playing an important role in the activity. If there are impurities present then these could be reducing catalytic activity and hence catalytic activity decreases could be due to this. It should be noted that for complex III isomerisation could be detrimental to the catalytic activity of that complex. The two isomers being cis and trans in nature. It is plausible that one isomer might be an effective CTA whilst the other is not. It was however not possible to determine which isomer if both were present was the active one.

From the results outlined in tables 3.5 and 3.6 it can be seen that the complexes containing pyridine, see table 3.5, as the values obtained for the pyridine complexes (VIII – X) are roughly half to three quarters less than those for the corresponding water analogues (XI – XIII). Water, although a base is a weak base and therefore imparts little if any effect on the cobalt–carbon bond. This would explain the high C_s values obtained when compared to the pyridine analogues. It should also be noted that the C_s values obtained for the water analogues are very close to those obtained for the cobalt (II) analogues, see table 3.2. The effect of decreasing initiator concentration leads to a reduction in chain transfer activity. Other relevant factors which could play an important role for the C_s values obtained for complexes II-XIII are the presence of isomers, purity and the substitution of the axial ligands with monomer. It is also possible that these factors could be responsible for the C_s values obtained to a greater or lesser extent as previously discussed within the relevant sections of this chapter.

The range of C_s values obtained for each complex by each method of determination in particular with reference to the 2/DPw and CLD methods offer a wide range of molecular weights. The differing values could be attributable to wide PDi values indicating a wide range of molecular weight in particular with respect to low molecular weight. The presence of low molecular weight polymer on the GPC trace would cause some non-linearity for the CLD values and hence provide differing C_s values. The 2/DPw method is the most reliable when this is the case. It should also be noted that the linearity of some of the plots obtained for complexes II-XIII do not directly follow the Mayo assumption of a straight line. The curvature and hence lines of best fit are indicative of some of these assumptions being broken and this was evident in repeat experiments for

these complexes. From the data obtained it appears that the majority of methods for the determination of C_s agree well with each other, with the odd exception. The CLD values are larger than those of 2/DPw which lies in between those of the former and the Mayo method. This observation agrees well with previous workers observations [1,6-8,12,13,20].

3.6 References.

1) Heuts, J. P. A.; Forster, D. J.; Davis, T. P. ; *Macromolecules,* **1999**, *32*, 5514.

2) Haddleton, D. M.; Maloney, D. R.; Suddaby, K. G.; Muir, A. V. G.; Richards, S. N. ; *Macromol. Symp.*, **1996**, *111*, 37.

3) Gridnev, A. A.; Gonocharov, A. V.; Lampeka, Y. D.; Gavrish, S. P. ; *Teor. Eks. Khim.*, **1989**, *25*, 698.

4) Davis, T. P.; Haddleton, D. M.; Richards, S. N. ; *J. Macromol. Sci.,Rev. Macromol. Chem. Phys.*, **1994**, *C34*, 243.

5) Davis, T. P.; Kukulj, D.; Haddleton, D. M.; Maloney, D. R. ; *Trends in Polymer Science,* **1995**, *3*, 365.

6) Moad, G.; Moad, C. L. ; *Macromolecules,* **1996**, *29*, 7727.

7) Mayo, F. R. ; *J. Am. Chem. Soc,* **1943**, *65*, 2324.

8) Gilbert, R. G.; Clay, P. A. ; *Macromolecules,* **1995**, *28*, 552.

9) Stickler, M.; Meyerhoff, G. ; *Makromol. Chem.*, **1978**, *179*, 2729.

10) Olaj, O. F.; Zifferer, G.; Gleixner, G.; Stickler, M. ; *Eur. Polym. J.*, **1986**, *22*, 585.

11) Clay, P. A.; Gilbert, R. G. ; *Macromolecules.*, **1997**, *30*, 1935.

12) Heuts, J. P. A.; Kukulj, D.; Forster, D. J.; Davis, T. P. ; *Macromolecules,* **1998**, *31*, 2894.

13) Suddaby, K. G.; Maloney, D. R.; Haddleton, D. M. ; *Macromolecules,* **1997**, *30*, 702.

14) Moad, G.; Moad, C. L.; Krstina, J.; Rizzardo, E.; Thang, S.; Fryd, M. ; World Patent 96/15158, (**1996**).

15) Smirnov, R. R.; Morozova, I. S.; Marchenko, A. P. ; *Doklady Akademii Nauk SSSR,* **1980**, *253*, 891.

16) Mironychev, V. Y.; Mogilevich, M. M.; Smirnov, B. R.; Shapiro, Y.; Golikov, I. V. ; *Vysokomol Soyed,,* **1986**, *A28*, 1891.

17) Hawthorne, D. G. ; World Patent 87/03605, (**1987**).

18) Hawthorne, D. G. ; European Patent 0249614 A1, (**1992**).

19) Davis, T. P.; Kukujl, D.; Maxwell, I. A. ; *Macromol.Theory Simul.,* **1995**, *4*, 195.

20) Kukulj, D.; Heuts, J. P. A.; Davis, T. P. ; *Macromolecules,* **1998**, *31*, 6034.

Chapter 4

Bulk polymerisation of Styrene using CCTP with no external initiator and different temperatures.

4.0. Bulk polymerisation of styrene using CCTP with no external initiator and different temperatures.

4.1. Aim.

The aim of this work was to see how the chain transfer constants for complexes II-IV, VIII-XIII as described in chapter 3 varied for styrene. Styrene undergoes thermal initiation hence no external initiator is required. Different temperatures were investigated to see the temperature dependence of the chain transfer constants.

It was also interesting to directly compare the cobalt (II) and cobalt (III) water and pyridine analogues with each other. For example, it was interesting to see if the same trends observed in chapter three were observed for styrene, i.e. would cobalt (III) pyridine analogues give the lowest C_s values when directly compared to its cobalt (III) water and cobalt (II) analogues. It would also be interesting to see what relationship there was between C_s and the activation energy for transfer.

4.2. Introduction.

It is known from previous work that CCTP is reliant on a constant radical feed to replenish radicals consumed by radical-radical termination in order for an acceptable rate of polymerisation to be maintained. It has been reported that CCTP will still occur but at a slower rate when no external initiating source is used, the work reporting this observation used MMA and various other monomers[1-5]. No comparisons have been made between thermal radical initiator containing and initiator free systems and the effect temperature has on this. The work reported in this chapter has used styrene in the

presence of complexes reported in chapter 2, with no external radical source. Styrene undergoes thermal initiation by a Diels-Alder mechanism at elevated temperatures producing primary radicals which propagate and follow normal CCTP by chain transfer to cobalt. The mechanism of thermal self-initiation of styrene follows a Diels - Alder mechanism, which was proposed by Mayo [6,7] and has been confirmed by other investigations [8,9], see figure 4.1.

Figure 4.1. Mechanism of thermal self-initiation of styrene.

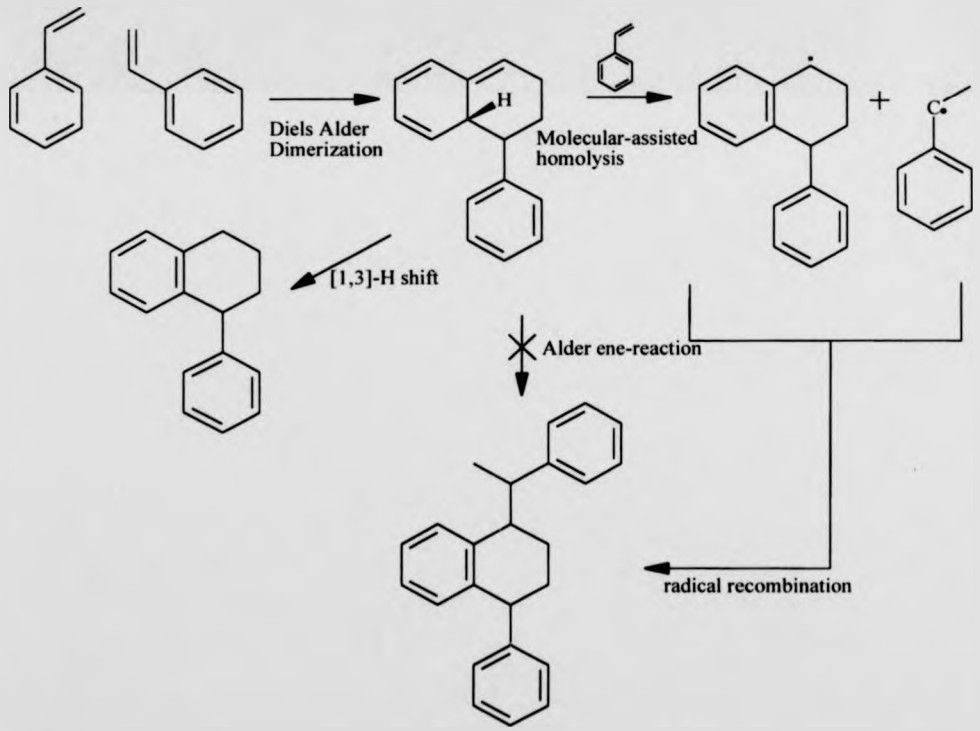

The temperature's used in the study were 80, 90, 100, 120 and 140 °C. Previous workers investigating temperature effects in order to determine thermodynamic parameters have reported two very different trends. O'Driscoll et al used MMA and found that C_s was temperature dependant, however Haddleton and Davis have both found independently using a wider range of temperatures (50,60, and 70 °C Haddleton and 40, 50, 60 and 70 °C Davis) and also reanalysis of O'Driscolls' data using various monomers including MMA that C_s is not dependant on temperature. Although none of the previous studies have used styrene it would be expected that the C_s values will also be temperature independent. However if one ignores these observations and studies the thermodynamics and kinetics of the reaction one would assume that as temperature is increased the thermal initiation of styrene would increase leading to an increase in C_s

This study will enable the calculation of the activation energies for transfer for each complex. This is of special interest with respect to the cobalt (III) systems as it is presumed that the pyridine cobalt (III) analogues will give the highest value for the activation energy of transfer owing to the strength of the pyridine ligand. This strength will impart a decrease in activity and mobility to undergo effective CCTP and produce low molecular weight polymers. Work reported in chapter 3, showed that for MMA bulk polymerisations, the chain transfer constants for the pyridine complexed cobalt (III) complexes exhibit a lower value for C_s than those containing water or for the cobalt (II) analogues. It was assumed that this is attributable to the pyridine imparting a strengthening to the Co-C bond making the dissociation of this bond harder than that of water.

4.3. Results.

The chain transfer constants for complexes II – IV and VIII – XIII were evaluated for polymerisations of styrene in bulk in the absence of thermal initiator. Polymerisations were terminated at appropriate times depending on the temperature used, table 4.1. Experimental conditions and molecular weight/conversion data is reported in appendix 3, together with chain transfer constants. Conversions were obtained by gravimetry. The values contained in this chapter are samples of the repeat runs obtained for each complex at each temperature.

Table 4.1. Time and temperature information for bulk polymerisation in styrene, using complexes II-IV and VIII – XIII.

Temperature, °C	80/90	100	120	140
Time (mins)	60	45	30	15

4.3.1. Temperature dependence of catalytic chain transfer of styrene by cobalt (II) complexes – an investigation into complex structure and the effect of temperature.

This work was carried out to investigate the effect of the equatorial alkyl groups on the chain transfer constant, figure 4.2, and to determine the effect of temperature had on C_s for these compounds. It was also interesting to see whether the trend reported in chapter three, was reproduced, i.e., whether an increase in skeletal carbons causes a decrease in chain transfer activity. The molecular weight and conversion data for these complexes can be found in appendix 3, tables 1-3 respectively.

Figure 4.2. Structure of cobalt (II) complexes.

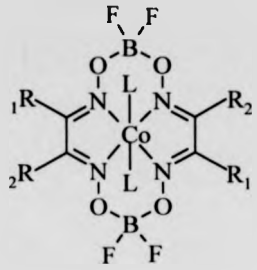

Where $R_1 + R_2 = CH_3$ (Complex II) L = CH_3OH

$R_1 = CH_3$ and $R_2 = CH_2CH_3$ (Complex III) L = CH_3OH

$R_1 + R_2 = CH_2CH_3$ (Complex IV) L = CH_3OH.

Table 4.2 gives C_s values for complexes II-IV using the Mayo, 2/DPw and CLD methods of determination so as to compare methods, effect of temperature and complex structure on the chain transfer constant values. Values are also illustrated graphically in figures 4.3 – 4.11.

From the results obtained for complexes II – IV it would appear that there is no change in C_s with an increase in temperature. It is also apparent that the trend observed in chapter 3 is also observed here, increasing the skeletal carbon's decreases the value of C_s. The observation that C_s is not temperature dependant agrees with the observations of both Haddleton [10] and Davis [11]. The values here are considerably lower with styrene than those obtained with MMA, also agreeing with previous workers. Another possible factor for complex III is the effect of isomerisation since there are two possible isomers cis and trans. It is quite possible for both isomers to have been synthesised and that both would therefore participate in the reaction with this in mind it is therefore plausible that the one

isomer is an effective CCTA whilst the other is not. It was however not possible during this work to isolate either and determine this. Another factor which could affect Cs values are the purity of the CCTA. Results in Chapter 3 for complex IV would suggest that purity affects Cs. With this in mind it is important to consider that likewise for other complexes and monomers the Cs values obtained could be reduced or increased owing to CTA purity. From the plots obtained for complexes II-IV some non-linearity is observed indicative of some assumptions being broken with regard to Mayo assumptions.

Styrene gives a lower C_s value than MMA in CCTP under identical conditions owing to the unlikely formation of an internal double bond on the styrene polymer and also the formation of secondary radicals in styrene are more stable than the tertiary radicals formed in MMA [12]. The cobalt -styrene bond is a lot stronger than the Co-MMA bond and therefore transfer in styrene is limited owing to the bond strength. Styrene also complexes directly to the cobalt center where one of the ligands has broken off at the beginning of CCTP. With regard to an increase in skeletal carbons leading to a decrease in C_s, the decrease in activity is probably attributable to an increase in electron density around the cobalt. The crowding must strengthen the Co-C bond and make the dissociation of this bond harder, this results in more energy being required to break the bond and therefore a slowing in the CCTP process and a decrease in the chain transfer constant is observed. It is interesting to note that the trend is complex II > IV > III, which is identical to the trend in chapter three. The methods used to obtain the C_s values also give slightly different values. Haddleton [10] postulated that that the bulkiness of the equatorial groups can affect the mobility owing to the strength of the cobalt polymer bond and hence affect the chain transfer constant value obtained as this bond must break

to allow continuation of the CCTP cycle. The CLD values obtained throughout this chapter are significantly lower than the other two procedure values. This could be due to the pattern of the GPC trace as linearity was a problem in calculating C_s via this procedure, owing to the presence of low molecular weight polymer present in the trace. Also the CLD values could be lower owing to the possibility that the polymerisations are not dominated by chain transfer.

The Mayo, CLD and 2/DPw values vary considerably when compared to each other. As stated previously some non linearity is observed in the plots indicating some deviation from the Mayo ideal. The PDi values are varied and sometimes wide indicating a variation in molecular weight. Reliable C_s values are obtained with narrow PDi and this may be a contributing factor to explain the wide range of C_s values.

Table 4.2. Chain transfer constants for complexes II-IV.

Complex + Temp °C	Mayo	Error +/-	2/DPw	Error +/-	CLD	Error +/-
II						
90	2080	719	2370	408	35	10
120	2810	444	1560	207	850	113
140	3140	390	2570	476	755	1382
III						
80	230	12.0	220	8.0	200	39.0
100	270	36	230	12	210	19
120	140	7.00	76	5	34	4
140	220	45	157	35	96	70
IV						
90	65	69	77	45	65	35
100	450	130	190	60	110	30
120	320	65	270	55	130	20
140	270	40	150	40	70	10

4.3.1.1.Temperature dependence of CCT with complex II in the bulk polymerisation of styrene.

Figures 4.3 – 4.5 shows no temperature dependence on C_s.

The results obtained by a Mayo plot give higher chain transfer constant values than those determined by the methods of 2/DPw and CLD procedures, the latter giving much lower values. The Mayo plots in figure 4.3 however show that there is a temperature dependence which is not noted by the other two procedures. The discrimination between values in for each procedure combined with the observation by the Mayo procedure of temperature dependence for C_s highlights the importance of using more than one procedure to obtain data to evaluate trends and values.

Figure 4.3. Mayo plot overlay for the CCTP of styrene with complex II in the absence of solvent and initiator at 90, 120 and 140°C.

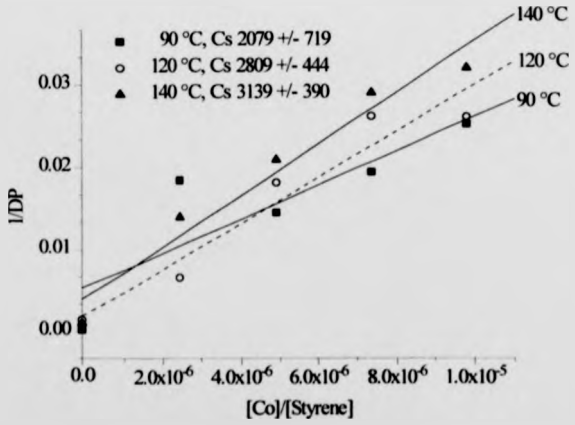

The Mayo plots in figure 4.3 behave linearly and fit well with the linear regressions with minimal errors, giving a maximum C_s value of 3139 at 140°C.

Figure 4.4. 2/DPw overlay for the CCTP of styrene with complex II in the absence of solvent and initiator at 90, 120 and 140°C.

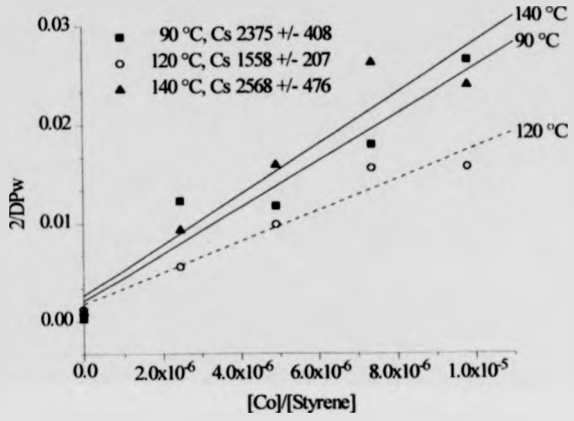

Figure 4.5. CLD overlay for the CCTP of styrene using complex II in the absence of solvent and initiator at 90, 120 and 140°C.

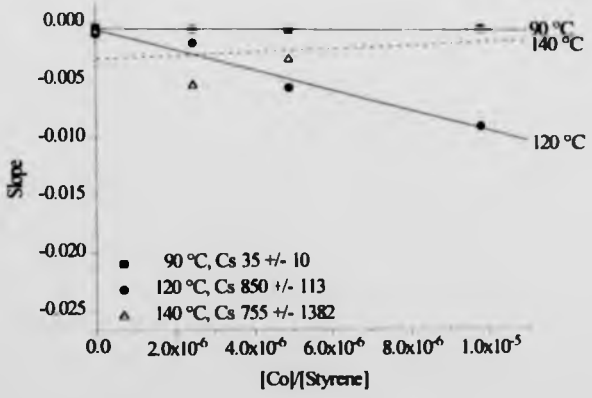

The CLD values are significantly lower than those of both 2/DPw, figure 4.4, and the Mayo procedure, figure 4.3. Again the plots for the 2/DPw and CLD procedures behave linearly and minimal error is observed. The highest C_s value given from the 2/DPw plot is 2570 at 140 °C whilst the highest value from the CLD plot is 850 at 120 °C.

4.3.1.2. Temperature dependence of CCT with complex III in the bulk polymerisation of styrene.

The values given in table 4.2 and illustrated in figures 4.6 – 4.8, for complex III again illustrate temperature independence at chain transfer. Again the Mayo plots give higher values than the other two procedures, followed by 2/DPw and then CLD.

Figure 4.6. Mayo plot for the CCTP of styrene with complex III in the absence of solvent and initiator at 80, 100, 120 and 140°C.

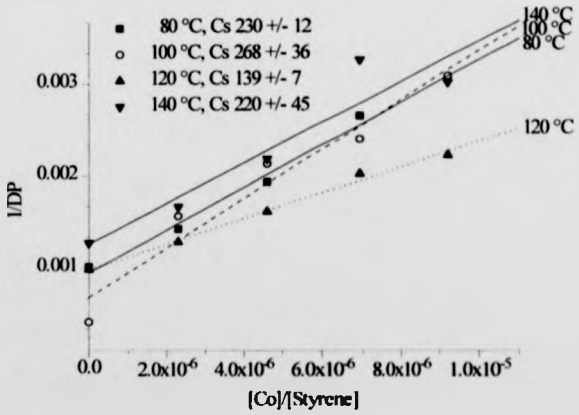

The Mayo plots in figure 4.6 follow linearity with minimal error giving a maximum C_s value of 268 at 100°C.

Figure 4.7. 2/DPw plot for the CCTP of styrene with complex III in the absence of solvent and initiator at 80, 100, 120 and 140°C.

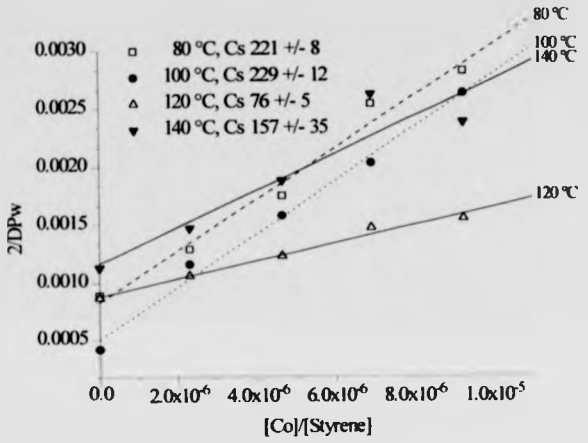

Figure 4.8. CLD overlay for the CCTP with styrene with complex III in the absence of solvent and initiator at 80, 100, 120 and 140°C.

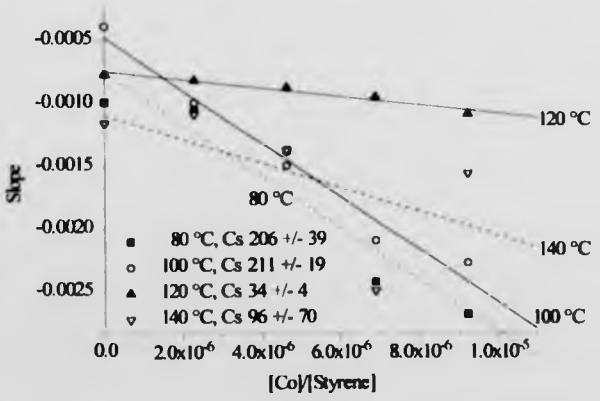

The 2/DPw plots in figure 4.7 behave linearly with minimal error however, the CLD plots in figure 4.8 do not although, values from both give some similar values. The highest C_s value given from the 2/DPw plots is 229 at 100°C, whilst the maximum value obtained from the CLD plots is 211 at 100°C.

4.3.1.3. CCT of styrene by complex IV in the absence of solvent and initiator.

The values of chain transfer reported in table 4.2 for complex IV show that the chain transfer values are not temperature dependant. The Mayo procedure appears to give the highest C_s values at all temperatures with good plots obtained. The maximum C_s value of 449 was found at 100°C.

Figure 4.9. Mayo plot overlay for the CCTP of styrene with complex IV in the absence of external initiator and solvent at 80, 100, 120 and 140°C.

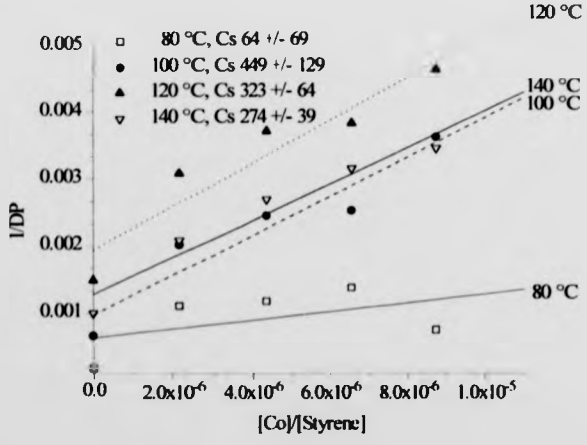

Figure 4.10. 2/DPw overlay for the CCTP of styrene with complex IV in the absence of solvent and external initiator at 80, 100, 120 and 140°C.

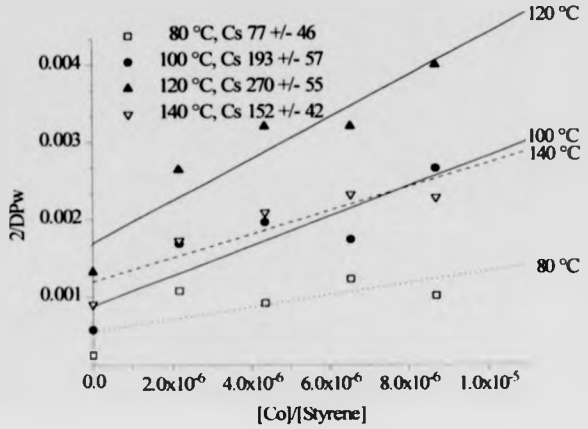

From the overlays in figure 4.10 the highest C_s value of 270 coincides with 120°C, although it should be noted that there is scatter on all plots.

Figure 4.11. CLD overlay for the CCTP of styrene with complex IV in the absence of solvent and initiator at 80, 100, 120 and 140°C.

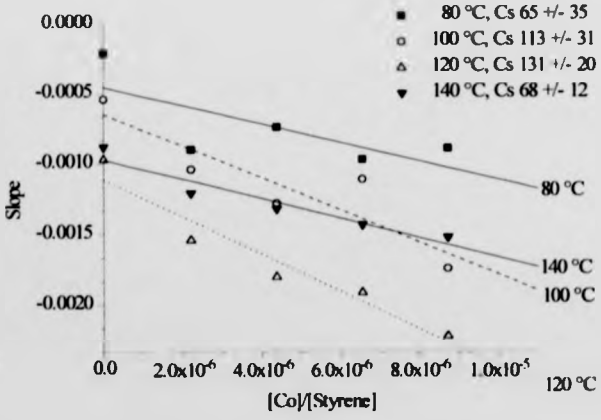

The CLD plots in figure 4.11 show linearity with minimal error, giving a maximum C_s of 131 at 120°C.

4.3.2. CCT of styrene in the absence of solvent by cobalt (III) complexes with pyridine as the equatorial ligand - an investigation into complex structure including the nature of the axial ligand and the effect of temperature.

The purpose of this work was to investigate the effect of the pyridine axial ligand on the chain transfer constant as compared to cobalt (II) and cobalt (III) (water) analogues. This was to investigate any temperature dependence effects. It was also interesting to see whether the combined effect of increased skeletal carbons and pyridine would strengthen or weaken the cobalt carbon bond and compare both with cobalt (II) and cobalt (III) water axial analogues, see figure 4.12.

Tables 4 - 6 in appendix 3 give molecular weight and conversion data for complexes VIII – X containing pyridine as one of the axial ligands.

Figure 4.12. Structure of cobalt (III) complexes containing pyridine as the axial base ligand.

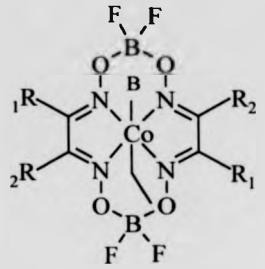

Where B= pyridine and

$R_1+R_2 = CH_3$ (Complex VIII)

$R_1 = CH_3$, $R_2 = CH_2CH_3$ (Complex IX)

$R_1 + R_2 = CH_2CH_3$ (Complex X).

Table 4.3 gives C_s values for complexes VIII - X using the Mayo, 2/DPw and CLD methods of determination, effect of temperature and complex structure on the chain transfer constant values.

Both figures 4.23 and 4.24 show that complex VIII, which contains the least number of carbons gives the highest C_s value, followed by complex X and then complex IX in agreement with earlier work. This is also the overall trend observed for this series of catalysts, i.e. the less sterically hindered - complex VIII gives the highest value followed by complex X,- symmetrical equatorial ligands and then the unsymmetrical complex IX. This trend was also observed in Chapter three for cobalt (II) complexes II-IV. A factor to consider when commenting on C_s values is the purity of the complex. Results for complex IV in chapter 3 would indicate that complex purity plays an important role. It is

therefore important to remember this factor when comparing C_s values as the relative purities of the other complexes is varied. When complex IX is considered it is important to take into account the possible presence of both cis and trans isomers as only one of the isomers may be effective as a CCTA. Once again the CLD procedure gives the lowest values for C_s, again this could be attributable to the fact that the system is not dominated by chain transfer. PDi values obtained vary greatly and the linearity of some plots is varied. The non linear behavior suggests deviation from the assumptions of Mayo. The combination of PDi and deviation from linearity could therefore pose an explanation for the variation in C_s values. When considering complexes VIII-X one must take into account the presence of different axial ligands. X-ray crystal data and NMR data suggest the presence of pyridine and ethyl axial ligands prior to the insertion of the complexes into the CCTP system. However, one must consider the possibility that during polymerisation axial ligands could be replaced by monomer in both axial positions this could lead to a decrease in activity.

Table 4.3. Chain transfer constants for complexes VIII – X in the polymerisation of styrene.

Complex + Temp °C	Mayo	Error	2/DPw	Error	CLD	Error
VIII 80	3080	443	2990	339	2210	377
100	4990	1190	1370	235	771	290
120	2450	235	1400	267	164	310
140	3530	470	2680	290	460	50
IX						
80	50	15	40	14	30	20
100	100	20	90	14	60	8
120	180	30	190	30	160	30
140	160	9	160	10	135	20
X						
80	710	80	610	80	450	100
100	450	130	550	55	360	60
120	870	120	600	50	570	25
140	700	50	630	25	485	43

4.3.2.1.CCTP of styrene with complex VIII in the absence of solvent and initiator.

Figure 4.13 – 4.15 show Mayo, 2/DPw and CLD plots respectively, for the polymerisation of styrene with complex VIII as the chain transfer agent.

Figure 4.13. Mayo overlay for the CCTP of styrene complex VIII in the absence of initiator and solvent at 80, 100, 120 and 140°C.

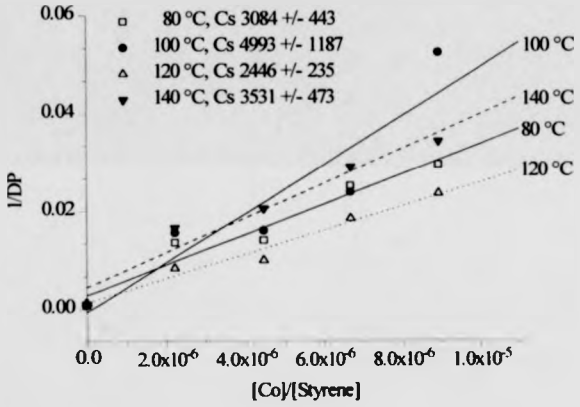

Temperatures shown in figure 4.13 give linear plots with a maximum C_s value of 4990 at 100°C.

Figure 4.14. 2/DPw overlay for the CCTP of styrene with complex VIII in the absence of initiator and solvent at 80, 100, 120 and 140°C.

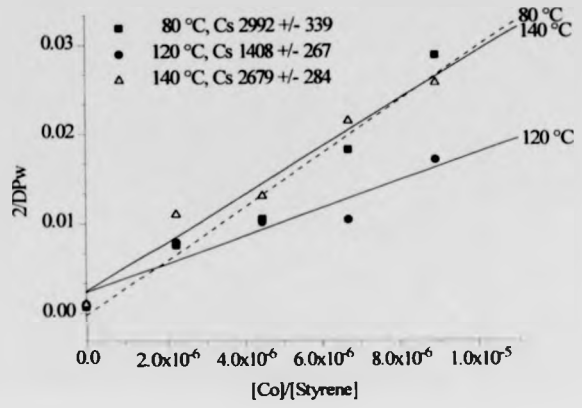

Figure 4.15. CLD overlay for the CCTP of styrene with complex VIII in the absence of solvent and initiator at 80, 100, 120 and 140°C.

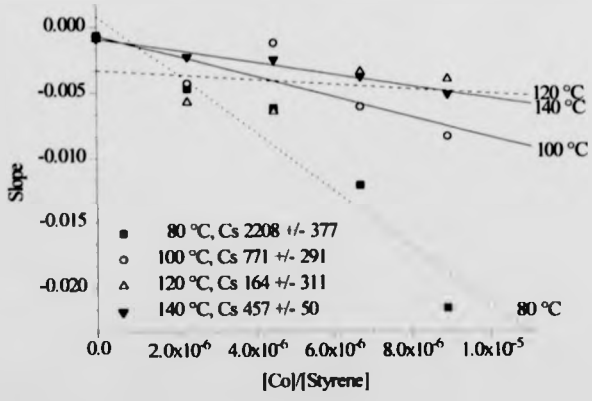

The 2/DPw plots in figure 4.14 giving a maximum C_s value of 2990 at 80° C. The CLD plots in figure 4.15 gives a C_s of 2210 at 80°C.

4.3.2.2. CCTP of styrene with complex IX in the absence of initiator and solvent.

The results reported in table 4.3 and in figures 4.16 - 4.18 show no temperature dependence on C_s. Again the Mayo method gives higher values than those of the 2/DPw and CLD procedures. As can be seen in figure 4.16 the Mayo plots are all relatively linear, with a maximum C_s value of 180 at 120°C.

Figure 4.16. Mayo plot overlay for the CCTP of styrene with complex IX in the absence of solvent and initiator at 80, 100, 120 and 140°C.

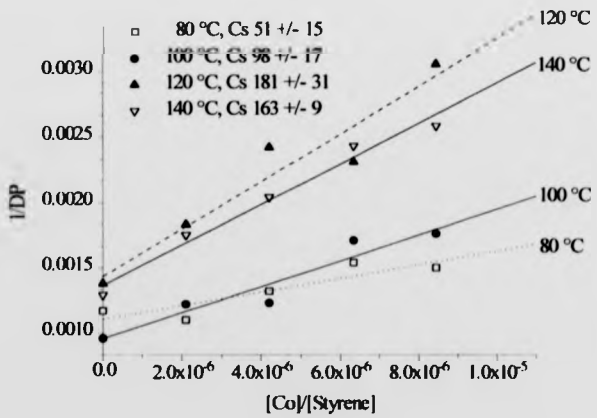

Figure 4.17. 2/DPw overlay for the CCTP of styrene with complex IX in the absence of initiator and solvent at 80, 100, 120 and 140°C.

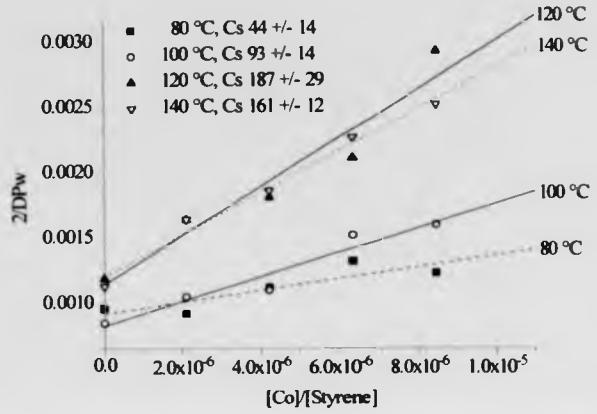

Figure 4.18. CLD overlay for the CCTP of styrene with complex IX in the absence of solvent and initiator at 80, 100, 120 and 140°C.

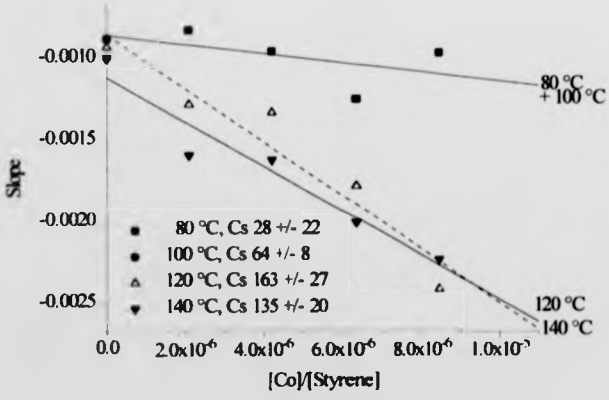

Again the 2/DPw and CLD plots, figure 4.17 and 4.18 respectively exhibit linearity with the 2/DPw method giving a maximum C_s value of 187 at 120 °C and the CLD method giving a maximum C_s value of 163 at 120°C.

4.3.2.3. Catalytic chain transfer of styrene with complex X in the absence of solvent and initiator.

The results in table 4.3 and in figures 4.19 - 4.21 indicate that there is no temperature dependence on C_s. Again the Mayo method generally gives higher values than those of the 2/DPw and CLD procedures.

Figure 4.19. Mayo overlay for the CCTP of styrene with complex X in the absence of initiator and solvent at 80, 100, 120 and 140°C.

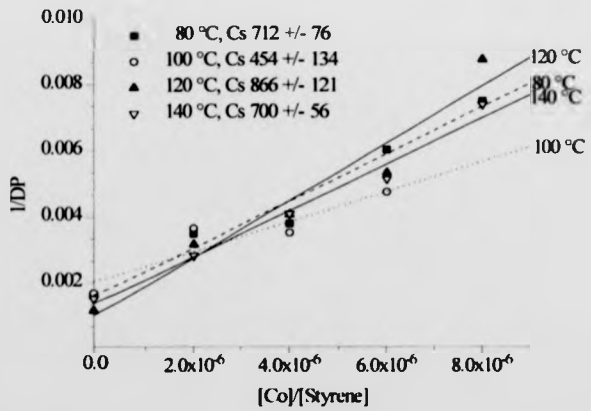

The Mayo plots in figure 4.19 are relatively linear with a C_s value of 866 at 120°C.

Figure 4.20. 2/DPw overlay for the CCTP of styrene with complex X in the absence of initiator and solvent at 80, 100, 120 and 140°C.

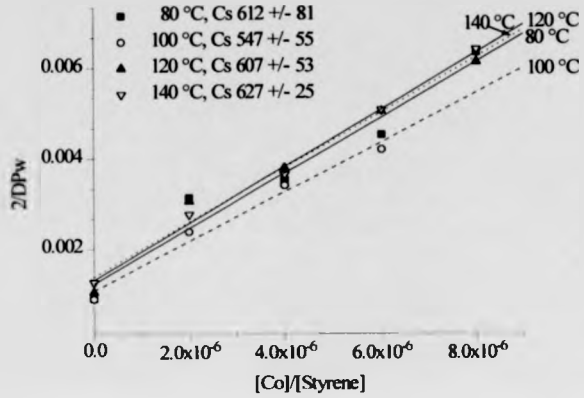

The 2/DPw plots in figure 4.20 giving a maximum C_s of 627 at 140°C the CLD plots in figure 4.21 over-page also give linear plots with a maximum C_s of 569 at 120 °C.
The Mayo and 2/DPw values for C_s at most temperatures are relatively close indicating little error and that both groups of results can be considered reliable when compared to each other.

Figure 4.21. CLD overlay for the CCTP of styrene with complex X in the absence of initiator and solvent.

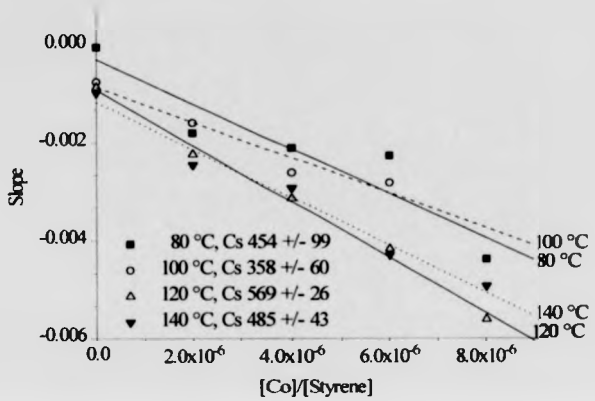

4.3.3. The CCTP of styrene using cobalt (III) complexes containing water as an equatorial ligand in the absence of solvent and initiator – an investigation into complex structure, in particular the effect of the axial ligand and the effect of temperature.

The purpose of this work was to investigate what effect water as the axial ligand had on the chain transfer constant and to see whether an increase in temperature would increase the complexes activity. The other purpose was to see whether the combined effect of increased skeletal carbons and water would strengthen or weaken the cobalt carbon bond and compare these results with both the cobalt (II) cobalt (III) pyridine axial analogues, see figure 4.2.2.

Figure 4.22. Structure of cobalt (III) complexes containing water as a base ligand.

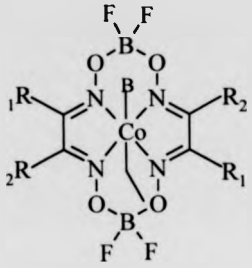

Where B= water and

$R_1+R_2 = CH_3$ (Complex VIII)

$R_1 = CH_3$, $R_2 = CH_2CH_3$ (Complex IX)

$R_1 + R_2 = CH_2CH_3$ (Complex X).

Tables 7 - 9 in appendix 3 give molecular weight and conversion data for the CCTP of styrene using complexes XI – XIII containing water as one of the axial ligands. Again the same temperatures and times were used as for the previous complexes. Table 4.4 gives C_s values for complexes XI - XIII using the Mayo, 2/DPw and CLD methods of determination in order to compare methods, effect of temperature and complex structure on the chain transfer constant values. Again the trend of least sterically hindered complex giving the highest C_s value is once again observed. This is the same trend as has been observed for chapter three and in the previous sections of this chapter. It is also important to consider other factors which could be affecting the C_s values obtained. CCTA purity as mentioned in earlier sections could be playing an important role than previously considered. Isomerisation is also a potential source of reduced catalytic activity in

complex XII where both cis and trans isomers are possible and potentially only one of the isomers is effective as the CCTA. Axial ligand exchange with monomer during the polymerisation process is also a possible factor leading to reduced C_s activity and this factor should also be taken into consideration. There is also no temperature dependence and the Mayo method of determination for C_s gives consistently the highest values when compared to the other methods of determination. From the C_s data obtained it is evident that the 3 different methods for obtaining C_s show some variation. This could be due in part to large PDi values and non-linearity in the Mayo plots. The combination of these factors could possibly account for variation in obtained C_s values.

Table 4.4. Chain transfer constants for complexes XI – XIII.

Complex + Temp°C	Mayo	Error	2/DPw	Error	CLD	Error
XI 80	3490	260	3370	210	2875	630
100	2460	410	1530	540	690	310
120	2880	270	2420	190	720	210
140	2180	420	1540	590	380	400
XII						
80	1180	110	900	80	530	140
100	1480	300	500	150	330	120
120	1390	300	1230	170	1130	90
140	1690	260	1180	290	730	720
XIII						
80	1300	90	920	50	470	70
100	1130	270	440	120	280	110
120	650	300	440	280	480	240
140	1090	180	480	90	180	80

4.3.3.1 The catalytic chain transfer polymerisation of styrene using complex XI in the absence of initiator and solvent.

It would appear that from the results in table 4.4 and illustrated in figures 4.23 - 4.25, there is no connection between temperature increase and an increase in C_s. C_s is independent of temperature. Again the Mayo method gives higher values than those of the 2/DPw and CLD procedures. Figure 4.23 gives results obtained from the Mayo procedure at all temperatures.

Figure 4.23. Mayo plot overlay for the CCTP of styrene with complex XI in the absence of initiator and solvent at 80, 100, 120 and 140°C.

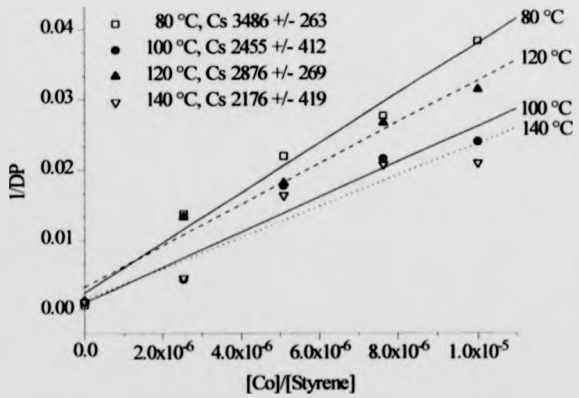

The Mayo plots in figure 4.23 behave linearly with minimal error, giving a maximum value for C_s of 3490 at 80°C.

Figure 4.24. 2/DPw overlay for the CCTP of styrene using complex XI in the absence of both initiator and solvent at 80, 100, 120 and 140°C.

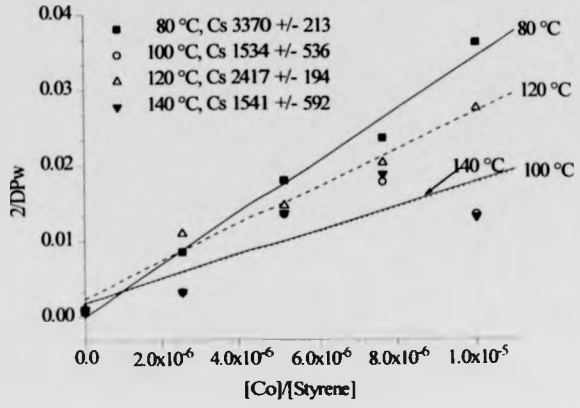

Figure 4.25. CLD overlay for the CCTP of styrene using complex XI in the absence of initiator and solvent at 80, 100, 120 and 140°C.

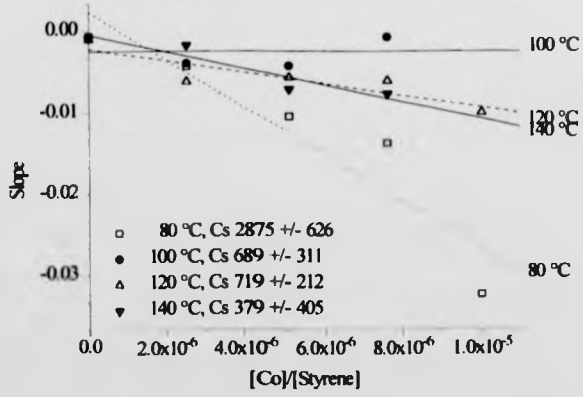

From the 2/DPw overlays in figure 4.24 A maximum value for C_s of 3370 is given corresponding to 80 °C. The CLD overlays in figure 4.25 give a maximum C_s value of 2875 at 80°C.

4.3.3.2 Catalytic chain transfer of styrene using of complex XII as the chain transfer agent in the absence of solvent and initiator.

It would appear that from the results in table 4.4 and illustrated graphically in figures 4.26 - 4.28 that values for C_s are independent of temperature. Again the Mayo method gives higher values than those of the 2/DPw and CLD procedures. Figure 4.26 gives results from the Mayo procedure at all temperatures.

Figure 4.26. Mayo overlay for the CCTP of styrene using complex XII in the absence of solvent and initiator at 80, 100, 120 and 140°C.

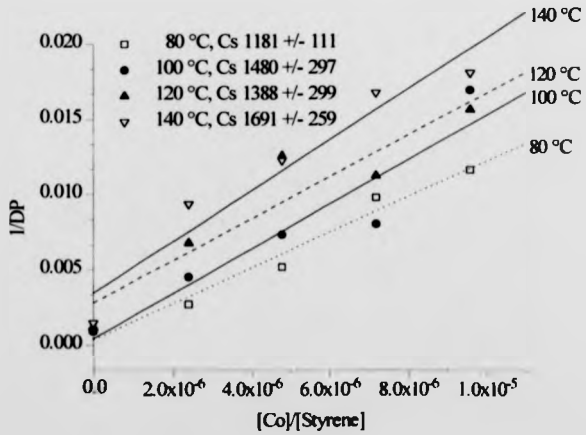

From the overlay in figure 4.26 it would appear that there is some scatter, however a maximum value for C_s of 1690 was found at 140°C.

Figure 4.27. 2/DPw overlay for the CCTP of styrene using complex XII in the absence of solvent and initiator at 80, 100, 120 and 140°C.

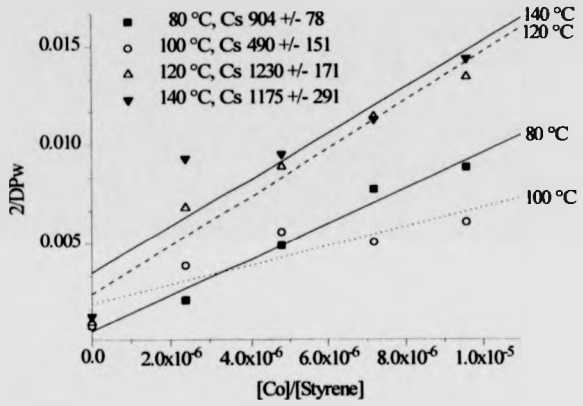

From figure 4.27 a maximum C_s of 1230 at 120°C was found.

Figure 4.28. CLD overlay for the CCTP of styrene using complex XII in the absence of solvent and initiator at 80, 100, 120 and 140°C.

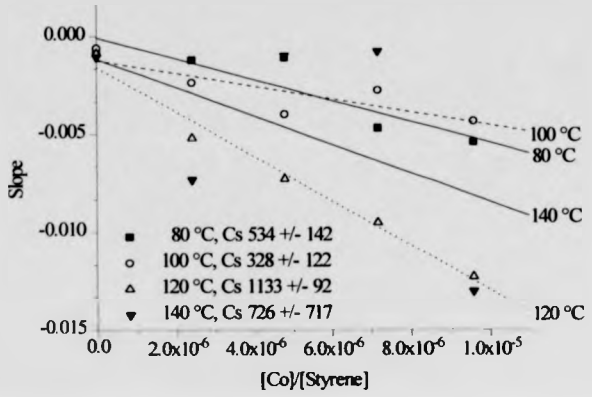

From the CLD overlays in figure 4.28 linear plots are observed giving a maximum C_s value of 1130 at 120°C.

4.3.3.3 The catalytic chain transfer polymerisation of styrene using of complex XIII in the absence of solvent and initiator.

It would appear that from the results in table 4.4 there is no connection between temperature increase and an increase in C_s. C_s is independent of temperature. Again the Mayo method gives higher values than those of the 2/DPw and CLD procedures. Figure 4.29 gives results from the Mayo procedure at all temperatures.

Figure 4.29. Mayo plot overlay for the CCT polymerisation of styrene using complex XIII at 80, 100, 120 and 140°C.

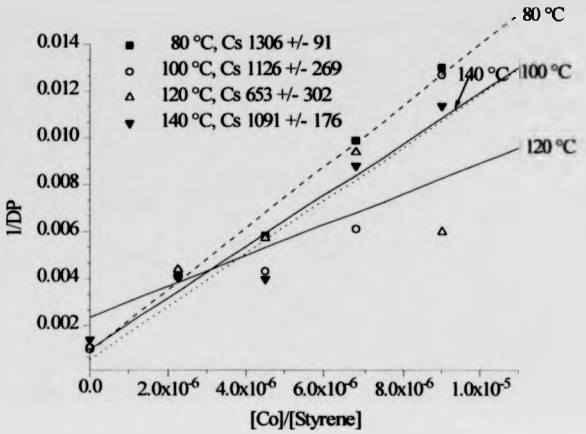

Figure 4.30. 2/DPw overlay for CCT polymerisation of styrene using complex XIII in the absence of solvent and initiator at 80, 100, 120 and 140°C.

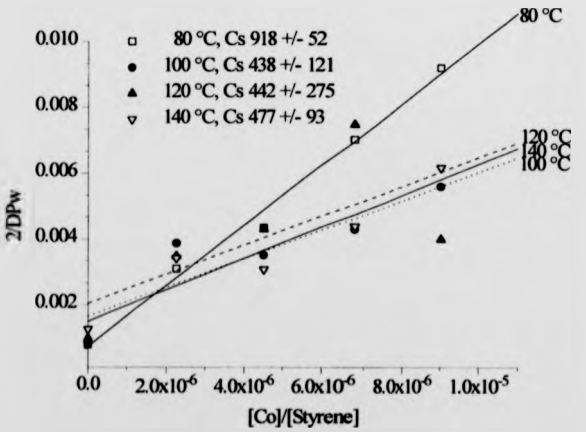

Figure 4. 31. CLD overlay for the CCT polymerisation of styrene using complex XIII in the absence of solvent and initiator at 80, 100, 120 and 140°C.

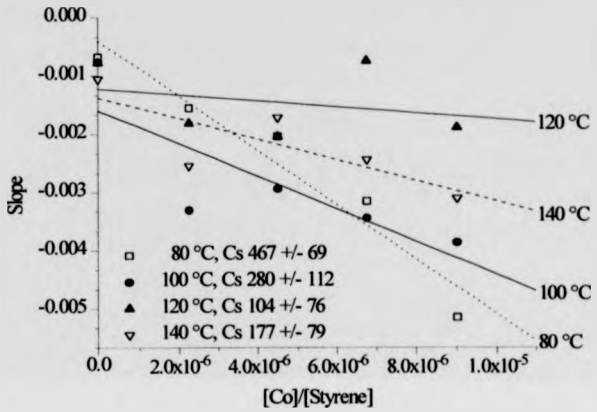

From figure 4.29 a maximum C_s of 1310 at 80°C was found. The 2/DPw overlay in figure 4.30 gives a maximum C_s value of 920 at 80°C whilst the CLD overlay in figure 4.31 gives a maximum C_s value of 467 at 80°C.

It is also important to compare each set of complex analogues with each other at all temperatures to see what effect different axial ligands have on the C_s value. Would the water ligand analogue give similar results to its cobalt (II) analogue and will the pyridine ligand analogue in each set give the lowest C_s value. The most suitable method to achieve this comparison is by overlaying the 2/DPw plots for each analogue taken from tables 4.2, 4.3 and 4.4 at 120°C. The plots show that the same trend is observed here as previously, i.e., the water analogue gives the highest chain transfer value and is therefore assumed to be the most effective, followed by the cobalt (II) analogues and finally the pyridine analogues. The fact that the pyridine analogues give consistently the lowest C_s

values when compared to the other analogues agrees well with the postulation that the pyridine ligand itself hinders the abstraction of the ethyl group possibly by strengthening the cobalt carbon between the ethyl and cobalt. The observed reduction in activity could however be due to a reduction in mobility of the CCTA containing pyridine as the pyridine ligand is considered to be bulky when compared to its water analogues. It is however equally likely that the strength of the cobalt alkyl bond is very strong and can therefore not reduce to cobalt (II). Possibly the strength of the pyridine ligand causes the cobalt (III)- alkyl polymer intermediate bond strengths to become stronger and therefore its dissociation and continuation of the cycle is greatly affected.

Figure 4.32. 2/DPw overlay for the CCTP of styrene at 120°C using complexes II, VIII and XI.

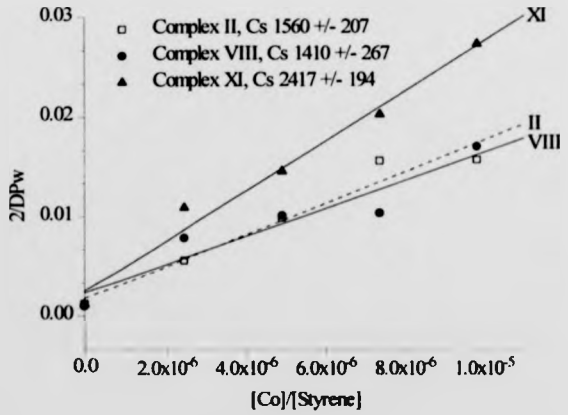

Figure 4.33. 2/DPw overlay for the CCTP of styrene at120°C using complexes III, IX and XII

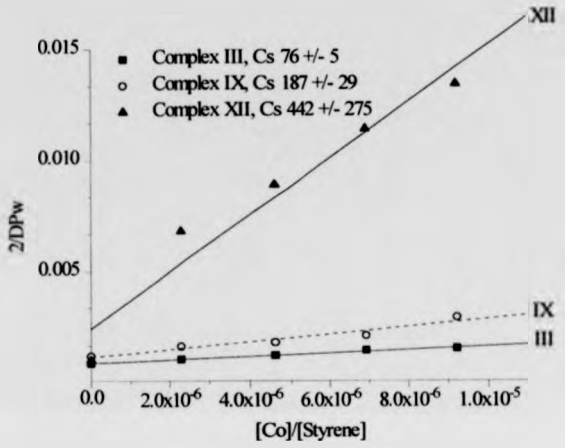

Figure 4.34. 2/DPw overlays for the CCTP of styrene at 120°C using complexes IV, X and XIII.

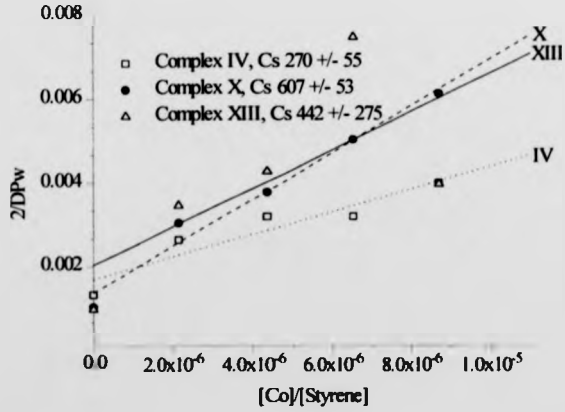

4.3.4. Calculation of activation energies for complexes II-IV, XIII-XIII in the catalytic chain transfer polymerisation of styrene.

In free radical polymerisation propagation is the 'growth stage' for polymer molecules. In CCTP this growth stage is modified by the use of a CCTA. The higher the value for the chain transfer constant the more effective the complex is at reducing the molecular weight of the product. It should be noted that for chain transfer to be effective it must dominate over the propagation step. If the value for chain transfer is low then either the CCTA is ineffective at reducing molecular weight or the energy required to undergo transfer is larger than that for propagation, transfer will still occur but propagation will dominate. In both cases where C_s is low or the activation energy is high for transfer, high molecular weight polymer is formed. A value for the activation energy for propagation for styrene is given in appendix 5 along with $E_{transfer}$ and $A_{transfer}$ values for all the complexes used in this investigation, see table 1.

By measuring chain transfer coefficients at the minimum of three different temperatures it was possible to plot ln C_s versus 1/T (Arrhenius plot). An example calculation for the determination of the E_a transfer and $A_{transfer}$ values can be found in appendix 5. Values for slopes and intercepts for each complex can also be found in appendix 5, table 1.

It was of interest to investigate whether a similar observation is noted with regard to a strong base decreasing activity and requiring more energy to break the bond and therefore $E_{transfer}$ is higher than $E_{propagation}$. This is the postulated explanation for reduced activity of cobalt (III) complexes containing pyridine as the axial ligands for both MMA and styrene bulk polymerisation.

Results in chapter 3 with MMA show that the pyridine complex chain transfer values are significantly lower than the cobalt (II) and cobalt (III) water analogues. The water analogue values give slightly higher values than cobalt (II). This would suggest that $E_{transfer}$ would be higher for pyridine. The results in this chapter also show that again the water analogue values for chain transfer are higher than cobalt (II) followed by pyridine. Values from all methods for the determination of C_s were used to calculate both E_{tr} and A_{tr} and compared. Figure 4.40 shows a plot of ln C_s versus 1/T for complex II using all methods of determination for C_s. Table 4.5 shows $E_{transfer}$ and $A_{transfer}$ values for all complexes using all methods of determination. If the value for $E_{transfer}$ is larger than $E_{propagation}$ then the complex will give a low value for chain transfer activity and produce high molecular weight polymer and will be considered ineffective at reducing molecular weight. Propagation and termination via free radical mechanisms will dominate in this situation. However if the $E_{transfer}$ is lower than $E_{propagation}$ then transfer will dominate and control of molecular weight will be established.

Figure 4.35. Arrhenius plot for the CCTP of styrene using complex II.

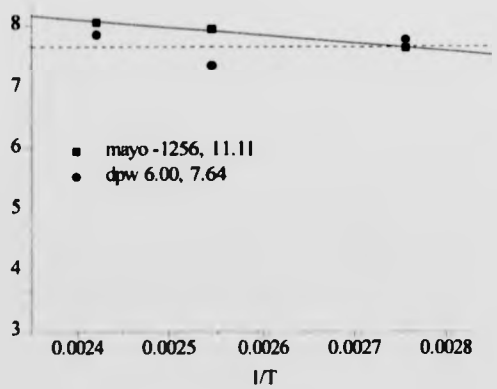

All plots behave linearly with minimal scatter. From the values given for slope and intercept it was possible to calculate $E_{transfer}$ and $A_{transfer}$ for each method and compare. Table 4.5 gives $E_{transfer}$ and $A_{transfer}$ values for all complexes. The results in table 4.5 show that for each complex most methods of determination give different values, however sometimes these values are close. Complex II has three very different values for $E_{transfer}$, complex III has a very low value when the CLD procedure is used although the other two methods give similar but not brilliant values in agreeance with each other. Complex IV has $E_{transfer}$ values which are very close to each other regardless of method, it was not possible to obtain a value for complex VIII using the CLD values as there was too much error in the data. Complex IX values are very different when compared to each other and therefore determination of an absolute average value is difficult. For complexes X and XI all methods give similar values and therefore an estimation using an average value would be possible for $E_{transfer}$. The scatter and high values of $E_{transfer}$ can be explained by the fact that during CCTP the time taken to establish an equilibrium between cobalt (II) and cobalt (III) formation is long. The result of this is manifested in low monomer conversion and it would have been more suitable to have run the experiments for a longer period of time. This would have resulted in higher monomer conversion and thus a more accurate measure of $E_{transfer}$ would have been obtained. Both complexes XII and XIII give similar values using all three methods although the Mayo and 2/DPw methods give the most comparable results.

Table 4.5. Table of $E_{transfer}$ and $A_{transfer}$ values for complexes II-IV and VIII - XIII.

Complex	Mayo E_{tr}	Mayo A_{tr}	2/DPw E_{tr}	2/DPw A_{tr}	CLD E_{tr}	CLD A_{tr}
II	42600	2.85E +12	32100	8.87E +10	114000	1.21E +21
III	27200	1.85E +09	18900	1.01E +08	6650	1.49E +06
IV	59400	4.59E +12	47100	7.17E +11	32500	4.24E +09
VIII	30400	8.26E +10	29400	3.53E +10		1.07E +15
IX	56400	9.64E +12	3830	3.37E +13	82900	2.39E +16
X	36000	8.33E +10	33500	3.43E +10	36400	6.77E +10
XI	24900	1.03E +10	20800	2.23E +09		3.14E +05
XII	38650	4.17E +11	42450	8.76E +11	45520	1.58E +12
XIII	25550	4.78E +09	35200	4.36E +11	20710	3.62E +08

If we consider the results in table 4.5 for the complexes in order of grouping i.e. cobalt (II), cobalt (III) – pyridine and then cobalt (III)- water and consider only the 2/DPw values we can see that although the least sterically hindered complex (II) gives the highest C_s value it does not correspondingly give the lowest $E_{transfer}$ value. This is interesting because it is the second most sterically hindered complex III that does give the lowest $E_{transfer}$ value. Therefore for this group there is no connection between a high C_s value and a low $E_{transfer}$ value. For the cobalt (III)-pyridine sets complex VIII again the least sterically hindered equatorially gave the highest C_s value but did not have the lowest $E_{transfer}$ value, however it had the intermediate value of the three complexes.

With regard to the cobalt (III) group containing water as the axial ligand there is some connection between C_s and $E_{transfer}$ as highlighted by complex XI, this gave the highest C_s value and has the lowest $E_{transfer}$ value. If we now consider the results in terms of analogue comparisons we see that when $R = CH_3$ only there is a connection between $E_{transfer}$ and C_s. A low value for $E_{transfer}$ corresponds to a high value for C_s. It should also be noted that the $E_{transfer}$ values for complex XI are lower than those for $E_{propagation}$, this is also the case for complex VIII. It should also be noted that the $E_{transfer}$ value for the water analogue is lower than that for its corresponding pyridine analogue, this therefore agrees with the postulation that the energy involved for a pyridine analogue to undergo CCTP is higher than that for water. When $R_1 = CH_2CH_3$ and $R_2 = CH_3$ there seems to be no direct connection between C_s and $E_{transfer}$. Although the cobalt (III) - water analogue gives a lower $E_{transfer}$ value than the cobalt (III) - pyridine analogue. When R_1 and $R_2 = CH_2CH_3$there again appears to be no connection between C_s and $E_{transfer}$. However the value of $E_{transfer}$ for the water analogue is smaller than that of the pyridine analogue.

The overall C_s values for styrene are lower than those for MMA, this is however expected and both monomers cannot directly be compared in this thesis owing to the obvious fact that the MMA polymerisations in chapter 3 used an external initiating source whilst in this work no external initiating source was used. It was however hoped that here the reaction at elevated temperatures would give an increase in activity although it was assumed that the chain transfer values would not increase with an increase in temperature. The decrease in chain transfer activity for styrene bulk polymerisations could be due to propagation dominating and also there being no external source of radicals present, this will limit the number of radicals being able to replenish the exhausted stocks, CCTP is reliant on a continuous supply of radicals. If k_p is fast and k_t is slow then there will be an insufficient number of radicals present. MMA bulk polymerisation values are higher for two reasons, the structure of the radicals formed are less stable than styrene radicals and the presence of an external initiator. The styrene values are lower owing to structure and no external initiator being present. $E_{transfer}$ is larger than $E_{propagation}$.

4.4. Conclusions.

The chain transfer constants obtained for bulk polymerisation of styrene are lower than those with MMA using identical complexes owing to the absence of a terminal methyl group. C_s is independent of temperature. An increase in skeletal carbons decreases chain transfer activity and the presence of a strong base as an axial ligand further reduces its effectiveness. Both cobalt (II) and cobalt (III) water analogues give similar chain transfer values. Complex purity is one explanation for decreased activity along with the possibility of cis/trans isomerisation for complexes III,IX and XII. It is quite possible that

although both isomers are probably formed only one isomer may be an effective CCTA. The lability and presence of axial ligands offers another explanation for the results obtained. From NMR and X-ray crystal data (where applicable) indicate/confirm the presence of the desired axial ligands. It is unconfirmed whether both ligands remain attached during polymerisation or whether both are replaced by monomer ligands. The energy of transfer ($E_{transfer}$) does not seem to be reliant on the structure of the catalyst when all three analogues are compared, but when only the cobalt (III) systems are compared there is a connection between a strong base giving a higher value for $E_{transfer}$ when compared to the identical water analogue. It appears from these results that an effective CCTP does not rely on $E_{transfer}$ being smaller then $E_{propagation}$ neither does a high C_s correspond to a low $E_{transfer}$ value. The wide scatter of values obtained for $E_{transfer}$ could be attributed to the time required for equilibrium to be established between co(II) and co(III). It would have therefore been better to take these polymerisations to higher conversion as a significant amount of formed polymer is wasted during this equilibrium stage. The lower values for C_s given by the CLD procedure could be attributable to a number of factors such as chain transfer is not dominating in the systems [13], this is plausible owing to the fact that the energy of transfer values for all complexes are on the whole larger that the energy for propagation suggesting that although transfer does occur propagation and hence termination via another process dominates. Davis [13] has reported that the CLD procedure is only reliable if transfer dominates. It is also possible to state that the non-linearity observed in some plots implies that some assumptions may be broken with respect to the Mayo equation. Some large PDi values are also observed which could possibly explain why the 2/DPw+ CLD values differ. The presence of low

molecular weight polymer in the GPC trace could cause curvature in the CLD plot resulting in differing values. They also suggest that the linearity of the ln N(M) plots also play an important role in obtaining accurate C_s values. They suggest that the 2/DPw method of determination for C_s is the most accurate.

4.5. References.

1) Davis, T. P.; Haddleton, D. M.; Richards, S. N. ; *J. Macromol. Sci.,Rev. Macromol. Chem. Phys.*, **1994**, *C34*, 243.

2) Davis, T. P.; Kukulj, D.; Haddleton, D. M.; Maloney, D. R. ; *Trends in Polymer Science*, **1995**, *3*, 365.

3) Hawthorne, D. G. ; European Patent 0249 614 B1, (**1986**).

4) Hawthorne, D. G. ; World Patent 87/03605, (**1987**).

5) Hawthorne, D. G. ; European Patent 0249614 A1, (**1992**).

6) Mayo, F. R. ; *Polym. Prep.*, **1961**, *2*, 55.

7) Mayo, F. R. ; *J. Am. Chem. Soc.*, **1968**, *90*, 1289.

8) Buzanowski, W. C.; Graham, J. D.; Priddy, D. B.; Shero, E. ; *Polymer*, **1992**, *33*, 3055.

9) Chong, Y. K.; Rizzardo, E.; Solomon, D. H. ; *J. Am. Chem. Soc.*, **1983**, *105*, 7761.

10) Haddleton, D. M.; Maloney, D. R.; Suddaby, K. G.; Muir, A. V. G.; Richards, S. N. ; *Macromol. Symp.*, **1996**, *111*, 37.

11) Heuts, J. P. A.; Forster, D. J.; Davis, T. P. ; *Macromolecules*, **1999**, *32*, 5514.

12) Plotnikov, V. D. ; *Vysokomolekulyarnye Soedineniya Seriya A & Seriya B*, **1997**, *39*, 406.

13) Heuts, J. P. A.; Davis, T. P.; Russell, G. T. ; *Macromolecules.*, **1999**, *32*, 6019.

Chapter 5

Partitioning of cobalt (II) and cobalt (III) complexes.

5.0. Partitioning of cobalt (II) and cobalt (III) complexes.

5.1. Aim.

The aim of this work was to evaluate the solubility of a series of CCT complexes in water and monomer, MMA. It was interesting to see how the structure of the catalyst affected its solubility in both phases.

5.2. Introduction.

A major potential end use application for the catalysts synthesised in the previous chapters is in emulsion polymerisation [1-6]. It has been shown that when CCTA's are used in emulsion polymerisation they are effective in controlling the molecular weight of the polymer formed [7]. Monomer and water are immiscible with water acting as a dispersion medium and initiation occurs within the water layer, as the monomer is slightly water soluble allowing initiation to occur. It is important for the catalyst to be slightly soluble in the water phase as the emulsion is a diffusion controlled process and monomer propagation and termination is controlled by both the monomer and CCTA's ability to diffuse from one droplet to a particle and then into another. If however, monomer depletion occurs before the CCTA has had time to control the molecular weight then the CCTA will be termed ineffective at reducing the molecular weight of the polymer. Before emulsions are carried out it is important to ascertain the catalysts solubility properties. A typical emulsion consists of monomer (MMA) and water phase, it is therefore important to investigate the solubility of the catalysts in each phase. A CCTA is deemed to be effective if it leads to the production of a low molecular weight polymer by the fast

termination via transfer mainly to monomer. The formed chains will be shorter and therefore their mobility is increased, large chains are formed when a less effective or smaller amount of CCTA is used leading to a lower rate of transfer resulting in higher molecular weight products.

The partitioning properties of a CCTA are reliant on both its structure and the monomer used. The effect of catalyst structure upon partitioning is investigated in this chapter. Little work has been carried out on the partitioning properties of CCTA's however the results from other workers will be discussed and compared with the findings of this work. A known quantity of catalyst was added to either a 50/50, 90/10 or 10/90 solution of both monomer and water. The purpose behind the 90/10 and 10/90 percentage composition mixtures was to ascertain if the complexes had a saturation point. This is an important aspect as it could be possible that the catalyst could become saturated in one phase and therefore diffuse into the other layer and give inaccurate values and conclusions about the catalysts activity.

5.3 Results.

Stock solutions of each catalyst in both MMA and water were made and UV/VIS spectra recorded. The values detailed in this thesis are samples of repeat measurements. Plots of absorbance versus concentration for each catalyst in each phase were plotted. A known quantity of catalyst was then added to a stirred solution of either 50/50, 90/10 and 10/90 compositions of monomer/water. Each layer was then separated and a UV/vis spectrum of each phase was recorded independently of each other. By obtaining the absorbance value for each layer it was then possible to calculate the concentration of catalyst present

in each layer. The exact quantities and procedure can be found in the experimental section of Chapter 6.

5.3.1. The use of Cobalt (II) complexes for partitioning between MMA and water.

The aim of this section was to investigate what effect increasing skeletal carbons had on the solubility of the catalysts in monomer and water. The complexes used for this investigation were II, III and IV, see figure 5.1.

Figure 5.1. Structure of cobalt (II) complexes to be used in partitioning experiments.

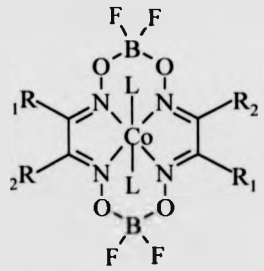

Where Complex II, $R_1 + R_2 = CH_3$ L = CH_3OH

Complex III, $R_1 = CH_3$ and $R_2 = CH_2CH_3$ L = CH_3OH

Complex IV, $R_1 + R_2 = CH_2CH_3$ L = CH_3OH.

Tables 5.1 and 5.2 give absorbance and concentration information for the stock solutions of complex II in both water and monomer respectively. Tabular information for complexes III and IV can be found in appendix 5, tables 1 and 2 respectively.

Table 5.1. Absorbance and wavelength information for complex II water stock solutions.

Solution	Concentration (M) x 10^{-4}	Absorbance at λ max	λ max	ε ($L\ mm^{-1}mol^{-1}$)
S1A	5.14	1.73	455.5	336.5
S1B	3.84	1.26	455.6	328.1
S1	3.46	1.19	455.6	343.9
S2	1.66	0.49	455.6	295.1
S3	0.97	0.30	456.0	309.2
S4	0.83	0.28	456.0	337.4

Table 5.2 Absorbance and wavelength information for complex II MMA stock solutions.

Solution	Concentration (M) x 10^{-4}	Absorbance at λ max	λ max	ε ($L\ mm^{-1}mol^{-1}$)
S1A	4.99	1.91	446.2	382.7
S1B	3.64	1.41	446.2	387.3
S1	3.24	0.90	446.8	277.7
S2	1.60	0.42	447.2	262.5
S3	0.65	0.20	446.4	308.6

Figures 5.2 – 5.4 illustrate graphically the Beer-Lambert plots for complexes II-IV for both monomer and water stock solutions.

Figure 5.2. Plot of absorbance at λ max versus concentration for complex II, for MMA and water stock solutions.

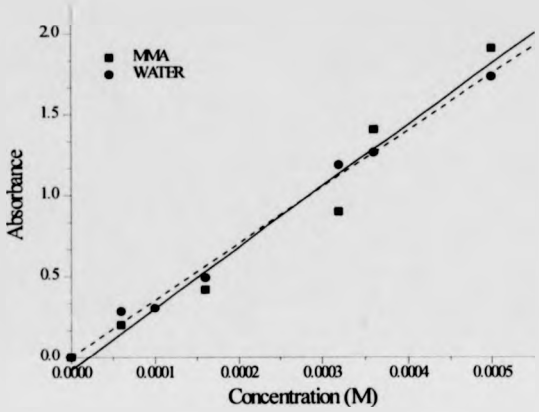

Figure 5.2 shows that both the plots behave linearly with minimal scatter and therefore the results obtained for complex II should give accurate values for the percentage of complex in each phase at various compositions.

The plots in figure 5.3 show that results derived from these plots involving complex III show some scatter with respect to the MMA and it is therefore tentatively assumed that these results are reliable.

Figure 5.3. Plot of absorbance at λ max versus concentration for complex III for both MMA and water stock solutions.

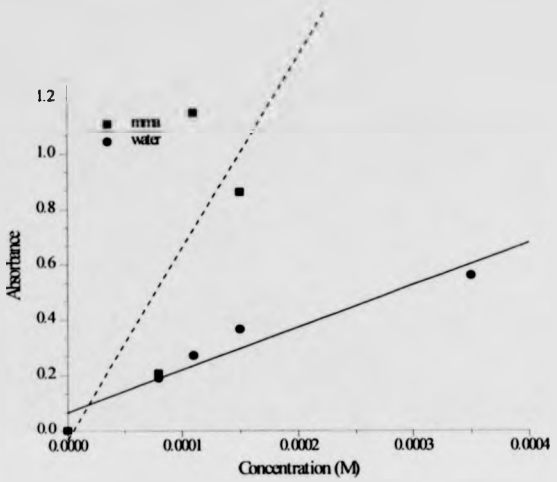

Figure 5.4. Absorbance at λ max vs concentration plot for complex IV both MMA and water stock solutions.

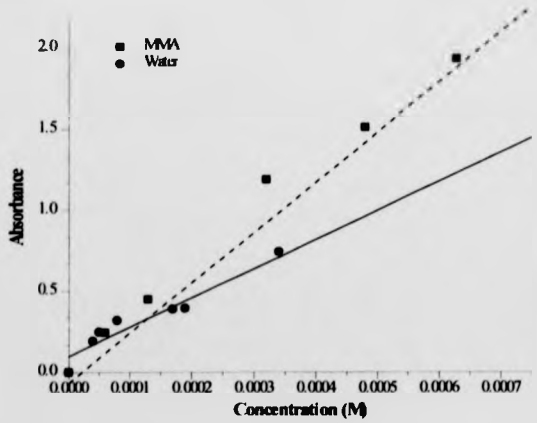

Again figure 5.4 shows that the MMA plot exhibits minimal error whilst the water plot does give some scatter, therefore the error in this phase will be larger.

From the absorbance values obtained for each complex in each phase it was then possible to calculate the percentage catalyst in each phase for all compositions using the formulae $y = mx + c$. Where y = Absorbance, x = concentration, m = slope and c = error

Table 5.3 gives percentage composition of complex in each phase for complexes II – IV at all composition mixtures.

Table 5.3. Percentage values for complexes II – IV in both MMA and water phases at each composition.(p = partition coefficient)

Complex	90/10 (%)		50/50 (%)		10/90 (%)	
	MMA	Water	MMA	Water	MMA	Water
II	45	55 p = 0.79	45	55 p = 0.82	51	49 p = 1.04
III	14*	86* p = 0.16	89	11.0 p = 0.81	69	31 p = 2.23
IV	74	26 p = 0.06	99	1.0 p = 0.04	93	7.0 p = 0.19

*The absorbance readings for this catalyst were only possible for the MMA phase, it was not possible to obtain a value for the water phase, therefore this is only a theoretical value after calculating the number of grams of complex present in the MMA phase.

From the results in table 5.3 it would appear that for complex II the percentage of catalyst in each phase does vary with composition. Both 90/10 and 50/50 compositions give similar values indicating that the catalyst is not saturated in one layer and that the catalyst was equally soluble in both layers at both of these compositions, however just more

hydrophilic than hydrophobic. However, with the 10/90 composition of MMA/water it would appear that although there is significantly more water than MMA the catalyst does appear to prefer the monomer layer. It is possible that at 90% water, the catalyst has become saturated and has diffused into the monomer layer, this is not the case for the 90% monomer layer. The results for this complex agree well with those of Suddaby [7] and Kukulj [8], who independently found that complex II was approximately equally soluble in a 50/50 composition of monomer/water. Neither author however investigated what effect varying the composition of monomer/water had on the partitioning properties of complex II.

For complex III it would appear from the results for the 50/50 and 10/90 compositions that the catalyst concentration in each layer varies with composition. However, both compositions tell us that the complex prefers monomer to water and that even in a 10% monomer phase the complex would prefer to stay in that phase and become saturated before diffusing into the larger water phase, however it is significantly soluble in water. It should also be noted that the irregularity of values for complex III in 90/10 MMA/water phase could be due to the absence of the water absorbance peak in the spectra.

Again with complex IV the concentration of catalyst present in each phase changes with fluctuations in composition. However, again the complex prefers monomer i.e. it is hydrophobic in nature although again quite soluble in water.

From table 5.3 it can be concluded that an increase in skeletal carbons leads to an increase in hydrophobicity. These results indicate that complexes II – IV should be effective in emulsion polymerisations owing to their solubility in both monomer and

water. It should also be noted that the presence of any impurities could affect complex partitioning and possibly lead to inaccurate results. The results for complex II agree well with previous workers findings [7]. Work by a coworker [4] has in fact shown that complex IV is more than three times more effective at reducing molecular weight in emulsion polymerisations when compared to complex II and is one and a half times more effective than complex III.

5.3.2. The use of cobalt (III) complexes containing pyridine as an axial ligand in the partitioning investigation with MMA and water.

The purpose of this section of work was to investigate what effect having a strong base as an axial ligand, see figure 5.5, had on the partitioning properties of the complexes and compare these results with both cobalt (II) and cobalt (III) water containing analogues. Again information regarding absorbance and concentration values for complexes VIII – X for stock solutions and phase compositions can be found in appendix 5, tables 4-6.

Figure 5.5. Structure of cobalt (III) complexes containing pyridine as the axial ligand used in the partitioning experiments with MMA and water.

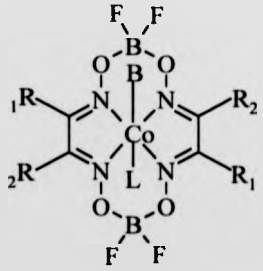

Where B= pyridine and complex VIII, R_1+R_2 = CH_3,complex IX, R_1 = CH_3, R_2 = CH_2CH_3,complex X, R_1 + R_2 = CH_2CH_3.

Figure 5.6 shows the Beer-Lambert plots for complex VIII for both water and monomer stock solutions.

Figure 5.6. Plot of absorbance at λ max versus concentration for complex VIII for both MMA and water stock solutions.

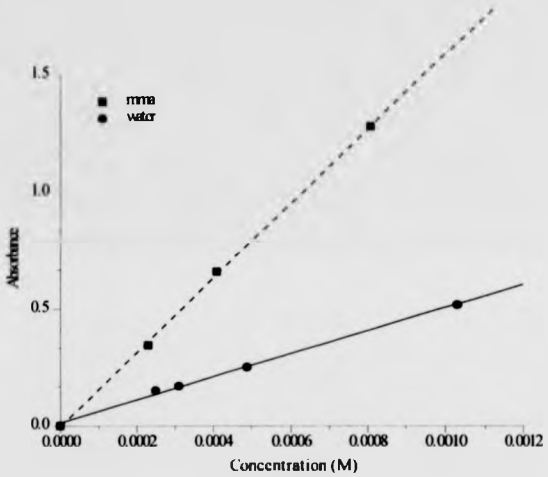

From figure 5.6 it can be seen that both plots exhibit linearity with minimal error and therefore the results obtained by using both plots give reliable results. From figure 5.7 it can be seen that linearity is also observed here for both sets of solutions and that therefore the results obtained for complex IX are reliable.

Figure 5.7. Plot of absorbance at λ max versus concentration for complex IX for both MMA and water stock solutions.

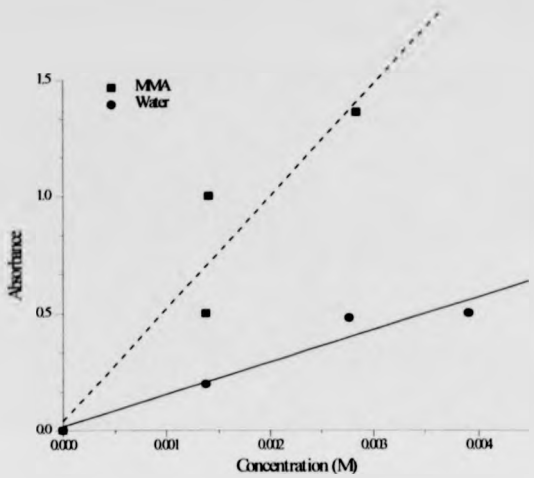

The plots in figure 5.7 show minimal error for both stock solutions and therefore results for complex IX are reliable.

Again excellent linearity is observed for both plots in figure 5.8. Table 5.4 gives percentage composition of complex in each phase for complexes VIII – X at all composition mixtures.

Figure 5.8. Plot of absorbance at λ max versus concentration for complex X, for both MMA and water stock solutions.

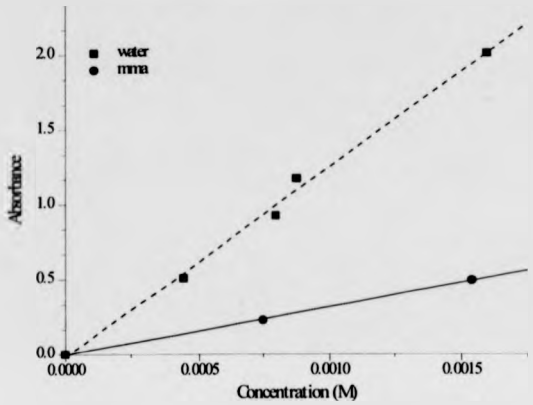

Table 5.4. Percentage values for complexes VIII – X in both the MMA and water phases for each composition. (p = partition coefficient)

Complex	90/10 (%)		50/50 (%)		10/90 (%)	
	MMA	Water	MMA	Water	MMA	Water
VIII	78	22 p = 0.28	93	7.0 p = 0.07	92	8.0 p = 0.08
IX	58	42 p = 0.70	98	2.0 p = 0.02	75	25 p = 0.32
X	41	59 p = 1.47	88	12.0 p = 0.13	98	2.0 p = 0.20

From the results in table 5.4 for complex VIII it is clear that percentage complex in each phase changes with composition. However, results at all composition tell us that the complex is hydrophobic in nature, i.e. more catalyst is present in the monomer phase than

water phase at each composition. It is however interesting to note that the complex at both 50/50 and 10/90 compositions of monomer and water gives similar values indicating that the catalyst is not saturated in either the 50/50 or 90/10 compositions. It is however interesting to note that at 90/10 monomer/water composition, less of the complex is present in the monomer phase, why this is so is unexplainable.

With regard to complex IX it would appear that again the percentage of the complex in each phase varies with composition. Again the complex is most definitely more hydrophobic in nature at all compositions, however again the percentage complex present in 90/10 mixture is less than that of 50/50 and 10/90. Complex X also exhibits hydrophobicity but not at all compositions. Again the value given in the 90/10 mixture is less than that of 50/50 and 10/90. The lability of the axial ligands could affect the partitioning values of complexes as it is possible that monomer or indeed water can replace one or both of the identified axial ligands when the complex is added to the monomer/water mixture. The presence of impurities could also influence the partitioning properties of the complex thus resulting in inaccurate values. It can be concluded that all three complexes should be effective in emulsion polymerisation.

5.3.3. The use of cobalt (III) complexes containing water as an axial ligand in partitioning investigations.

The purpose of this section of work was to investigate what effect having a weak base as an axial ligand, see figure 5.9, had on the partitioning properties of the complexes and compare these results with both cobalt (II) and cobalt (III) pyridine containing analogues. Again information regarding absorbance and concentration values for complexes XI-XIII for stock solutions and phase compositions can be found in tables 8-10 in appendix 5.

Figure 5.9. Structure of cobalt (III) complexes containing water as the axial ligand.

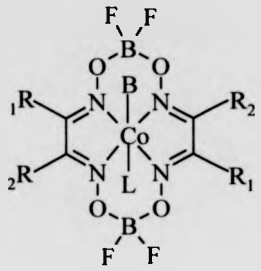

Where B= water and

Complex VIII, $R_1 + R_2 = CH_3$

Complex IX, $R_1 = CH_3$, $R_2 = CH_2CH_3$

Complex X, $R_1 + R_2 = CH_2CH_3$.

The following figures show Beer - Lambert plots for complexes XI - XIII using both water and monomer stock solutions.

Figure 5.10. Plot of absorbance at λ max versus concentration for complex XI.

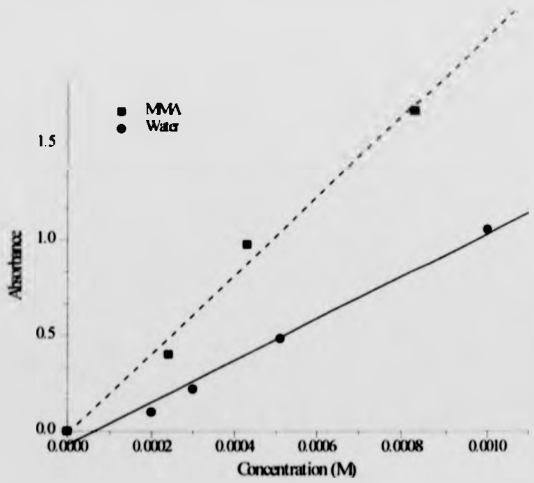

From both plots in figure 5.10 it appears that both exhibit linearity. Figure 5.11 also shows linearity for both MMA and water plots and therefore the results obtained for this complex from these plots will be reliable.

Figure 5.11. Plot of absorbance at λ max versus concentration for complex XII for both MMA and water stock solutions.

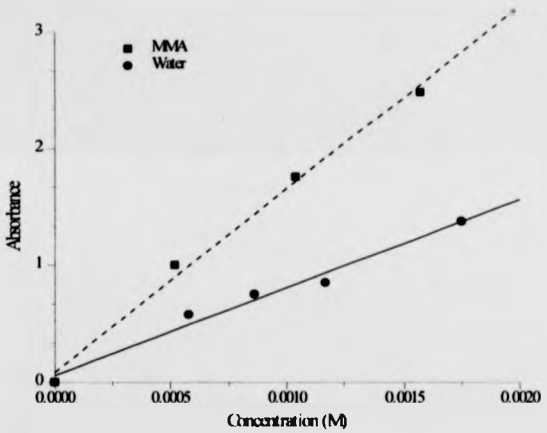

Again linearity is observed for both plots in figure 5.12. Table 5.5 gives partitioning values in percent for complexes XI – XIII at each composition.

Figure 5.12. Plot of absorbance at λ max versus concentration for complex XIII from both MMA and water stock solutions.

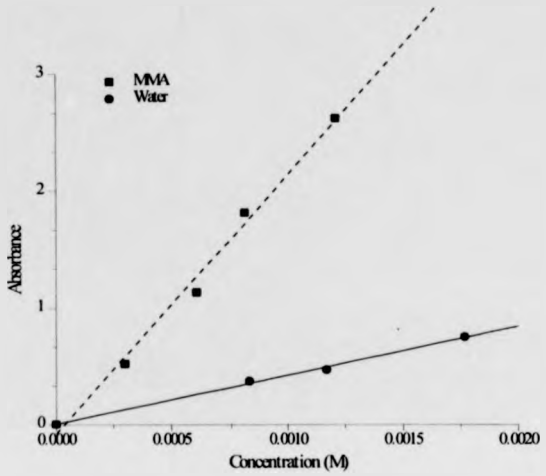

Table 5.5. Percentage values for complexes XI –XIII in both the MMA and water phases at all compositions.(p = partition coefficient)

Complex	90/10 (%)		50/50 (%)		10/90 (%)	
	MMA	Water	MMA	Water	MMA	Water
XI	64.0	36.0 p=0.55	58.0	42.0 p=0.73	92.0	8.0 p=0.09
XII	79.0	21.0 p=3.74	92.0	8.0 p=0.08	98.0	2.0 p=0.02
XIII	74.0	26.0 p=0.34	95.0	5.0 p=0.06	98.0	2.0 p=0.03

From the results in table 5.5 for complex XI it can once again be seen that the complex is hydrophobic in nature and its percentage values in each phase vary with composition. Complex XII is hydrophobic in nature for both 50/50 and 10/90 percentage compositions.

Complex XIII is hydrophobic at each composition and its values change for each composition. From the results obtained for the three complexes it should be noted that complex purity could influence the complexes hydrophobic properties. The identity of the axial ligands was proven before experimentation but once the complex was added to the monomer/water mixtures these axial ligands could have been exchanged by monomer or water as the ligand. It can be concluded that this set of complexes should be effective in emulsion polymerisations owing to their solubility in both phases allowing diffusion from one phase to the other.

In order to compare each analogue directly with each other it is necessary for ease of explanation and observation to illustrate values in a tabular form, table 5.6 and figure 5.13. Only 50/50 compositions will be compared.

Figure 5.13. Structure of complexes.

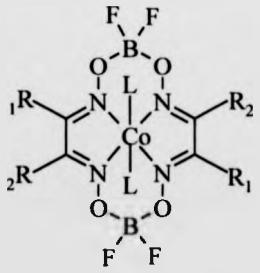

Where Cobalt (II) L= CH_3OH

Cobalt (III) Py L = Pyridine and Ethyl

Cobalt (III) Water L = Water and Ethyl

Table 5.6. Comparison of percentage complex per layer for 50/50 percentage composition of monomer to water, for complexes II – IV, VIII – X and XI - XIII.

$R_1 + R_2$	Cobalt (II) (%)		Cobalt(III)Py (%)		Cobalt(III)H_2O (%)	
	MMA	Water	MMA	Water	MMA	Water
II, VIII + XI $R_1 + R_2 = CH_3$	45	55	93	7	58	42
III, IX +XII $R_1 = CH_3$ $R2 = CH_2CH_3$	95	5	98	2	92	8
IV, X + XIII $R_1 + R_2 =$ CH_2CH_2	99	1	88	12	95	5

In general the results in table 5.6 show that the pyridine ligand in each analogue set increases the hydrophobicity of the complex whilst the water and cobalt (II) analogues decreases hydrophobicity. However for the pyridine and water analogues for when $R_1 + R_2$ are equal to ethyl it can be seen that this is not the case. It would appear that in this instance the pyridine analogue increases hydrophobicity whilst the water decreases hydrophobicity. Possible explanations for this include experimental error and possibly complex purity. The cobalt (II) and cobalt (III) water analogues give similar results when compared to each other.

5.4 Conclusions.

From the results in this chapter it is possible to conclude that from these preliminary results each complex would be effective as a CCTA in emulsion polymerisation. It is also possible to conclude that the structure of the catalyst plays an important role in its partitioning properties. The presence of increased alkyl groups on the equatorial arms of

the complexes increases hydrophobicity. When this is coupled with the interaction of a strong base present as one axial ligand the complexes hydrophobic property is further increased. The replacement of this ligand with water allows the catalyst to become increasingly hydrophilic. It is also possible to conclude that both cobalt (II) and cobalt (III) water analogues are in general more hydrophilic in nature than the pyridine containing cobalt (III) analogues, although it should be noted that all complexes are hydrophobic in nature. The change in monomer and water compositions allow the properties of the complexes to be further changed with regard to their hydrophilic and hydrophobic nature. The results found for complex II at a 50/50 composition of monomer/water agree well with previous workers findings. It should be remembered that as stated earlier in various sections of this chapter that purity and lability of axial ligands could also be influencing the results obtained.

5.5. References.

1) Haddleton, D. M.; Muir, A. V.; Leeming, S. W. ; World Patent 95/17435, (**1995**).

2) Haddleton, D. M.; Padget, J. C.; Overbeek, G. C. ; World Patent 95/04767, (**1995**).

3) Haddleton, D. M.; Muir, A. V. ; World Patent 95/04759, (**1995**).

4) Morsley, D. R. ; Ph.D. Thesis, , University of Warwick, Coventry, UK, (**1999**).

5) Janowicz, A. H. ; United States Patent 5 028 677, (**1991**).

6) Melby, L. R.; Janowicz, A. H.; Ittel, S. D. ; European Patent 0199436 A1, (**1986**).

7) Suddaby, K. G.; Haddleton, D. M.; Hastings, J. J.; Richards, S. N.; O'Donnell, J. P. ; *Macromolecules,* **1996**, *29*, 8083.

8) Kukulj, D. ; Ph.D. Thesis, , University of New South Wales, Sydney, Australia., (**1997**).

Chapter 6

Experimental section

6.0. Experimental section.

6.1. General experimental procedures.

Polymer molecular weight data was obtained by gel permeation chromatography using a Polymer Laboratories modular GPC system. THF was used as the elutent at 1 mL min^{-1} equipped with a differential refractive index and UV detectors. Calibration was performed using narrow PMMA standards (Mp = 1040 – 1577000) and narrow PS standards (Mp = 580 – 3150000) which were obtained from Polymer Laboratories.

Yields of polymerisation were calculated by drying a known mass of reaction mixture to constant weight in a vacuum oven at 80 °C for MMA and 110 °C for styrene. 1H and ^{13}C NMR spectra were obtained using either a Bruker ACF 250 or DPX 300 MHz spectrometer. Infrared spectra of compounds were obtained on a Bruker Vector 22 FTIR equipped with a Graseby Specac golden gate single reflectron diamond ATR cell. Ultraviolet – visible spectra were obtained using a Phillips PU 8720 UV/VIS scanning spectrophotometer. Magnetic susceptability of complexes were measured using a Johnson Mathey Chemicals (JMC) magnetic susceptibility balance.

6.2. Preparation of cobalt (II) and cobalt (III) complexes.

The synthetic routes to cobalt (II) and cobalt (III) complexes are shown in figures 6.1 and 6.2 respectively. Both procedures require the use of a suitable dioxime as the starting material which can be synthesised from the corresponding diketone.

Figure 6.1. Synthesis of cobalt (II) complexes.

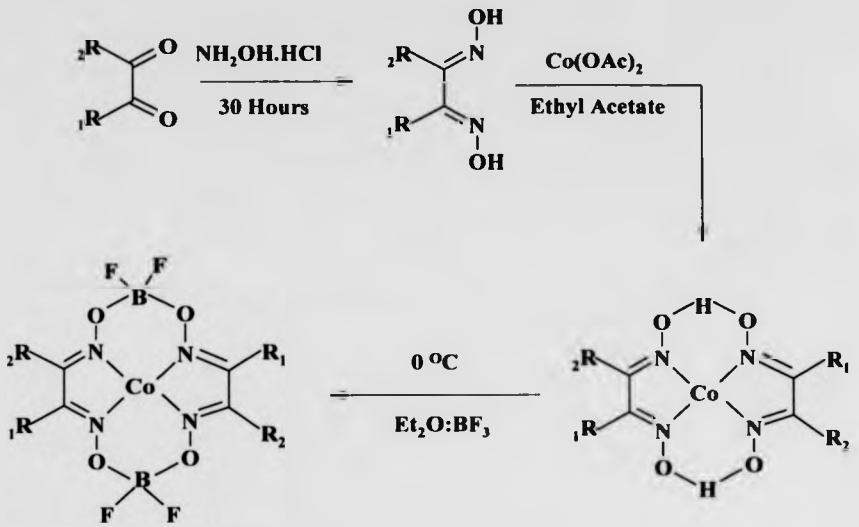

Figure 6.2. Synthesis cobalt (III) complexes.

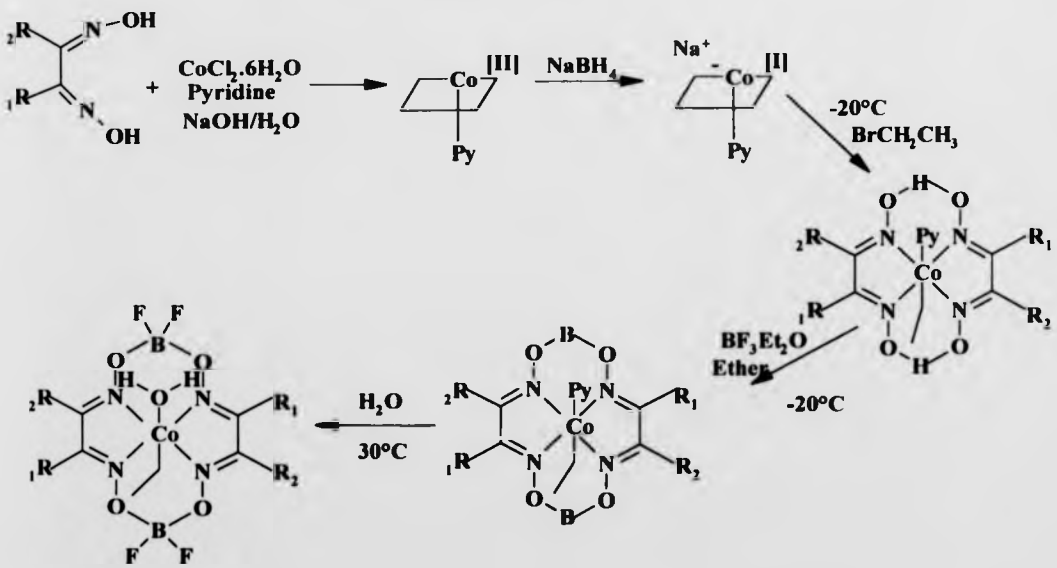

6.3. Synthesis of diketones.

The first stage in the synthesis of the diketone involved the preparation of the grignard reagent :-3-Pentyl magnesium bromide..

6.3.1. Synthesis of 3,6-diethylocta-4,5-magnesium bromide, (3-Pentyl magnesium bromide).

6.3.1.1. Reagents and suppliers.

THF - HiDry, Aldrich.

Magnesium turnings, Aldrich.

3-Bromopentane, Aldrich.

6.3.1.2. Procedure.

A three neck round bottomed flask, equipped with a magnetic follower, condenser and dropping funnel, was pre flushed with nitrogen for twenty minutes. Magnesium turnings and THF (10 mL) were added to the round bottomed flask maintained under a nitrogen atmosphere. 3-Bromopentane (7.55 g, 0.05 mol) and THF (40 mL) were placed in the dropping funnel and approximately 5 mL of the halide solution was added to the magnesium turnings. The reaction vessel was then heated to reflux temperature, once reflux was attained the remaining halide solution was added dropwise at a rate which maintained a constant reflux until no halide solution remained. Stirring was continued for a further fifteen minutes, by which time the magnesium turning had been consumed.

6.3.2. Synthesis of 3.6-diethylocta-4,5-diketone.

6.3.2.1. Reagents and sources.

Lithium bromide, anhydrous, Aldrich.

Copper Bromide, Aldrich.

3,6-diethylocta-4,5-magnesium bromide, as synthesised above,

Oxalyl chloride, Aldrich.

6.3.2.2. Procedure [1].

A THF solution of anhydrous LiBr (30 mL, 16.52 mmol) was added at room temperature under nitrogen to a stirred suspension of CuBr (30 mL, 8.26 mmol) in THF. The resulting mixture was stirred until it became homogeneous, it was then cooled to –78 °C. A freshly prepared solution of 3,6-diethylocta-4,5-magnesium bromide (10.32 mL, 8.26 mmol) was added followed shortly by the addition of oxalyl chloride (0.29 mL, 3.44 mmol) in THF (15 mL, 3.44 mmol) to the stirred solution of the salts. The mixture was stirred at –78 °C, for 15 mins, quenched with saturated ammonium chloride solution and extracted with ethyl acetate. The organic extracts were dried over Na_2SO_4 and concentrated under vacuum. The resulting yellow diketone was purified by vacuum distillation on a Kugel Rohr, Bpt 69-71°C Lit Value 68-70°C [2].

Anal calculated for $C_{12}H_{22}O_2$: C 72.73, H 11.11, Found, C 71.43, H 10.91. FAB MS + (m/z) = 198, FTIR (ATR, liquid), 2966, 2936, 1706 (C=O), 1460, 1384, 1363, 1043, 1023, 951, 907, 849, 797, 667. NMR, 13C {^{1}H}($CDCl_3$, 100.6 MHz, 298K,). 203.0 (C=O), 47.0, 23.0, 11.0, ^{1}H ($CDCl_3$, 250.13 MHz, 298K). 3.56 (m, *J* 5.8 Hz, 2H), 1.90 (m, *J* 8.3 Hz, 8H), 1.18 (t, *J* 7.6 Hz, 12H). Yield (average) 1.89 g, (40%).

6.4. Synthesis of dioximes .

6.4.1. Reagents and sources.

Hydroxylamine hydrochloride, Aldrich,

Potassium carbonate, Aldrich,

Methanol, Fisons,

2,3-Pentanedione, 2,3-Hexanedione, 3,4-Hexanedione, 2,3-Heptanedione, 3-Methyl-1,2-cyclopentanedione, 3,6-diethylocya-4,5-dione, as prepared previously.

6.4.2.1. General procedure[3].

The diketone (20 mmol), hydroxylamine hydrochloride (8.34 g, 120 mmol), potassium carbonate (8.29 g, 60 mmol) and methanol (340 cm^3) were placed in a three necked round bottomed flask fitted with magnetic follower and reflux condenser and heated at reflux for 30 hours. At the end of that time, the boiling solution was filtered through Celite and the methanol was removed under reduced pressure. The white residue was stirred with 100 cm^3 of water for 30 minutes, filtered, washed several times with 10 cm^3 portions of water and dried under vacuum. The white product was recrystallised from aqueous methanol and dried in vacuo.

6.4.2.2. 2,3-Pentanedione dioxime.

The above procedure (6.4.2.1) was followed, 2,3-pentane dione (2.00 g) was added to the reaction vessel as described above.

Anal calculated $C_5H_{10}N_2O_2$ C 46.15, H 7.69, N 21.53, Found C 46.21, H 7.71, N 21.64.

FTIR (ATR, Solid) 3198, 2982, 2942,1634 (C=N), 1445, 1430, 1368, 1248, 1145, 1073, 1049, 1007, 984, 965, 895, 810, 732, 697, 656, 620. NMR, $^{13}C\{^1H\}$

(CD_3COCD_3, 100.6 MHz, 298 K,). 159.00 (C=N), 153.00 (C=N), 17.56, 11.57, 9.53., ^1H (CD_3COCD_3, 250.13 MHz, 298 K), 10.87 (s, 1H), 10.82 (s, 1H), 3.00 (q, *J* 7.6 Hz, 2H), 2.39 (s, 3H), 1.40 (t, *J* 7.5 Hz, 3H). +EI MS (m/z) = 130.07, Yield (average) = 3.39 g (65%). Mpt found 170 – 179 °C, literature 170 – 174 °C [4]

6.4.2.3. 2,3-Hexanedione dioxime.

The above procedure (6.4.2.1) was followed, 2,3-hexane dione (2.00g) was added to the reaction vessel as described above.

Anal calculated $C_6H_{12}N_2O_2$, C 50.00, H 8.33, N 19.44, Found C 50.06, H 8.33, N 19.56. FTIR (ATR, Solid) 3201, 2966, 2933, 2873, 1635 (C=N), 1465, 1444, 1427, 1374, 1355, 1300, 1146, 1110, 1067, 1007, 979, 920, 894, 879, 733, 702, 645, 620. NMR ^{13}C {1H} (CD_3COCD_3, 100.6 MHz, 298 K,).158.41 (C=N), 154.25 (C=N), 26.18, 20.83, 14.84, 9.53. ^1H (CD_3COCD_3, 250.13 MHz, 298K) 10.47 (s, 1H), 10.43 (s, 1H), 2.60 (t, *J* 3.1 Hz, 3H), 1.98 (s, 3H), 1.50 (m, *J* 7.2 Hz, 2H), 0.87 (t, *J* 7.2Hz , 2H). +EI MS (m/z) = 144. Yield (Average) 3.52 g, (61%). Mpt found 175 – 177 °C, literature 174 – 175 °C [5].

6.4.2.4. 3,4-Hexanedione dioxime.

The above procedure (6.4.2.1) was followed, 2,3-hexane dione (2.00 g) was added to the reaction vessel as described above.

Anal calculated for $C_6H_{12}N_2O_2$ C 50.0, H 8.33, N 19.44, Found C 49.99, H 8.33, N 19.24. FTIR (ATR, Solid) 3191, 2990, 1628 (C=N), 1475, 1350, 1267, 1146, 1068, 1027, 950, 890, 820, 780, 750, 689, 600.

NMR ^{13}C {1H} (CD_3COCD_3, 100.6 MHz, 298 K) 160.0 (C=N), 17.5, 11.5. 1H (CD_3COCD_3, 250.13 MHz, 298 K) 10.74 (s, 2H), 3.00 (q, *J* 7.3Hz, 4H), 1.39 (t, *J*

6.5Hz, 6H). +FAB MS (m/z) = 145. Yield (Average) 1.24 g, (43%). Mpt found 146 – 147 °C, literature 147 – 149 °C [6].

6.4.2.5. 2,3-Heptanedione dioxime.

The above procedure (6.4.2.1) was followed, 2,3-heptane dione (2.56 g) was added to the reaction vessel as described above.

Anal calculated for $C_7H_{14}N_2O_2$ C 53.16, H 8.86, N 17.72, Found C 52.95, H 8.84, N 17.82. FTIR (ATR, Solid). 3203, 2959, 2931, 2874, 1620 (C=N), 1445, 1427, 1374, 1354, 1204, 1146, 1100, 1074, 1011, 979, 931, 910, 831, 783, 731, 704, 648. NMR, ^{13}C {^1H} (CD_3COCD_3, 100.6MHz, 298 K), 158.62 (C=N), 154.24 (C=N), 29.18, 24.02, 23.90, 14.43, 9.53. ^1H (CD_3COCD_3, 250.13MHz, 298 K) 10.46 (s, 1H), 10.41 (s, 1H), 2.60 (t, *J* 7.0Hz, 2H), 1.96 (s, 3H), 1.35 (m, *J* 6.0 Hz, 4H), 0.86 (t, *J* 7.3Hz, 3H). +EI MS (m/z) = 158. Yield (Average) 4.78 g (75%). Mpt 177.2 – 177.6, literature 173 °C [6].

6.4.2.6. 3-Methyl-1,2-cyclopentanedione dioxime.

The above procedure (6.4.2.1) was followed, 3-methyl-1,2-cyclopentanedione (2.56 g) was added to the reaction vessel as described above. However it was necessary to recrystallise with a solution of water and acetone in place of methanol.

Anal calculated for $C_6H_9N_2O_2$ C 50.66, H 7.04, N 19.70, Found C 43.75, H 6.13, N 16.29 ; FTIR (KBr disk) 3450, 3200, 3000, 2900, 2850, 1637 (C=N), 1616 (C=N), 1462, 1425, 1401, 1318, 1274, 1256, 1197, 1173, 1116, 1078, 1062, 1014, 989, 952, 920, 814, 778, 711, 668, 631. NMR, ^{13}C {^1H} (CD_3COCD_3, 100.6 MHz, 298 K) 161.38 (C=N), 157.54 (C=N), 34.77, 25.61, 18.09, 17.16. ; ^1H (CD_3COCD_3, 250.13MHz, 298 K) 10.99 (s, 2H), 3.70 (s, 1H), 3.10 (t, 9.0 Hz, 2H), 2.90 (m, 9.0 Hz,

2H), 1.50 (d, 2.0Hz, 3H). +FAB MS (m/z) = 143, Yield (Average) 3.66 g, 65 %. Mpt 145-146°C Lit. Value 145-146°C [7].

6.4.2.7. 3,6-Diethylocta-4,5-dioxime.

The procedure outlined previously was followed but smaller quantities of each reactant were used owing to the low yields of diketone synthesised. After analysis of product and literature it was apparent that this procedure did not work, this procedure was repeated a further two times, using other solvents such as dry methanol and ethanol. Other synthetic routes were attempted [8-10] but with no success, also other diketones were used as controls for each route to ensure that it was the dione and not the route which was the obstacle. From analysis it emerged that the monoxime had been made, see figure 6.3 [2].

Figure 6.3. Structure of monoxime.

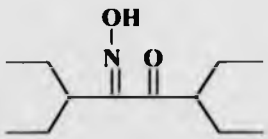

Anal calculated for $C_{12}H_{23}O_2N$ C 67.60, H 10.79, N 6.57, found C 67.09, H 10.85, N 6.69. NMR ^{13}C {^1H} ($CDCl_3$, 100.6 MHz, 298 K) 203.57 (C=O), 161.23 (C=N), 48.18, 39.64, 24.60, 24.34, 12.35, 11.62. ^1H ($CDCl_3$, 250.13MHz, 298 K), 3.85 (m, *J* 5.4Hz, 1H), 3.57 (m, *J* 5.0Hz, 1H), 2.43 (m, *J* 2.5Hz, 2H), 2.15 (m, *J* 7.6Hz, 2H), 2.00 (m, *J* 7.0Hz, 2H), 1.92 (m, *J* 5.1Hz, 2H), 1.29 (t, *J* 2.0Hz, 6H), 1.18 (t, *J* 2.7Hz, 6H). FTIR 3395 (OH), 1672ν (C=O).+EI MS (m/z) = 213, Mpt 59.0°C, Lit Value 60.5°C [2].

6.5 Synthesis of cobalt (II) complexes.

6.5.1. Reagents and sources.

Cobalt acetate tetrahydrate, Aldrich, boron trifluoride etherate, Aldrich, ethyl acetate, Fisons, sodium hydrogen carbonate, Aldrich., methanol, Fisons. 2,3-Pentanedione dioxime, 2,3-Hexanedione dioxime, 3,4-Hexanedione dioxime, 2,3-Heptanedione dioxime, 3-Methyl-1,2-cyclopentanedione dioxime, as prepared previously.

Glyoxime, Aldrich.

A nitrogen atmosphere was maintained throughout the preparation and isolation. The purification stage was not carried out under nitrogen. However, the time that the catalyst spends wet with either ethyl acetate or methanol was kept to a minimum. The source of cobalt used was cobalt (II) acetate tetrahydrate. In order to keep the amount of water in the preparation to a minimum, this is first dried by heating under vacuum ,100 °C, 5-6 hours, the pink powder eventually changes to a purple colour when dry. The ethyl acetate was deoxygenated by purging thoroughly with nitrogen prior to use.

6.5.2.1 Preparation of $CoEt_2Me_2BF$ [11].

To a Schlenk equipped with a magnetic follower under a nitrogen atmosphere, 2,3-pentanedionedioxime (4.47 g, 0.0344 mol) and anhydrous cobalt acetate (3.14 g, 0.0126 mol) were added. The boron trifluoride etherate (13.03 mL, 0.09 mol) was added via syringe over a period of 10 minutes immediately following the addition of ethyl acetate (77.12 mL, 0.87 mol), with vigorous stirring. A slight exotherm was noted and the reaction solution became a deep orange/yellow colour prior to the complete addition of the BF_3. The resulting solution was warmed to 50 °C and held at this temperature for 15 minutes to complete the reaction prior to cooling back to room temperature. Sodium bicarbonate (3.57 g, 0.042 mol) was then added in portions so as

to avoid excessive frothing. When the bicarbonate addition was complete, the reaction mixture was cooled to around 10 °C, and stirred for 1 hour to allow the product to crystallise. In situ filtration was then attempted followed by washing with water and methanol. However due to the excessive solubility of the product in these solvents minimal washing was carried out. Once washing was complete the filtrate was placed in the refrigerator to allow the powder to crystallise, this was then filtered to separate the powder from the solvent. Anal calculated for $C_{12}H_{18}N_4O_6F_4B_2Co$ C 30.19, H 3.77, N 11.74, Found C 27.79, H 4.47, N 12.69. + FAB MS (m/z) = 460. Yield 1.89 g, 35%.

6.5.2.2. Preparation of $CoEt_4BF$.

The procedure outlined above was followed with the exception that 3,4-hexanedione dioxime (3.20 g, 0.02 mol) was used with cobalt acetate (2.25 g, 9 mmol), boron trifluoride etherate (10 mL, 0.07 mol), ethyl acetate (55 mL, 0.62 mol), sodium hydrogen carbonate (2.56 g, 0.03 mol) and methanol (36 mL). A portion of the product was recrystallised from a 75/25 solution of methanol / water. The X-ray diffraction structure in chapter 2 shows the presence of two methanol groups bonded to the cobalt atom. Anal calculated for $C_{14}H_{22}N_4O_6B_2F_4Co$ C33.27, H 4.36, N 11.09, Found C 24.63, H 4.09, N 9.39. From FAB MS the presence of two methanol groups was not observed.

6.5.2.3. Preparation of CoH_4BF.

The procedure outlined previously was followed but with the exception that glyoxime was used (4.35 g, 0.049 mol) with cobalt acetate (3.05 g, 0.012 mol), boron trifluoride etherate (13 mL, 0.09 mol), ethyl acetate (75 mL), sodium hydrogen carbonate (3.48

g, 0.041 mol). The product was washed with methanol at the purification stage. The complex proved to be only sparingly soluble in methanol therefore repetitive washes were carried out. Anal calculated for $C_6H_6N_4O_6F_4B_2Co$, C 18.32, H 1.52, N 14.25, Found C 9.42, H 1.31, N 10.47. +FAB MS (m/z) = 392. Yield 3.97 g, (84%).

6.5.2.4. Preparation of $CoMe_2Prop_2BF$.

The procedure outlined above was followed with the exception that 2,3-hexanedione dioxime (3.20 g, 0.02 mol) was used with cobalt acetate (2.25 g, 9 mmol), boron trifluoride etherate (10 mL, 0.07 mol), ethyl acetate (55 mL, 0.62 mol), sodium hydrogen carbonate (2.56 g, 0.03 mol) and methanol (36 mL).

The first attempt at synthesising this complex resulted in a low yield being obtained. This was mainly due to the high solubility of the complex in methanol, therefore during the repeat synthesis no in-situ filtration was carried out. Water was added to the ethyl acetate solution to remove impurities. The whole solution was placed in a separating funnel and the water layer removed. $MgSO_4$ was then added to the ethyl acetate solution to remove any residual water, the solution was then filtered to remove the $MgSO_4$ and the solvent was removed by rotary evaporation. The resulting product was then dried in a vacuum dessicator over P_2O_5 for a few days to give brown powder. Yield 3.00 g, (38%).

6.5.2.5. Preparation of $CoMe_2Bu_2BF$.

The procedure outlined above was followed with the exception that 2,3-heptanedione dioxime (3.16 g, 0.02 mol) was used, and new quantities used were cobalt acetate (2.25 g, 9 mmol), boron trifluoride etherate (10 mL, 0.07 mol), ethyl acetate (55 mL, 0.62 mol), sodium hydrogen carbonate (2.56 g, 0.03 mol) and methanol (36 mL).

The first time this product was synthesised it was washed with both water and methanol but this proved unsatisfactory owing to the fact that no product remained on the filter, therefore during the repeat synthesis no insitu filtration occurred. Water was added to the ethyl acetate solution to remove impurities. The whole solution was placed in a separating funnel and the water layer removed. $MgSO_4$ was then added to the ethyl acetate solution to remove any residual water, the solution was then filtered to remove the $MgSO_4$, and the solvent was removed by rotary evaporation. The remaining product was then dried in a vacuum dessicator over P_2O_5 for a few days to give brown powder. Yield 3.50 g, (43%).

6.5.2.6. Preparation of Co(3–Methyl-1,2-Cyclopent)BF.

3-Methyl-1,2-Cyclopentanedione dioxime 1.84 g, 0.013 mol, cobalt acetate 1.05 g, 0.0042 mol, boron trifluoride etherate 4.38 mL, ethyl acetate 25.91 mL, sodium hydrogen carbonate 1.20 g, methanol 17.28 mL.

The procedure outlined previously was followed however, to give a water soluble product which was purified by transferring to a round bottomed flask and the water was subsequently removed by rotary evaporation yielding a brown powder. +FAB MS (m/z) = 468. Yield 0.8339 g, (46%).

6.6. The synthesis of cobalt (III) complexes [12].

As shown in figure 6.2 it can be seen that this synthesis involves three key stages and that isolation and characterisation at each stage is possible. This section will therefore be split into the three stages and dealt with individually. The dioximes used were identical to the ones detailed above for the cobalt (II) complexes.

6.6.1. The synthesis of ethyl pyridinato-cobaloximes.

6.6.1.1 Reagents and sources.

Methanol, Hi dry, Fisons, $CoCl_2.6H_2O$, Aldrich, sodium hydroxide, Aldrich, water, pyridine, Aldrich, sodium borohydride, Aldrich, ethyl bromide, Aldrich. dimethyl glyoxime, Aldrich, 2,3-pentanedione dioxime, 3,4-Hexanedione dioxime, as prepared previously.

6.6.1.2. Preparation of $CoMe_4H_2O$/PyEt.

Methanol (50 mL) was degassed by purging with nitrogen for 20 minutes at room temperature. To this $CoCl_2.6H_2O$ (2.0171 g, 0.008 mol) and dimethyl glyoxime (3.00 g, 0.025 mol) were added. After ten minutes the solution S1 (sodium hydroxide: 0.819 g, 0.02 mol; water 0.819 g) was added followed by the slow addition of pyridine (0.670 mL, 0.008 mol). The reaction mixture was cooled to –20 °C, and stirring under nitrogen was continued for 20 minutes. The second sodium hydroxide solution, S2 (sodium hydroxide: 0.532 g, 0.013 mol; water 0.532 g) and the sodium borohydride (0.365 g, 0.096 mol) were added slowly. Ethyl bromide (0.590 mL, 0.008 mol) was added dropwise over 20 minutes and the reaction mixture was allowed to reach room temperature. Half of the solvent was removed by rotary evaporation and 40 mL of cold water was added. The orange compound was filtered and washed with a pyridine/water (5/95) solution, and dried over P_2O_5. Anal calculated for $C_{11}H_{26}O_4N_5Co$, C 39.18, H 7.77, N 20.76, Found C 43.26, H 5.99, N 18.61. NMR, $^{13}C\{^1H\}$ (CD_3COCD_3, 100.6 MHz, 298 K), 150.95, 149.87 (C=N), 139.10, 126.37, 16.19, 12.06, 9.48. ^1H (CD_3COCD_3, 300 MHz, 298 K) 8.53 (d, *J* 4.9Hz, 2H), 7.90 (t, *J* 1.5Hz, 1H), 7.48 (t, *J* 1.5Hz, 2H), 2.09 (s, 12H), 1.57 (q, *J* 7.6Hz, 2H),

0.33 (t, *J* 7.6Hz, 3H). FTIR (ATR, solid).3201, 2969, 2914, 1601 (C=N), 1557 (C=N), 1491, 1446, 1377, 1362, 1226, 1165 (N-O), 1084, 1070, 1026, 972, 908, 731, 708, 693, 649, 631, 580. +FAB MS (m/z)= Yield 3.16 g, (99%).

6.6.1.3. Preparation of $CoMe_2Et_2H_2O$/PyEt.

The above procedure was followed with the exception that 2,3-pentanedione dioxime (2.47 g, 0.020 mol) was used.

Anal calculated for $C_{17}H_{28}N_5O_4Co$, C47.95, H 6.58, N 16.45, Found C 45.45, H 6.17, N 15.68. NMR, ^{13}C {^1H} (CD_3COCD_3, 100.6 MHz, 298 K). 150.82, 149.50, 139.13, 126.36, 19.65, 16.08, 11.97, 10.91. ^1H (CD_3COCD_3, 300 MHz, 298 K) 8.54 (d, *J* 4.5Hz, 2H), 7.90 (t, *J* 1.9Hz, 1H), 7.48 (t, *J* 1.5Hz, 2H), 2.59 (q, *J* 3.8Hz, 4H), 2.07 (s, 6H), 1.57 (q, *J* 7.6Hz, 2H), 0.94 (t, *J* 2.7Hz, 6H), 0.34 (t, J 7.6Hz, 6H). FTIR (ATR, solid), 3108, 3075, 3045, 2962, 2930, 2911, 2867, 1600 (C=N), 1548 (C=N), 1505, 1489, 1442, 1367, 1318, 1269, 1225, 1166 (N-O), 1138, 1106, 1059, 1023, 947, 863, 805, 768, 703, 634, 586. Yield 2.56 g, (75%).

6.6.1.4. Preparation of $CoEt_4H_2O$/PyEt.

Again the procedure outlined previously was adhered to with the exception that 3,4-hexanedione dioxime (3.00 g, 0.02 mol) was used in place of the dimethyl glyoxime.

Anal calculated for $C_{19}H_{32}N_5O_4Co$, C 50.34, H 7.06, N 15.46, Found 48.83, H 6.86, N 15.52. NMR ^{13}C {^1H} (CD_3COCD_3, 100.6 MHz, 298 K), 154.99, 150.71, 139.16, 126.34, 19.76, 16.00, 11.11. ^1H (CD_3COCD_3, 300 MHz, 298 K), 13.10 (s, 1H), 13.02 (s, 1H), 8.54 (d, *J* 5.1Hz, 2H), 7.90 (t, *J* 7.6Hz, 1H), 7.50 (d, *J* 6.8Hz, 2H), 2.60 (q, *J* 7.6Hz, 8H), 1.52 (q, *J* 4.8Hz, 2H), 0.97 (t, *J* 7.5 Hz, 12H), 0.38 (t, *J* 7.6 Hz, 3H). FTIR (ATR, solid), 3212 (O-H), 2972, 2939, 2912, 2871, 1601 (C=N), 1548 (C=N), 1445, 1366, 1323, 1265, 1219, 1161 (N-O), 1109, 1066, 1036, 1013, 964, 913,

883, 855, 827, 767, 699, 632. +FAB MS (m/z) = 453. Yield 2.74 g, (75%).

6.6.2. Bridging of cobaloximes using boron trifluoride etherate.

6.6.2.1. Reagents and sources.

Boron trifluoride etherate, Aldrich, ether, Hi dry, $CoMe_4H_2O$/PyEt, $CoMe_2Et_2H_2O$/PyEt, and $CoEt_4H_2O$/PyEt as prepared previously.

6.6.2.2. Preparation of $CoMe_4BF$/PyEt, (CoBF/PyEt).

Boron trifluoride etherate (7.20 g, 0.05 mol) and ether (3.90 mL) were cooled under a nitrogen atmosphere at –20 °C for 40 minutes. The cobaloxime ($CoMe_4H_2O$/PyEt, 2.77 g, 0.0069 mol) was added over twenty minutes. The reaction was allowed to reach room temperature, then the compound was isolated by filtration and washed with ether.

Anal calculated for $C_{15}H_{22}N_5O_4B_2F_4Co$, C 36.51, H 4.46, N 14.19, Found C 33.00, H 4.32, N 12.89.+FAB MS (m/z) = 493.03. Yield 1.75g, (52%).

6.6.2.3. Preparation of $CoEt_2Me_2BF$/PyEt.

The procedure outlined above was followed with the exception that $CoEt_2Me_2H_2O$/PyEt (2.00 g (4.71 mmol) was used in place of $CoMe_4H_2O$/PyEt. New quantities for ether (2.92 mL) and $BF_3.Et_2O$ (5.39 g, 0.03 mol) were also used. Anal calculated for $C_{15}H_{21}N_5O_4B_2F_4Co$, C 39.19, H 4.80, N 11.52, Found C 33.82, H 3.63, N 8.25. +FAB MS (m/z) = 521. Yield 0.72 g, (30%).

6.6.2.4. Preparation of $CoEt_4BF$/PyEt.

Again the procedure outlined previously was adhered to with the exception of a different complex and new quantities being used. $CoEt_4H_2O$/PyEt 2.35 g, 0.005 mol;

$BF_3.Et_2O$ 6.14 g, 0.04 mol, ether 3.33 mL. Anal. calculated for $C_{19}H_{30}N_5O_4B_2F_4Co$, C 41.64, H 5.48, N 12.78, Found C 34.91, H 4.51, N 9.85. +FAB MS (m/z) = 524.57 Yield 1.33 g, (49 %).

6.6.3.Replacement of pyridine ligands for water in cobalt III complexes.

6.6.3.1. Reagents and sources.

$CoMe_4BF/PyEt$, $CoEt_2Me_2BF/PyEt$ and $CoEt_4BF/PyEt$, as prepared previously, Water.

6.6.3.2. Preparation of $CoMe_4BF/H_2OEt$.

Water (10.16 mL) was degassed by purging with nitrogen at 30°C for 10 minutes. The $CoMe_4BF/PyEt$ complex (0.50 g, 0.0010 mol) was added and the solution heated to 30 °C for 40 minutes. The solution was allowed to cool to room temperature and the compound was isolated by filtration, and washed with water. Anal calculated for $C_{10}H_{19}N_4O_5B_2F_4Co$, C 27.78, H 4.40, N 13.38, Found C 27.93, H 4.43, N 12.89. +FAB MS (m/z) = 433. Yield 0.28 g, (65%).

6.6.3.3. Preparation of $CoMe_2Et_2BF/H_2OEt$.

The procedure outlined above was followed and repeated a number of times it was however apparent that this synthetic method did not work for this complex. It however emerged from an X-ray crystal structure that the solution at the end of procedure 6.6.2.3., after leaving for a couple of weeks yielded the above desired compound.

Anal calculated for $C_{12}H_{23}N_4O_5B_2F_4Co$, C 31.33, H 5.00, N 12.19, found C 28.79, H 4.85, N 10.92. +FAB MS (m/z)= 533 (Se 28). Yield. = 1.20 g

6.6.3.4. Preparation of $CoEt_4BF/H_2OEt$.

Again the procedure outlined previously was attempted but again it did not work. However, the discovery of keeping the solution from section 6.5.2.4., led to the formation of the desired product. Anal calculated for $C_{14}H_{27}N_4O_5B_2F_4Co$, C 34.46, H 5.54, N 11.49, found C 34.01, H 5.52, N 11.12. +FAB MS (m/z) = 488.Yield = 0.50 g

6.7. Bulk polymerisations of cobalt (II) and cobalt (III) complexes at 60 °C with MMA.

The following experimental procedure describes the commonly used method of obtaining the catalytic chain transfer constant (C_s) of catalytic chain transfer agents. C_s is a measure of molecular weight reduction obtained during a polymerisation using a chain transfer agent with that of an identical polymerisation with the chain transfer agent being absent.

The monomer was passed down a basic alumina column to remove inhibitor and degassed prior to use. All solutions were prepared under an atmosphere of nitrogen.

6.7.1. Reagents and sources.

Methyl methacrylate, Aldrich, CoBF, $CoEt_2Me_2BF$, $CoEt_4BF$, $CoMe_2Prop_2BF$, $CoMe_2Bu_2BF$, CoBF/PyEt, $CoEt_2Me_2BF$/PyEt, $CoEt_4BF$/PyEt, CoBF/H_2OEt, $CoEt_2Me_2BF/H_2OEt$, $CoEt_4BF/H_2OEt$.

6.7.2. Procedure:

Firstly 3 stock solutions were made up:

S1

Contained 2.5mg of the catalyst under investigation and 10ml of methyl methacrylate (MMA).

S2

This contained 1ml of S1 and 9ml of MMA.

S3

This stock solution contained 150mg of AIBN and 24ml of MMA.

From stock solutions S2 and S3 five other solutions were made.

Table 6.1 below, indicates the quantities of each stock solution required and the amount of MMA added for each sample.

Table 6.1. Quantities of stock solutions used for bulk polymerisations of MMA at 60 °C, using cobalt II and cobalt III complexes.

Solution	Volume S2/mL	Volume S3/mL	Volume MMA/mL
A	0.00	4.00	1.00
B	0.10	4.00	0.90
C	0.20	4.00	0.80
D	0.30	4.00	0.70
E	0.40	4.00	0.60

Solutions A-E were then freeze pumped thawed three times before heating to 60°C in a water bath for 15 minutes, after which time the reactions were quenched by placing

in ice to allow the samples to return to room temperature. GPC's of each sample were then run and the Mn and PDi noted. From the information obtained it was then possible to calculate the chain transfer constant of the desired complex by one of the three methods outlined in this work.

6.8 Bulk polymerisations of Styrene at 80, 90, 100, 120 and 140 °C using cobalt (II) and cobalt (III) complexes.

From this procedure it was possible to evaluate the chain transfer constant for each complex. The monomer was passed down a basic alumina column to remove inhibitor and degassed prior to use. Again all solutions were prepared under an atmosphere of nitrogen.

6.8.1. Reagents and sources.

Styrene, Aldrich, CoBF, $CoEt_2Me_2BF$, $CoEt_4BF$, CoBF/PyEt, $CoEt_2Me_2BF$/PyEt, $CoEt_4BF$/PyEt, CoBF/H_2OEt, $CoEt_2Me_2BF$/H_2OEt, $CoEt_4BF$/H_2OEt.

6.8.2. Procedure.

S1

This contained 48 mg of the desired complex and 10 mL of ethyl acetate.

S2

This contained 1 mL of S1 and 9 mL of Styrene

Five solutions containing varying quantities of S2 and styrene were then prepared, table 6.2 gives relevant quantities of each.

Table 6.2. Quantities of stock solution and monomer required for bulk polymerisation of styrene.

Sol[n]	S2 (mL)	Sty (mL)
A	0.0	5.0
B	0.10	4.90
C	0.20	4.80
D	0.30	4.70
E	0.40	4.60

All five solutions were then freeze pump thawed three times and heated in an oil bath at the relevant temperature and time. Once complete the solutions were quenched in liquid nitrogen and allowed to reach room temperature. GPC and conversion analysis was undertaken. Table 6.3, gives time and temperature information for the bulk polymerisations of styrene.

Table 6.3. Time and temperature information for the bulk polymerisations of styrene using cobalt II and cobalt III complexes.

Time (mins)	Temperature (°C)
60	80
60	90
45	100
30	120
15	140

6.9. Partitioning experiments for cobalt II and cobalt III complexes in MMA and Water.

Partition values play an important role in the evaluation of the chain transfer agent because if the complex is to be used for emulsion polymerisations it must be soluble in both the water and monomer phase. The monomer under investigation here is methylmethacrylate (MMA). Both monomer and water were degassed prior to use and inhibitor removed from the MMA.

6.9.1. Procedure.

Before any solutions were made up, the volumetric flasks were vacuum/degassed, an air sensitive cell was used to record the UV spectra.

6.9.1.1. Water stock solutions for the partitioning experiments.

In total 4 solutions were made. Stock solution (S1) was made up to a known concentration of catalyst, this was then filled up to the line with de-ionised water and weighed. From this solution various quantities were taken and placed in other volumetric flasks which were then filled up to the line with de-ionised water (S2 onwards). A UV spectrum of each solution was then recorded and a graph of concentration versus absorbance was plotted, which would then be used in the final stage of evaluation of the catalyst.

Catalysts investigated in this way were CoBF, $CoMe_2Et_2BF$, $CoEt_4BF$, CoBF/PyEt, $CoEt_2Me_2BF$/PyEt, $CoEt_4BF$/PyEt, CoBF/H_2OEt, $CoEt_2Me_2BF$/H_2OEt, $CoEt_4BF$/H_2OEt.

Appendix 5 gives concentrations and absorbance values for the stock solutions of each complex.

6.9.1.2. MMA stock solutions for the partitioning experiments.

Stock solution (S1) containing a known concentration of catalyst was made, this time being filled up to the line with MMA and again weighed empty, plus complex plus monomer. From this solution known quantities were taken and placed in other volumetric flasks and filled up to the line with MMA (S2 onwards). A UV spectrum of each solution was then recorded and a graph of concentration versus absorbance was plotted, for use in the final stage of evaluation of the complex. Complexes evaluated were CoBF, $CoMe_2Et_2BF$, $CoEt_4BF$, CoBF/PyEt, $CoEt_2Me_2BF$/PyEt, $CoEt_4BF$/PyEt, CoBF/H_2OEt, $CoEt_2Me_2BF$/H_2OEt, $CoEt_4BF$/H_2OEt.

Appendix 5 gives concentrations and absorbance values for each complex and its respective stock solutions.

In total three different compositions of monomer water were used to evaluate the complexes partitioning properties, 50/50, 90/10 and 10/90 monomer/water respectively. The combinations consisted of a total volume of 6 mL, therefore for a 50/50 composition 3 mL of each component was used. To achieve this 20 mg of the desired complex was added to a stirred solution of monomer/water of chosen composition. This solution was then allowed to settle and the two layers were then analysed individually on the UV-VIS spectrometer and their respective absorbances recorded. The concentration of catalyst in each phase was determined and interpreted as a percentage of catalyst in each layer from the plots of concentration versus absorbance for each phase.

6.10. References.

1) Babudri, F.; Fiandanese, V.; Marchese, G.; Punzi, A. ; *Tett.Lett.*, **1995**, *36*, 7305.

2) Burkin, A. R.; Preston, J. S. ; *J. Inorg. Nucl. Chem.*, **1975**, *37*, 2187.

3) Abusamleh, A. A. ; *J. Coord. Chem.*, **1991**, *23*, 91.

4) Ponzio, J. ; *Gazz. Chim. Ital.*, **1901**, *31*, 404.

5) Helmann; Baret ; *J. CR Seances Acad. Sci. Ser. D*, **1968**, *267*, 579.

6) Boureault; Locquin ; *Bull. Soc. Chim. Fr.*, **1906**, *3*, 653.

7) Tischtschenko; Lischkewitsch; Skulskaja ; *Zh. Prikl. Khim. (Leningrad)*, **1936**, *3*, 375.

8) Lance, K. A.; Dzugan, S.; Busch, D. H. ; *Gazz. Chim. Ital.*, **1996**, *126*, 251.

9) Nakamura, A.; Konishi, A. ; *J. Am. Chem. Soc.*, **1978**, *100*, 3443.

10) Paping, L. R. M.; Rummens, C. P. J. ; *Polyhedron*, **1985**, *4*, 723.

11) Bakac, A.; Brynildson, M. E.; Espenson, J. H. ; *Inorg. Chem.*, **1986**, *25*, 4108.

12) Moad, G.; Moad, C. L.; Krstina, J.; Rizzardo, E.; Thang, S.; Fryd, M. ; World Patent 96/15158, (**1996**).

Chapter 7

Conclusions

7.0. Conclusions.

The infra red results in chapter 2 show that catalyst structure affects certain stretching frequencies, NMR data shows the presence of characteristic peaks which are indicative of a successful synthesis. X-ray crystallography confirms the structure of three of the complexes.

The chain transfer constants in bulk polymerisations with MMA (Chapter 3) are affected by the equatorial and axial ligands. An increased number of carbons on the skeletal backbone tends to decrease C_s. The presence of strong axial base ligands such as pyridine in cobalt (III) complexes lower C_s due to an increase in electron density around the cobalt center which imparts a strengthening of the cobalt carbon bond, allowing ease of abstraction to be decreased. Cobalt (III) complexes with water as the axial ligands behave similarly to the cobalt (II) analogues giving very similar C_s values and conversions. Axial pyridine ligands in cobalt (III) complexes however give approximately half the value for C_s. Decreasing initiator concentration leads to a decrease in C_s and rate of polymerisation. The C_s values of which are approximately half their value when compared to the increased initiator concentration C_s values. A decrease in percentage conversion is observed with a lowering of initiator concentration. The decrease in C_s is attributable to the fact that CCTP is reliant on a constant radical feed, the source of radicals in a reduced initiator system is therefore decreased and generation of these radicals is more reliant on the CCTP process generating these. Fewer radicals results in fewer propagating species and therefore fewer transfer steps.

The bulk polymerisation of styrene in the presence of CCTA's resulted in lower values for C_s being obtained. There seems to be no correlation between an increase in temperature and an increase in C_s. The $E_{transfer}$ values are not directly

connected with catalyst structure although if one only considers the cobalt (III) analogues containing water and pyridine as axial ligands it would appear that a lower value of $E_{transfer}$ is found for the water analogues. The cobalt (III)-water analogues behave similarly to their cobalt (II) analogues and sometimes exhibit higher chain transfer constants. It can therefore be concluded that the pyridine axial ligand does hinder chain transfer activity. For accurate $E_{transfer}$ values it would have been better to run the polymerisations to higher conversion owing to the fact that an equilibrium between Co(II) and Co(III) complexes must be established before effective CCTP is observed and accurate $E_{transfer}$ values would be obtained.

Preliminary results conclude that the complexes would be effective as chain transfer agents in emulsion polymerisations. The structure of the complex plays an important role in its partitioning properties. The presence of increased alkyl groups on the equatorial arms of the complexes increases the hydrophobic properties of the complex. When this is combined with the interaction of a strong base, pyridine in this work, the hydrophobic properties of the complex is further increased. The replacement of the pyridine axial ligand with water reduces the hydrophobic nature of the complex. Cobalt (II) and cobalt (III)- water analogues when compared with cobalt (III) – pyridine analogues are more hydrophilic in nature, although all complexes are hydrophobic in nature. The change of monomer and water compositions allows the properties of the complexes to be further changed with regard to their hydrophilic nature. When analysing the C_s values for all complexes in both monomers it is important to consider the possibility that both impurity and axial ligand labilty and hence insertion of monomer molecules on to the complex could all influence the C_s values obtained.

Appendix 1

Example of a magnetic moment calculation.

Method for magnetic moment calculation for complex II (CoBF)

A. Weight of tube and sample (g)	0.9518
B. Weight of empty tube (g)	0.8045
C. Weight of sample (g)	0.1473
D. Length of sample (cm)	2.20
E. Room Temperature (K)	291.55
F. Reading of empty tube	-30
G. Reading of packed tube	132 131 134
H. Average reading of packed tube	132.333
I. Tube constant	1.151
J. Magnetic susceptibility (c.g.s. units)	2.791E-06
K. Magnetic susceptibility	3.507E-08
L Relative molar mass (kg mol^{-1})	4.468E-01
M. Molar magnetic susceptibility (m^3 mol^{-1})	1.576E-08
Magnetic Moment (BM)	1.705

Calculation of magnetic moment using the labels from the table above:

$J = I \times D \times ((H - F)/(C \times 10^{9})$ {c.g.s. units}

$K = 4 \times \pi \times 10^{-3} \times J$ {S.I. units}

$M = K \times L$

Appendix 2

X-ray crystallography data

$CoEt_4BF$ Crystal data

Table 1. Crystal data and structure refinement for 1(jencm).

Identification code	jencm
Empirical formula	$C_{14}H_{26}B_2CoF_4N_4O_6$
Formula weight	502.94
Temperature	200(2) K
Wavelength	0.71073 Å
Crystal system	Monoclinic
Space group	$P2_1/n$
Unit cell dimensions	a = 11.5701(3) Å alpha = 90° b = 7.83080(10) Å beta = 90.7830(10)° c = 11.9889(3) Å gamma = 90°
Volume, Z	1086.13(4) $Å^3$, 2
Density (calculated)	1.538 Mg/m^3
Absorption coefficient	0.862 mm^{-1}
F(000)	518
Crystal size	0.50 x 0.20 x 0.10 mm
θ range for data collection	2.43 to 28.55°
Limiting indices	$-12 \le h \le 15$, $-10 \le k \le 9$, $-16 \le l \le 13$
Reflections collected	6263
Independent reflections	2510 (R_{int} = 0.0251)
Absorption correction	SADABS
Max. and min. transmission	1.0000 and 0.8553
Refinement method	Full-matrix least-squares on F^2
Data / restraints / parameters	2510 / 0 / 142
Goodness-of-fit on F^2	1.015
Final R indices [I>2σ(I)]	R1 = 0.0338, wR2 = 0.0768(for 1968reflections)
R indices (all data)	R1 = 0.0514, wR2 = 0.0834
Largest diff. peak and hole	0.552 and -0.288 $eÅ^{-3}$

Table 2. Atomic coordinates [x 10^4] and equivalent isotropic displacement parameters [$Å^2$ x 10^3] for 1. U(eq) is defined as one third of the trace of the orthogonalized U_{ij} tensor.

	x	y	z	U(eq)
Co(1)	0	0	0	20(1)
B(1)	348(2)	2758(3)	-1865.9(19)	25(1)
O(1)	-658.0(11)	1602.3(19)	-2080.8(11)	25(1)
O(2)	1438.3(12)	1908.1(19)	-1491.2(11)	25(1)
O(3)	-484.3(12)	2339(2)	1024.4(12)	29(1)
N(1)	-997.0(14)	685(2)	-1167.0(13)	21(1)
N(2)	1346.6(13)	1090(2)	-482.4(13)	20(1)
F(1)	34.5(11)	3979.8(16)	-1069.4(10)	32(1)
F(2)	585.0(10)	3486.8(17)	-2879.1(10)	33(1)
C(1)	-2059.0(16)	174(3)	-1120.4(16)	20(1)
C(2)	-2993.9(18)	676(3)	-1933.7(17)	27(1)
C(3)	-3632(2)	2254(3)	-1523(2)	41(1)
C(4)	2279.8(16)	858(3)	105.5(16)	20(1)
C(5)	3440.3(17)	1544(3)	-211.2(18)	25(1)
C(6)	3523(2)	3472(3)	-70(2)	38(1)
C(7)	-1572(2)	2564(3)	1560(2)	42(1)

Table 3. Bond lengths [Å] and angles [°] for 1.

Co(1)-N(2)#1	1.875(2)	Co(1)-N(2)	1.875(2)
Co(1)-N(1)	1.879(2)	Co(1)-N(1)#1	1.879(2)
Co(1)-O(3)	2.279(2)	Co(1)-O(3)#1	2.279(2)
B(1)-F(2)	1.373(3)	B(1)-F(1)	1.403(3)
B(1)-O(2)	1.490(3)	B(1)-O(1)	1.494(3)
O(1)-N(1)	1.372(2)	O(2)-N(2)	1.374(2)
O(3)-C(7)	1.432(3)	N(1)-C(1)	1.294(2)
N(2)-C(4)	1.294(2)	C(1)-C(4)#1	1.486(3)
C(1)-C(2)	1.499(3)	C(2)-C(3)	1.524(3)
C(4)-C(1)#1	1.486(3)	C(4)-C(5)	1.500(3)
C(5)-C(6)	1.522(3)		

N(2)#1-Co(1)-N(2)	180.0	N(2)#1-Co(1)-N(1)	81.68(7)
N(2)-Co(1)-N(1)	98.32(7)	N(2)#1-Co(1)-N(1)#1	98.32(7)
N(2)-Co(1)-N(1)#1	81.68(7)	N(1)-Co(1)-N(1)#1	180.0
N(2)#1-Co(1)-O(3)	89.31(6)	N(2)-Co(1)-O(3)	90.69(6)
N(1)-Co(1)-O(3)	91.08(6)	N(1)#1-Co(1)-O(3)	88.92(6)
N(2)#1-Co(1)-O(3)#1	90.69(6)	N(2)-Co(1)-O(3)#1	89.31(6)
N(1)-Co(1)-O(3)#1	88.92(6)	N(1)#1-Co(1)-O(3)#1	91.08(6)
O(3)-Co(1)-O(3)#1	180.0	F(2)-B(1)-F(1)	112.0(2)
F(2)-B(1)-O(2)	105.9(2)	F(1)-B(1)-O(2)	109.0(2)
F(2)-B(1)-O(1)	105.3(2)	F(1)-B(1)-O(1)	108.8(2)
O(2)-B(1)-O(1)	115.8(2)	N(1)-O(1)-B(1)	114.21(14)
N(2)-O(2)-B(1)	113.47(14)	C(7)-O(3)-Co(1)	124.38(14)
C(1)-N(1)-O(1)	118.6(2)	C(1)-N(1)-Co(1)	116.94(14)
O(1)-N(1)-Co(1)	124.38(11)	C(4)-N(2)-O(2)	118.1(2)
C(4)-N(2)-Co(1)	117.31(13)	O(2)-N(2)-Co(1)	123.94(11)
N(1)-C(1)-C(4)#1	112.2(2)	N(1)-C(1)-C(2)	124.6(2)
C(4)#1-C(1)-C(2)	123.0(2)	C(1)-C(2)-C(3)	110.5(2)
N(2)-C(4)-C(1)#1	111.8(2)	N(2)-C(4)-C(5)	123.7(2)
C(1)#1-C(4)-C(5)	124.5(2)	C(4)-C(5)-C(6)	112.5(2)

Symmetry transformations used to generate equivalent atoms:

#1 -x,-y,-z

Table 4. Anisotropic displacement parameters [$Å^2 \times 10^3$] for 1.

The anisotropic displacement factor exponent takes the form:

$-2\pi^2 [(ha^*)^2 U_{11} + ... + 2hka^*b^* U_{12}]$

	U11	U22	U33	U23	U13	U12
Co(1)	13(1)	23(1)	23(1)	5(1)	-2(1)	-2(1)
B(1)	23(1)	27(1)	26(1)	7(1)	0(1)	-1(1)
O(1)	22(1)	31(1)	21(1)	9(1)	-2(1)	-4(1)
O(2)	18(1)	31(1)	24(1)	10(1)	1(1)	-1(1)
O(3)	29(1)	26(1)	32(1)	-2(1)	4(1)	0(1)
N(1)	19(1)	22(1)	21(1)	3(1)	0(1)	-1(1)
N(2)	18(1)	22(1)	21(1)	4(1)	1(1)	0(1)
F(1)	33(1)	25(1)	36(1)	2(1)	2(1)	0(1)
F(2)	28(1)	40(1)	31(1)	16(1)	0(1)	-3(1)
C(1)	15(1)	22(1)	23(1)	-1(1)	-2(1)	0(1)
C(2)	19(1)	37(1)	26(1)	3(1)	-6(1)	-3(1)
C(3)	33(1)	42(2)	48(1)	13(1)	-3(1)	13(1)
C(4)	17(1)	19(1)	25(1)	-2(1)	0(1)	-1(1)
C(5)	16(1)	29(1)	32(1)	2(1)	-1(1)	-3(1)
C(6)	33(1)	30(1)	52(2)	-5(1)	7(1)	-12(1)
C(7)	42(2)	41(2)	45(1)	-10(1)	16(1)	-3(1)

Table 5. Hydrogen coordinates (x 10^4) and isotropic displacement parameters ($Å^2$ x 10^3) for 1.

	x	y	z	U(eq)
H(2A)	-3547	-280	-2027	33
H(2B)	-2651	917	-2669	33
H(3A)	-4240	2563	-2063	62
H(3B)	-3086	3204	-1443	62
H(3C)	-3979	2008	-800	62
H(5A)	3591	1248	-999	30
H(5B)	4044	992	257	30
H(6B)	3387	3771	711	58
H(6C)	2940	4027	-547	58
H(6A)	4295	3858	-282	58
H(7A)	-1578	3664	1949	63
H(7B)	-1687	1640	2099	63
H(7C)	-2196	2540	999	63

Table 1. Crystal data and structure refinement for coxm.

$CoEt_4H_2O/PyEt$ crystal data

Identification code	coxm
Empirical formula	C19 H32 Co N5 O4
Formula weight	453.43
Temperature	183(2) K
Wavelength	0.71073 A
Crystal system, space group	?, ?
Unit cell dimensions	a = 7.9811(10) A alpha = 83.613(2) d b = 9.1812(11) A beta = 77.304(2) d c = 15.1302(18) A gamma = 87.836(2)
Volume	1074.8(2) A^3
Z, Calculated density	2, 1.401 Mg/m^3
Absorption coefficient	0.833 mm^-1
F(000)	480
Crystal size	0.2 x 0.06 x 0.04 mm
Theta range for data collection	1.39 to 24.00 deg.
Limiting indices	-8<=h<=9, -9<=k<=10, -11<=l<=17
Reflections collected / unique	4935 / 3324 [R(int) = 0.1137]
Completeness to theta = 24.00	98.3 %
Refinement method	Full-matrix least-squares on F^2
Data / restraints / parameters	3324 / 0 / 262
Goodness-of-fit on F^2	1.055
Final R indices [I>2sigma(I)]	R1 = 0.1280, wR2 = 0.2968
R indices (all data)	R1 = 0.1824, wR2 = 0.3539
Largest diff. peak and hole	1.200 and -1.458 e.A^-3

Table 2. Atomic coordinates (x 10^4) and equivalent isotropic displacement parameters (A^2 x 10^3) for coxm.
U(eq) is defined as one third of the trace of the orthogonalized Uij tensor.

	x	y	z	U(eq)
Co(1)	8661(2)	7489(2)	7487(1)	34(1)
N(1)	7311(12)	6852(10)	6747(6)	32(2)
N(2)	10066(12)	8159(9)	6352(7)	35(2)
N(3)	7248(12)	6864(10)	8610(7)	35(2)
N(4)	9998(12)	8155(10)	8218(7)	34(2)
N(5)	9979(12)	5496(10)	7467(6)	33(2)
O(1)	5803(10)	6166(9)	7083(6)	43(2)
O(2)	11538(10)	8834(8)	6271(6)	41(2)
O(3)	5744(10)	6221(9)	8710(6)	46(2)
O(4)	11512(10)	8851(9)	7889(6)	43(2)
C(1)	7897(16)	7125(12)	5884(8)	38(3)
C(2)	6920(16)	6760(13)	5191(9)	41(3)
C(3)	5885(19)	8109(16)	4886(11)	59(4)
C(4)	9509(16)	7859(11)	5630(8)	36(3)
C(5)	10563(16)	8193(13)	4694(8)	41(3)
C(6)	11690(16)	6859(14)	4393(9)	48(3)
C(7)	7812(16)	7129(12)	9346(8)	37(3)
C(8)	6803(15)	6797(12)	10279(8)	35(3)
C(9)	5730(20)	8126(16)	10630(12)	73(5)
C(10)	9438(15)	7874(11)	9068(8)	32(3)
C(11)	10474(16)	8143(13)	9761(10)	46(3)
C(12)	11647(18)	6839(16)	9909(12)	61(4)
C(13)	11703(17)	5404(13)	7262(9)	47(3)
C(14)	12607(19)	4098(14)	7244(9)	48(3)
C(15)	11723(19)	2821(14)	7464(9)	51(4)
C(16)	9932(18)	2871(13)	7707(9)	49(4)
C(17)	9184(17)	4235(14)	7674(9)	43(3)
C(18)	7440(15)	9471(11)	7539(9)	36(3)
C(19)	5810(20)	9663(16)	7263(13)	74(5)

Table 3. Selected bond lengths [A] and angles [deg] for coxm.

Co(1)-N(1)	1.866(10)
Co(1)-N(2)	1.886(10)
Co(1)-C(18)	2.032(11)
Co(1)-N(5)	2.076(9)
N(1)-C(1)	1.287(15)
N(1)-O(1)	1.349(12)
N(2)-C(4)	1.325(16)
N(2)-O(2)	1.325(12)
N(5)-C(17)	1.315(15)
N(5)-C(13)	1.344(16)
C(1)-C(4)	1.431(17)
C(1)-C(2)	1.509(18)
C(2)-C(3)	1.547(18)
C(4)-C(5)	1.486(17)
C(5)-C(6)	1.542(15)
C(13)-C(14)	1.376(18)
C(14)-C(15)	1.362(19)
C(15)-C(16)	1.397(19)
C(16)-C(17)	1.368(17)
C(18)-C(19)	1.451(19)
N(4)-Co(1)-N(1)	179.1(4)
N(3)-Co(1)-N(1)	97.7(4)
N(1)-Co(1)-N(2)	82.3(4)
N(1)-Co(1)-C(18)	92.5(5)
N(2)-Co(1)-C(18)	90.1(4)
N(1)-Co(1)-N(5)	90.0(4)
N(2)-Co(1)-N(5)	90.0(4)
C(18)-Co(1)-N(5)	177.5(5)
C(1)-N(1)-O(1)	121.4(10)
C(1)-N(1)-Co(1)	115.7(8)
O(1)-N(1)-Co(1)	123.0(7)
C(4)-N(2)-O(2)	121.8(10)
C(4)-N(2)-Co(1)	115.2(8)
O(2)-N(2)-Co(1)	123.0(8)
C(17)-N(5)-C(13)	115.3(10)
C(17)-N(5)-Co(1)	122.2(8)
C(13)-N(5)-Co(1)	122.4(8)
N(1)-C(1)-C(4)	115.0(11)
N(1)-C(1)-C(2)	122.5(12)
C(4)-C(1)-C(2)	122.4(11)
C(1)-C(2)-C(3)	110.8(11)
N(2)-C(4)-C(1)	111.8(11)
N(2)-C(4)-C(5)	121.1(11)
C(1)-C(4)-C(5)	126.9(11)
C(4)-C(5)-C(6)	110.7(10)
N(5)-C(13)-C(14)	123.6(12)
C(15)-C(14)-C(13)	118.8(13)
C(14)-C(15)-C(16)	119.4(12)
C(17)-C(16)-C(15)	116.1(12)
N(5)-C(17)-C(16)	126.7(12)
C(19)-C(18)-Co(1)	119.3(9)

Symmetry transformations used to generate equivalent atoms:

Table 4. Bond lengths [A] and angles [deg] for coxm.

Co(1)-N(4)	1.859(10)
Co(1)-N(3)	1.864(10)
Co(1)-N(1)	1.866(10)
Co(1)-N(2)	1.886(10)
Co(1)-C(18)	2.032(11)
Co(1)-N(5)	2.076(9)
N(1)-C(1)	1.287(15)
N(1)-O(1)	1.349(12)
N(2)-C(4)	1.325(16)
N(2)-O(2)	1.325(12)
N(3)-O(3)	1.329(12)
N(3)-C(7)	1.338(16)
N(4)-C(10)	1.265(15)
N(4)-O(4)	1.357(12)
N(5)-C(17)	1.315(15)
N(5)-C(13)	1.344(16)
C(1)-C(4)	1.431(17)
C(1)-C(2)	1.509(18)
C(2)-C(3)	1.547(18)
C(4)-C(5)	1.486(17)
C(5)-C(6)	1.542(15)
C(7)-C(10)	1.447(17)
C(7)-C(8)	1.469(16)
C(8)-C(9)	1.538(17)
C(10)-C(11)	1.516(18)
C(11)-C(12)	1.519(18)
C(13)-C(14)	1.376(18)
C(14)-C(15)	1.362(19)
C(15)-C(16)	1.397(19)
C(16)-C(17)	1.368(17)
C(18)-C(19)	1.451(19)
N(4)-Co(1)-N(3)	82.6(4)
N(4)-Co(1)-N(1)	179.1(4)
N(3)-Co(1)-N(1)	97.7(4)
N(4)-Co(1)-N(2)	97.4(4)
N(3)-Co(1)-N(2)	178.8(4)
N(1)-Co(1)-N(2)	82.3(4)
N(4)-Co(1)-C(18)	86.7(4)
N(3)-Co(1)-C(18)	88.7(4)
N(1)-Co(1)-C(18)	92.5(5)
N(2)-Co(1)-C(18)	90.1(4)
N(4)-Co(1)-N(5)	90.9(4)
N(3)-Co(1)-N(5)	91.1(4)
N(1)-Co(1)-N(5)	90.0(4)
N(2)-Co(1)-N(5)	90.0(4)
C(18)-Co(1)-N(5)	177.5(5)
C(1)-N(1)-O(1)	121.4(10)
C(1)-N(1)-Co(1)	115.7(8)
O(1)-N(1)-Co(1)	123.0(7)
C(4)-N(2)-O(2)	121.8(10)
C(4)-N(2)-Co(1)	115.2(8)
O(2)-N(2)-Co(1)	123.0(8)
O(3)-N(3)-C(7)	119.8(10)
O(3)-N(3)-Co(1)	124.2(8)
C(7)-N(3)-Co(1)	115.9(8)
C(10)-N(4)-O(4)	120.5(10)
C(10)-N(4)-Co(1)	115.6(8)
O(4)-N(4)-Co(1)	123.9(7)
C(17)-N(5)-C(13)	115.3(10)

C(17)-N(5)-Co(1)	122.2(8)
C(13)-N(5)-Co(1)	122.4(8)
N(1)-C(1)-C(4)	115.0(11)
N(1)-C(1)-C(2)	122.5(12)
C(4)-C(1)-C(2)	122.4(11)
C(1)-C(2)-C(3)	110.8(11)
N(2)-C(4)-C(1)	111.8(11)
N(2)-C(4)-C(5)	121.1(11)
C(1)-C(4)-C(5)	126.9(11)
C(4)-C(5)-C(6)	110.7(10)
N(3)-C(7)-C(10)	109.8(10)
N(3)-C(7)-C(8)	122.9(11)
C(10)-C(7)-C(8)	127.1(11)
C(7)-C(8)-C(9)	112.2(11)
N(4)-C(10)-C(7)	116.0(10)
N(4)-C(10)-C(11)	122.8(11)
C(7)-C(10)-C(11)	120.9(11)
C(10)-C(11)-C(12)	110.5(10)
N(5)-C(13)-C(14)	123.6(12)
C(15)-C(14)-C(13)	118.8(13)
C(14)-C(15)-C(16)	119.4(12)
C(17)-C(16)-C(15)	116.1(12)
N(5)-C(17)-C(16)	126.7(12)
C(19)-C(18)-Co(1)	119.3(9)

Symmetry transformations used to generate equivalent atoms:

Table 5. Anisotropic displacement parameters (A^2 x 10^3) for coxm. The anisotropic displacement factor exponent takes the form: -2 pi^2 [h^2 a*^2 U11 + ... + 2 h k a* b* U12]

	U11	U22	U33	U23	U13	U12
Co(1)	35(1)	26(1)	37(1)	2(1)	-1(1)	-4(1)
N(1)	40(5)	27(5)	27(6)	-3(4)	0(4)	-8(4)
N(2)	37(5)	20(5)	43(6)	3(4)	0(5)	2(4)
N(3)	31(5)	28(5)	43(6)	-1(5)	-5(5)	-5(4)
N(4)	41(5)	24(5)	33(6)	-9(4)	5(4)	2(4)
N(5)	35(5)	32(5)	30(6)	0(4)	-4(4)	5(4)
O(1)	40(5)	42(5)	42(5)	-5(4)	-1(4)	-4(4)
O(2)	34(4)	23(4)	56(6)	6(4)	10(4)	-8(3)
O(3)	39(5)	35(5)	56(6)	3(4)	0(4)	-12(4)
O(4)	41(5)	33(5)	55(6)	-8(4)	-5(4)	-13(4)
C(1)	57(8)	24(6)	36(8)	-13(5)	-13(6)	13(5)
C(2)	49(7)	33(7)	38(7)	-1(6)	-5(6)	4(5)
C(3)	55(9)	50(9)	71(11)	1(8)	-16(8)	12(7)
C(4)	52(7)	16(5)	41(8)	3(5)	-14(6)	0(5)
C(5)	54(8)	29(6)	32(7)	-1(5)	4(6)	1(5)
C(6)	43(7)	43(8)	50(8)	-13(7)	8(6)	10(6)
C(7)	50(7)	22(6)	36(7)	0(5)	-1(6)	7(5)
C(8)	44(7)	25(6)	35(7)	-6(5)	-5(6)	-3(5)
C(9)	84(11)	48(9)	79(12)	-17(8)	4(9)	7(8)
C(10)	47(7)	22(6)	32(7)	-16(5)	-15(6)	6(5)
C(11)	47(7)	28(6)	58(9)	-12(6)	3(6)	-5(5)
C(12)	49(8)	51(9)	84(12)	-5(8)	-16(8)	13(7)
C(13)	53(8)	30(7)	56(9)	4(6)	-9(7)	-7(6)
C(14)	59(8)	40(8)	45(8)	-1(6)	-10(7)	4(6)
C(15)	78(10)	32(7)	46(8)	-8(6)	-21(8)	22(7)
C(16)	63(9)	22(6)	54(9)	1(6)	3(7)	-8(6)
C(17)	44(7)	42(7)	44(8)	-3(6)	-14(6)	-6(6)
C(18)	41(7)	17(5)	42(7)	2(5)	3(6)	-3(5)
C(19)	73(11)	43(9)	113(15)	-25(9)	-31(10)	22(8)

Table 6. Hydrogen coordinates (x 10^4) and isotropic displacement parameters (A^2 x 10^3) for coxm.

	x	y	z	U(eq)
H(2A)	6126	5946	5459	49
H(2B)	7736	6434	4654	49
H(3A)	5273	7853	4431	89
H(3B)	6671	8915	4620	89
H(3C)	5054	8415	5415	89
H(5A)	11305	9040	4678	49
H(5B)	9799	8462	4265	49
H(6A)	12364	7097	3773	72
H(6B)	10954	6022	4408	72
H(6C)	12467	6610	4809	72
H(8A)	7591	6479	10688	42
H(8B)	6024	5976	10295	42
H(9A)	5079	7856	11251	109
H(9B)	4941	8436	10232	109
H(9C)	6503	8934	10631	109
H(11A)	9686	8310	10346	55
H(11B)	11172	9033	9544	55
H(12A)	12315	7035	10353	92
H(12B)	12429	6677	9330	92
H(12C)	10952	5964	10139	92
H(13A)	12331	6289	7123	57
H(14A)	13827	4087	7082	58
H(15A)	12320	1906	7451	62
H(16A)	9270	2007	7886	59
H(17A)	7964	4276	7816	51
H(18A)	7253	9720	8174	43
H(18B)	8238	10206	7155	43
H(19A)	5383	10668	7332	111
H(19B)	4976	8972	7646	111
H(19C)	5966	9478	6624	111

Table 8. Crystal data and structure refinement for cobrd.

$CoMe_2Et_2BF/H_2OEt$ crystal data

Identification code	cobrd
Empirical formula	C12 H23 B2 Co F4 N4 O5
Formula weight	459.89
Temperature	183(2) K
Wavelength	0.71073 A
Crystal system, space group	Monoclinic, P2(1)/c
Unit cell dimensions	a = 12.1953(4) A alpha = 90 deg. b = 13.0986(4) A beta = 113.5920(10 c = 12.7761(2) A gamma = 90 deg.
Volume	1870.29(9) A^3
Z, Calculated density	4, 1.633 Mg/m^3
Absorption coefficient	0.989 mm^-1
F(000)	944
Crystal size	0.16 x 0.09 x 0.08 mm
Theta range for data collection	1.82 to 24.00 deg.
Limiting indices	-8<=h<=13, -14<=k<=14, -14<=l<=10
Reflections collected / unique	8470 / 2928 [R(int) = 0.0702]
Completeness to theta = 24.00	99.9 %
Absorption correction	Semi-empirical from equivalents
Max. and min. transmission	0.928 and 0.746
Refinement method	Full-matrix least-squares on F^2
Data / restraints / parameters	2928 / 0 / 263
Goodness-of-fit on F^2	1.033
Final R indices [I>2sigma(I)]	R1 = 0.0544, wR2 = 0.1067
R indices (all data)	R1 = 0.1116, wR2 = 0.1313
Largest diff. peak and hole	0.706 and -0.624 e.A^-3

Table 9. Atomic coordinates (x 10^4) and equivalent isotropic displacement parameters (A^2 x 10^3) for cobrd.
U(eq) is defined as one third of the trace of the orthogonalized Uij tensor.

	x	y	z	U(eq)
Co(1)	2322(1)	401(1)	7521(1)	26(1)
N(1)	3240(4)	623(3)	6666(4)	26(1)
N(2)	3032(4)	1637(3)	8183(4)	25(1)
N(3)	1629(4)	-840(3)	6878(4)	25(1)
N(4)	1464(4)	175(3)	8414(4)	21(1)
O(1)	3328(3)	-74(3)	5896(3)	33(1)
O(2)	2710(3)	2185(3)	8929(3)	31(1)
O(3)	1921(3)	-1377(3)	6099(3)	36(1)
O(4)	1363(3)	849(3)	9183(3)	27(1)
O(5)	891(4)	1285(3)	6365(4)	33(1)
F(1)	2534(3)	-1370(3)	4635(3)	50(1)
F(2)	1266(3)	-100(3)	4698(3)	42(1)
F(3)	2007(3)	2238(2)	10333(3)	37(1)
F(4)	3379(3)	1010(2)	10442(3)	39(1)
B(1)	2254(6)	-711(6)	5328(6)	36(2)
B(2)	2391(6)	1555(5)	9738(6)	29(2)
C(1)	3941(5)	1406(4)	6934(5)	28(1)
C(2)	4853(5)	1628(5)	6456(5)	35(2)
C(3)	3758(5)	2052(4)	7802(5)	25(1)
C(4)	4339(5)	3075(4)	8152(5)	38(2)
C(5)	975(5)	-1274(4)	7320(5)	28(1)
C(6)	458(6)	-2348(5)	7001(6)	51(2)
C(7)	812(5)	-654(4)	8193(5)	32(2)
C(8)	-55(5)	-912(5)	8715(5)	36(2)
C(10)	3770(5)	-455(5)	8582(5)	38(2)
C(11)	3587(5)	-1190(5)	9410(5)	41(2)
C(81)	-1258(6)	-460(7)	8014(7)	77(3)
C(21)	6097(6)	1270(7)	7262(7)	75(3)

Table 10. Selected bond lengths [A] and angles [deg] for cobrd.

Co(1)-N(2)	1.870(4)
Co(1)-N(1)	1.873(4)
Co(1)-C(10)	2.072(5)
Co(1)-O(5)	2.123(4)
N(1)-C(1)	1.291(7)
N(1)-O(1)	1.377(5)
N(2)-C(3)	1.289(7)
N(2)-O(2)	1.371(5)
O(1)-B(1)	1.476(8)
O(2)-B(2)	1.490(8)
F(1)-B(1)	1.375(7)
F(2)-B(1)	1.401(8)
C(1)-C(3)	1.481(8)
C(1)-C(2)	1.496(8)
C(2)-C(21)	1.527(8)
C(3)-C(4)	1.498(8)
N(4)-Co(1)-N(1)	177.9(2)
N(3)-Co(1)-N(1)	98.6(2)
N(2)-Co(1)-N(1)	81.5(2)
N(4)-Co(1)-C(10)	93.1(2)
N(3)-Co(1)-C(10)	86.2(2)
N(4)-Co(1)-O(5)	90.34(17)
N(3)-Co(1)-O(5)	93.85(18)
C(10)-Co(1)-O(5)	176.5(2)
C(1)-N(1)-O(1)	118.9(5)
C(1)-N(1)-Co(1)	117.1(4)
O(1)-N(1)-Co(1)	123.3(3)
C(7)-N(4)-O(4)	118.1(4)
C(7)-N(4)-Co(1)	116.3(4)
O(4)-N(4)-Co(1)	125.2(3)
N(1)-O(1)-B(1)	114.7(4)
N(4)-O(4)-B(2)	116.3(4)
F(1)-B(1)-F(2)	111.6(5)
F(1)-B(1)-O(1)	105.7(5)
F(2)-B(1)-O(1)	110.4(5)
O(1)-B(1)-O(3)	115.4(5)
N(1)-C(1)-C(3)	111.8(5)
N(1)-C(1)-C(2)	124.6(6)
C(3)-C(1)-C(2)	123.6(5)
C(1)-C(2)-C(21)	111.5(5)
N(2)-C(3)-C(1)	111.9(5)
N(2)-C(3)-C(4)	125.4(5)
C(1)-C(3)-C(4)	122.7(5)
C(11)-C(10)-Co(1)	118.4(4)

Symmetry transformations used to generate equivalent atoms:

Table 11. Bond lengths [A] and angles [deg] for cobrd.

Co(1)-N(4)	1.855(4)
Co(1)-N(3)	1.865(4)
Co(1)-N(2)	1.870(4)
Co(1)-N(1)	1.873(4)
Co(1)-C(10)	2.072(5)
Co(1)-O(5)	2.123(4)
N(1)-C(1)	1.291(7)
N(1)-O(1)	1.377(5)
N(2)-C(3)	1.289(7)
N(2)-O(2)	1.371(5)
N(3)-C(5)	1.280(7)
N(3)-O(3)	1.376(5)
N(4)-C(7)	1.309(6)
N(4)-O(4)	1.362(5)
O(1)-B(1)	1.476(8)
O(2)-B(2)	1.490(8)
O(3)-B(1)	1.489(8)
O(4)-B(2)	1.490(7)
F(1)-B(1)	1.375(7)
F(2)-B(1)	1.401(8)
F(3)-B(2)	1.372(7)
F(4)-B(2)	1.380(7)
C(1)-C(3)	1.481(8)
C(1)-C(2)	1.496(8)
C(2)-C(21)	1.527(8)
C(3)-C(4)	1.498(8)
C(5)-C(7)	1.456(8)
C(5)-C(6)	1.529(8)
C(7)-C(8)	1.496(8)
C(8)-C(81)	1.501(9)
C(10)-C(11)	1.513(8)
N(4)-Co(1)-N(3)	82.20(19)
N(4)-Co(1)-N(2)	97.7(2)
N(3)-Co(1)-N(2)	179.3(2)
N(4)-Co(1)-N(1)	177.9(2)
N(3)-Co(1)-N(1)	98.6(2)
N(2)-Co(1)-N(1)	81.5(2)
N(4)-Co(1)-C(10)	93.1(2)
N(3)-Co(1)-C(10)	86.2(2)
N(2)-Co(1)-C(10)	93.1(2)
N(1)-Co(1)-C(10)	85.0(2)
N(4)-Co(1)-O(5)	90.34(17)
N(3)-Co(1)-O(5)	93.85(18)
N(2)-Co(1)-O(5)	86.88(18)
N(1)-Co(1)-O(5)	91.52(17)
C(10)-Co(1)-O(5)	176.5(2)
C(1)-N(1)-O(1)	118.9(5)
C(1)-N(1)-Co(1)	117.1(4)
O(1)-N(1)-Co(1)	123.3(3)
C(3)-N(2)-O(2)	118.2(4)
C(3)-N(2)-Co(1)	117.3(4)
O(2)-N(2)-Co(1)	123.9(3)
C(5)-N(3)-O(3)	118.7(4)
C(5)-N(3)-Co(1)	116.4(4)
O(3)-N(3)-Co(1)	124.2(3)
C(7)-N(4)-O(4)	118.1(4)
C(7)-N(4)-Co(1)	116.3(4)
O(4)-N(4)-Co(1)	125.2(3)
N(1)-O(1)-B(1)	114.7(4)

N(2)-O(2)-B(2)	114.8(4)
N(3)-O(3)-B(1)	113.4(4)
N(4)-O(4)-B(2)	116.3(4)
F(1)-B(1)-F(2)	111.6(5)
F(1)-B(1)-O(1)	105.7(5)
F(2)-B(1)-O(1)	110.4(5)
F(1)-B(1)-O(3)	105.2(5)
F(2)-B(1)-O(3)	108.4(5)
O(1)-B(1)-O(3)	115.4(5)
F(3)-B(2)-F(4)	112.3(5)
F(3)-B(2)-O(4)	105.1(5)
F(4)-B(2)-O(4)	109.7(5)
F(3)-B(2)-O(2)	105.4(5)
F(4)-B(2)-O(2)	109.7(5)
O(4)-B(2)-O(2)	114.7(5)
N(1)-C(1)-C(3)	111.8(5)
N(1)-C(1)-C(2)	124.6(6)
C(3)-C(1)-C(2)	123.6(5)
C(1)-C(2)-C(21)	111.5(5)
N(2)-C(3)-C(1)	111.9(5)
N(2)-C(3)-C(4)	125.4(5)
C(1)-C(3)-C(4)	122.7(5)
N(3)-C(5)-C(7)	113.0(5)
N(3)-C(5)-C(6)	123.6(5)
C(7)-C(5)-C(6)	123.3(5)
N(4)-C(7)-C(5)	111.8(5)
N(4)-C(7)-C(8)	124.6(5)
C(5)-C(7)-C(8)	123.6(5)
C(7)-C(8)-C(81)	110.0(5)
C(11)-C(10)-Co(1)	118.4(4)

Symmetry transformations used to generate equivalent atoms:

Table 12. Anisotropic displacement parameters (A^2 x 10^3) for cobrd. The anisotropic displacement factor exponent takes the form: -2 pi^2 [h^2 a*^2 U11 + ... + 2 h k a* b* U12]

	U11	U22	U33	U23	U13	U12
Co(1)	31(1)	27(1)	22(1)	-4(1)	13(1)	-9(1)
N(1)	24(3)	33(3)	19(3)	2(2)	8(2)	2(2)
N(2)	28(3)	25(3)	22(3)	1(2)	9(2)	-1(2)
N(3)	25(3)	27(3)	23(3)	-3(2)	9(2)	0(2)
N(4)	20(3)	26(3)	18(3)	-1(2)	8(2)	-2(2)
O(1)	36(2)	40(2)	29(2)	-6(2)	20(2)	1(2)
O(2)	37(2)	30(2)	29(2)	-8(2)	16(2)	-10(2)
O(3)	53(3)	29(2)	37(3)	-9(2)	29(2)	-9(2)
O(4)	32(2)	27(2)	26(2)	-9(2)	16(2)	-1(2)
O(5)	28(3)	39(3)	29(3)	-4(2)	11(2)	-2(2)
F(1)	66(3)	53(2)	44(2)	-19(2)	36(2)	-8(2)
F(2)	36(2)	54(2)	30(2)	-4(2)	8(2)	-1(2)
F(3)	43(2)	39(2)	31(2)	-13(2)	17(2)	-4(2)
F(4)	35(2)	46(2)	25(2)	-2(2)	2(2)	3(2)
B(1)	35(5)	44(5)	32(4)	-6(4)	16(4)	-2(4)
B(2)	27(4)	36(4)	25(4)	-5(3)	10(3)	-6(3)
C(1)	22(3)	32(4)	22(3)	9(3)	2(3)	0(3)
C(2)	33(4)	42(4)	36(4)	12(3)	21(3)	-1(3)
C(3)	17(3)	31(3)	20(3)	8(3)	-1(2)	0(3)
C(4)	43(4)	36(4)	34(4)	2(3)	16(3)	-14(3)
C(5)	30(3)	27(3)	30(4)	-5(3)	17(3)	-7(3)
C(6)	60(5)	47(4)	60(5)	-25(4)	39(4)	-31(4)
C(7)	34(4)	32(4)	36(4)	-8(3)	20(3)	-9(3)
C(8)	40(4)	38(4)	34(4)	-7(3)	20(3)	-11(3)
C(10)	34(4)	39(4)	36(4)	4(3)	11(3)	12(3)
C(11)	45(4)	41(4)	30(4)	10(3)	6(3)	9(3)
C(81)	58(5)	109(7)	63(6)	5(5)	23(4)	-5(5)
C(21)	48(5)	98(7)	88(7)	28(5)	36(5)	15(5)

Table 13. Hydrogen coordinates (x 10^4) and isotropic displacement parameters (A^2 x 10^3) for cobrd.

	x	y	z	U(eq)
H(051)	1100(50)	1510(50)	5900(50)	39
H(052)	260(50)	1020(40)	5910(50)	39
H(2A)	4872	2371	6327	42
H(2B)	4621	1280	5711	42
H(4A)	3898	3474	8505	57
H(4B)	4332	3437	7478	57
H(4C)	5167	2984	8703	57
H(6A)	477	-2546	6269	77
H(6B)	-370	-2356	6937	77
H(6C)	937	-2830	7594	77
H(8A)	242	-640	9503	43
H(8B)	-126	-1662	8752	43
H(10A)	4070	-851	8091	45
H(10B)	4413	26	9031	45
H(11A)	4340	-1545	9847	62
H(11B)	2972	-1691	8985	62
H(11C)	3330	-812	9934	62
H(81A)	-1839	-687	8319	116
H(81B)	-1519	-686	7220	116
H(81C)	-1203	286	8047	116
H(21A)	6674	1431	6928	113
H(21B)	6085	531	7376	113
H(21C)	6332	1619	7998	113

Appendix 3

Molecular Weight and Conversion data for Chapter 4

Table 1. Molecular weight and conversion data for the CCTP bulk polymerisation of complex II with Styrene.

Temp °C	[Co]/[Sty] x 10^{-6} Molar ratio	*Mn*	*Mw*	PDi	% Conv
90	0.0	583388	897802	1.54	1.30
	2.45	5660	17022	3.00	0.99
	4.90	7221	17805	2.46	0.99
	7.35	5373	11593	2.16	0.87
	9.80	4137	7869	1.90	0.78
120	0.0	74054	173248	2.34	6.61
	2.45	15955	37651	2.36	10.55
	4.90	5756	21178	3.68	10.19
	7.35	3986	13382	3.36	9.53
	9.80	4000	13305	3.33	10.55
140	0.0	103697	227004	2.19	4.40
	2.45	7493	22464	2.99	8.11
	4.90	4994	13138	2.63	7.62
	7.35	3597	7939	2.20	7.93
	9.80	3260	8712	2.67	7.74

Table 2. Molecular weight and conversion data for the CCTP bulk polymerisation of complex III with Styrene.

Temp °C	[Co]/[Sty]x 10^{-6} Molar ratio	*Mn*	*Mw*	PDi	% Conv
80	0.0	102767	232872	2.27	0.36
	2.30	73412	160861	2.20	1.63
	4.61	53939	118973	2.21	1.93
	6.91	39325	81875	2.08	1.85
	9.22	34077	73798	2.17	1.62
100	0.0	255283	496606	1.94	0.90
	2.30	66868	180196	2.70	2.63
	4.61	48861	131850	2.70	3.92
	6.91	43309	102426	2.37	4.16
	9.22	33766	79175	2.35	4.12
120	0.0	106331	239933	2.26	4.61
	2.30	81445	196427	2.41	6.79
	4.61	64792	169132	2.61	8.90
	6.91	51644	141983	2.75	9.65
	9.22	47020	134804	2.87	10.63
140	0.0	82044	183631	2.24	1.13
	2.30	62768	141413	2.25	3.46
	4.61	47700	110694	2.32	4.32
	6.91	31975	79456	2.49	4.59
	9.22	34617	87672	2.53	6.50

Table 3. Molecular weight and conversion data for the CCTP bulk polymerisation of complex IV with Styrene.

Temp °C	[Co]/[Sty]x 10^{-6} Molar ratio	*Mn*	*Mw*	PDi	% Conv
90	0.0	577948	914227	1.58	
	2.17	93949	194574	2.07	
	4.36	88605	228055	2.57	
	6.53	75576	170463	2.26	
	8.71	138588	208160	1.50	
100	0.0	156192	367925	2.36	1.52
	2.17	51569	123702	2.40	3.11
	4.36	42562	106110	2.50	3.50
	6.53	41098	120154	2.92	3.73
	8.71	28767	78627	2.73	4.39
120	0.0	70090	157223	2.24	7.73
	2.17	33782	78872	2.33	12.19
	4.36	28066	65074	2.32	12.62
	6.53	27177	65139	2.39	14.10
	8.71	22454	52167	2.32	14.17
140	0.0	104554	230897	2.20	4.99
	2.17	50022	121196	2.42	8.98
	4.36	38649	99918	2.59	9.11
	6.53	33062	90296	2.73	10.87
	8.71	30178	91799	3.04	12.24

Table 4. Molecular weight and conversion data for the CCTP bulk polymerisation of complex IV with Styrene.

Temp °C	[Co]/[Sty]x 10^{-6} Molar ratio	*Mn*	*Mw*	PDi	% Conv
80	0.0	132728	299396	2.26	0.39
	2.23	7672	27712	3.61	0.60
	4.46	7444	19994	2.69	0.57
	6.69	4150	11469	2.76	0.53
	8.92	3539	7243	2.05	0.41
100	0.0	129139	277721	2.15	2.34
	2.23	11183	28515	2.55	2.84
	4.46	11264	29308	2.60	3.09
	6.69	6551	20062	3.06	2.94
	8.92	4884	14382	2.94	2.62
120	0.0	84357	208553	2.47	6.47
	2.45	12493	26648	2.13	2.51
	4.90	10475	20653	1.97	3.09
	7.35	5661	20136	3.55	9.48
	9.80	4432	12254	2.78	4.37
140	0.0	102680	211969	2.06	5.10
	2.23	6304	19026	3.01	8.00
	4.46	5098	16062	3.15	11.85
	6.69	3594	9741	2.71	8.28
	8.92	3047	8121	2.66	10.36

Table 5. Molecular weight and conversion data for the CCTP bulk polymerisation of complex IX with Styrene.

Temp °C	[Co]/[Sty]x 10^{-6} Molar ratio	*Mn*	*Mw*	PDi	% Conv
80	0.0	88929	214142	2.40	0.24
	2.11	94507	224703	2.38	0.55
	4.22	78783	183717	2.33	0.72
	6.33	67469	156103	2.31	0.75
	8.45	69465	167517	2.41	0.79
100	0.0	108506	242652	2.24	0.89
	2.11	85146	195997	2.30	1.75
	4.22	84788	188005	2.22	1.71
	6.33	60829	136555	2.25	2.58
	8.45	59151	129320	2.19	2.84
120	0.0	75671	173526	2.29	3.11
	2.11	57065	126485	2.21	4.66
	4.22	42993	114267	2.66	4.97
	6.33	45051	98060	2.18	5.98
	8.45	34157	70864	2.08	4.61
140	0.0	80650	182751	2.27	1.69
	2.11	59577	126225	2.11	3.00
	4.22	51147	111350	2.17	3.45
	6.33	42776	91433	2.14	3.45
	8.45	40352	82176	2.04	3.76

Table 6. Molecular weight and conversion data for the CCTP bulk polymerisation of complex X with Styrene.

Temp °C	[Co]/[Sty]x 10^{-6} Molar ratio	*Mn*	*Mw*	PDi	% Conv
80	0.0	64678	234634	3.62	0.30
	2.00	29866	66665	2.23	0.63
	4.01	27468	59201	2.15	0.67
	6.01	17288	46124	2.65	0.58
	8.02	13922	32907	2.36	0.63
100	0.0	62066	237087	3.82	1.34
	2.00	28582	87873	3.07	2.06
	4.01	29602	61319	2.07	2.04
	6.01	21905	49667	2.27	2.49
120	0.0	90911	202359	2.22	3.18
	2.00	32931	68357	2.07	4.68
	4.01	25591	55041	2.15	5.54
	6.01	19555	41369	2.11	5.02
	8.02	11903	34012	2.85	5.92
140	0.0	68924	166439	2.41	4.20
	2.00	36949	75626	2.04	6.95
	4.01	25490	57237	2.24	7.14
	6.01	20284	41177	2.03	6.91
	8.02	14111	32580	2.30	6.51

Table 7. Molecular weight and conversion data for the CCTP bulk polymerisation of complex XI with Styrene.

Temp °C	[Co]/[Sty]x 10^{-6} Molar ratio	*Mn*	*Mw*	PDi	% Conv
80	0.0	140034	312701	2.23	0.37
	2.54	7609	24644	3.24	0.53
	5.09	4758	11678	2.45	0.58
	7.64	3780	8864	2.35	0.52
	10.1	2726	5777	2.12	0.53
100	0.0	86751	203706	2.35	1.99
	2.54	23804	65151	2.74	2.71
	5.09	5888	15508	2.63	2.85
	7.64	4843	11768	2.43	
	10.1	4357	15658	3.59	2.86
120	0.0	77698	178893	2.30	6.12
	2.54	7848	19160	2.44	9.02
	5.09	5759	14337	2.49	9.88
	7.64	3917	10307	2.63	9.66
	10.1	3327	7637	2.30	10.09
140	0.0	86976	203720	2.34	5.59
	2.54	23052	65062	2.82	7.96
	5.09	6401	15428	2.41	9.27
	7.64	5049	11162	2.21	11.10
	10.1	4995	16116	3.23	12.50

Table 8. Molecular weight and conversion data for the CCTP bulk polymerisation of complex XII with Styrene.

Temp °C	[Co]/[Sty]x 10^{-6} Molar ratio	*Mn*	*Mw*	PDi	% Conv
80	0.0	108035	249996	2.31	0.33
	2.39	38734	99033	2.56	0.69
	4.79	20127	42761	2.13	0.41
	7.19	10686	26929	2.52	0.29
	9.57	8998	23548	2.61	0.30
100	0.0	114047	260089	2.28	1.25
	2.39	23101	53916	2.33	1.79
	4.79	14250	37469	2.63	1.63
	7.18	13033	41310	3.17	1.83
	9.57	6167	34268	5.55	1.89
120	0.0	88018	207796	2.36	2.59
	2.39	15411	30590	1.99	3.55
	4.79	8293	23441	2.83	3.65
	7.19	9308	18263	1.96	3.84
	9.57	6684	15512	2.32	3.67
140	0.0	71017	163305	2.29	4.69
	2.39	11162	22410	1.99	7.49
	4.79	8514	21898	2.57	6.38
	7.18	6238	18476	2.96	5.27
	9.57	5776	14507	2.51	4.62

Table 8. Molecular weight and conversion data for the CCTP bulk polymerisation of complex XIII with Styrene.

Temp °C	[Co]/[Sty]x 10^{-6} Molar ratio	*Mn*	*Mw*	PDi	% Conv
80	0.0	100387	266120	2.65	0.29
	2.26	24348	67527	2.77	0.68
	4.51	17918	48192	2.69	0.69
	6.80	10557	29720	2.82	0.62
	9.02	8023	22669	2.83	0.69
100	0.0	105074	243247	2.31	0.89
	2.25	25613	53997	2.10	3.04
	4.51	24159	59473	2.46	2.96
	6.76	17072	48620	2.84	3.37
	9.02	8211	37297	4.51	2.84
120	0.0	94791	214064	2.25	2.86
	2.25	23805	60102	2.52	7.64
	4.51	18271	48677	2.66	7.635
	6.76	11108	27892	2.51	5.38
	9.02	17426	52483	3.01	12.07
140	0.0	74082	167087	2.25	4.10
	2.25	25755	61353	2.38	7.04
	4.51	.26270	68157	2.59	10.52
	6.77	11851	47801	4.03	11.16
	9.02	9181	33861	3.68	9.97

Appendix 4

Calculation of E_{tr} and A_{tr}

Table 1. Slope and intercept values for complexes II-IV and VIII-XIII, DRI detector

Complex	Mayo Slope	Mayo Intercept	2/DPw Slope	2/DPw Intercept	CLD Slope	CLD Intercept
II	-1256	11.11	6.0	7.64	-9848	30.98
III	595	3.77	1598	0.86	3067	-3.34
IV	-3274	13.89	-1798	9.73	-41	4.6
VIII	212	7.57	329	6.72	4719	-5.97
IX	-2920	12.33	-3407	13.58	-5105	20.15
X	-412	7.58	-117	6.69	-473	7.37
XI	920	5.49	1405	3.96	4455	-4.91
XII	-739	9.19	-1196	9.93	-1565	10.52
XIII	837	4.72	-323	6.93	1419	2.14

Example Calculation for E_{tr} and A_{tr}

$\ln Cs = \ln(A_{tr}/A_p) + ((E_p-E_{tr})/RT)$

Plot Ln Cs vs 1/T (K)

Slope = E_p-E_{tr}/R

and

Intercept = $\ln(A_{tr}/A_p)$

E_{tr}

Know Slope, R and E_p, therefore

Slope x $R-E_p=-E_{tr}$

If LHS is negative then the resulting value is positive

$\underline{A_p}$

Intercept = $Ln(A_{tr}/A_p)$

Inverse of Ln intercept value

Know A_p therefore substitute in value.

Intercept x $A_p = A_{tr}$

Appendix 5

Data for Chapter 5

Table 1. Concentration and Absorbance values for complex III, for both MMA and water stock solutions.

Solution	**Concentration (M) x 10^{-4}**	**Absorbance at λ max**	**λ max**	**ε ($L\ mm^{-1}mol^{-1}$)**
MMA				
S1	3.24	0.86	450.4	265
S2	1.63	1.146	449.6	703
S3	0.63	0.206	454.4	327
Water				
S1	3.46	0.559	458.4	162
S2	1.46	0.365	458.7	250
S3	1.07	0.271	459	253
S4	0.81	0.19	460	234

Table 2. Concentration and Absorbance values for complex IV, for both MMA and water stock solutions.

Solution	**Concentration (M) x 10^{-4}**	**Absorbance at λ max**	**λ max**	**ε (L $mm^{-1}mol^{-1}$)**
MMA				
S1A	6.34	1.93	457.2	304
S1B	4.78	1.51	457.1	315
S1	3.24	1.19	457.3	367
S2	1.26	0.45	458.4	357
S3	0.61	0.24	457.6	393
Water				
S1A	3.41	0.74	463.2	217
S1C	2.55	0.52	463.2	203
S1D	1.91	0.40	463.2	209
S1	1.73	0.74	463.7	427
S1B	1.70	0.39	463.2	229
S2	0.76	0.32	463.2	421
S3	0.54	0.25	463.2	463
S4	0.39	0.19	461.9	487

Table 3. Wavelength and Absorbance values for complexes II-IV, for both MMA at all partition compositions

	Concentration (M) x 10^{-4}		**Absorbance at λ max**		**λ max**		**ε (L $mm^{-1}mol^{-1}$)**	
Complex II Mon/Water	**Mon**	**Water**	**Mon**	**Water**	**Mon**	**Water**	**Mon**	**Water**
50/50	4.1	5.0	1.467	1.814	456.8	455.7	356	362
90/10	3.5	4.4	1.251	0.228	455.2	456	357	51
10/90	4.3	4.2	0.19	1.406	452	455.5	44	333
Complex III Mon/Water								
50/50	3.9	0.5	1.14	0.144	460.6	459.2	292	288
90/10	0.2		0.090		450		450	
10/90	4.74	1.5	0.095	0.30	450	450	2.02	
Complex IV Mon/Water								
50/50	13	0.13	2.074	0.12	465.7	434.9	159	923
90/10	6.7	0.83	2.11	0.041	465.5	455.1	31.5	49
10/90	48.3	3.172	2.511	0.668	459.2	463.2	51	222

Table 4. Concentration and Absorbance values for complex VIII, for both MMA and water stock solutions.

Solution	Concentration (M) x 10^{-4}	Absorbance at λ max	λ max	ε ($L\ mm^{-1}mol^{-1}$)
MMA				
S1	8.11	1.279	450.9	157
S2	4.09	0.658	448.5	160
S3	2.33	0.344	448.8	147
Water				
S1	10.3	0.517	448	51
S2	4.94	0.25	448.8	51
S3	3.09	0.17	448.8	55
S4	2.47	0.15	448.8	60

Table 5. Concentration and Absorbance values for complex IX, for both MMA and water stock solutions.

Solution	Concentration (M) x 10^{-4}	Absorbance at λ max	λ max	ε ($L\ mm^{-1}mol^{-1}$)
MMA				
S1	28.5	1.358	450	48
S2	14.1	1.0	450	71
S3	1.38	0.50	450	362
Water				
S1	39.1	0.50	450	13
S2	27.7	0.48	450	17
S3	13.8	0.20	450	15

Table 6. Concentration and Absorbance values for complex X, for both MMA and water stock solutions.

Solution	**Concentration (M) x 10^{-4}**	**Absorbance at λ max**	**λ max**	**ε ($L\ mm^{-1}mol^{-1}$)**
MMA				
S1	16.0	2.01	452.6	125
S2	8.75	1.17	452	133
S3	8.02	0.93	452	116
S4	4.37	0.51	451.2	117
Water				
S1	15.4	0.50	455.2	32
S2	7.51	0.23	452.2	31

Table 7. Wavelength and Absorbance values for complexes VIII-X, for both MMA at all partition compositions

	Concentration (M) x 10^{-4}		Absorbance at λ max		λ max		ε ($L\ mm^{-1}mol^{-1}$)	
Complex VIII Mon/Water	**Mon**	**Water**	**Mon**	**Water**	**Mon**	**Water**	**Mon**	**Water**
50/50	15.58	1.178	2.461	0.07	449.1	448.8	164	41
90/10	10	2.8	1.582	0.035	448.8	450	158	17
10/90	29.6	2.6	0.779	0.14	448.8	448.8	26	54
Complex IX Mon/Water								
50/50	22	0.36	1.10	0.015	450	450	50	42
90/10	20	14	1.358	0.042	450	450	68	3.0
10/90	6.16	2.0	0.089	0.04	450	450	15	20
Complex XI Mon/Water								
50/50	15.59	0.909	1.739	0.057	453.3	454	112	63
90/10	9.38	13.8	1.171	0.07	449.9	450.2	125	5.38
10/90	51	1.0	1.077	0.03	452.3	450.2	21	30

Table 8. Concentration and Absorbance values for complex XI, for both MMA and water stock solutions.

Solution	Concentration (M) x 10^{-4}	Absorbance at λ max	λ max	ε ($L\ mm^{-1}mol^{-1}$)
MMA				
S1	8.33	1.67	451.8	200
S2	4.28	0.98	450.2	228
S3	2.37	0.40	448.8	168
Water				
S1	10.0	1.05	449.9	105
S2	5.09	0.49	447.2	96
S3	3.04	0.22	450.0	72
S4	2.02	0.09	449.9	45

Table 9. Concentration and Absorbance values for complex XII, for both MMA and water stock solutions.

Solution	Concentration (M) x 10^{-4}	Absorbance at λ max	λ max	ε ($L\ mm^{-1}mol^{-1}$)
MMA				
S1	15.7	2.48	429.6	157
S2	10.4	1.75	429.6	168
S3	5.22	1.0	429.6	191
Water				
S1	17.5	1.37	450.2	78
S2	11.7	0.85	450.2	73
S3	8.62	0.75	452.9	87
S4	5.83	0.58	452.9	99

Table 10. Concentration and Absorbance values for complex XIII, for both MMA and water stock solutions.

Solution	**Concentration (M) x 10^{-4}**	**Absorbance at λ max**	**λ max**	**ε ($L\ mm^{-1}mol^{-1}$)**
MMA				
S1	12.1	2.62	454.1	216
S2	8.12	1.81	453.6	222
S3	6.09	1.13	452.0	186
S4	3.04	0.52	449.6	171
Water				
S1	17.7	0.75	452.0	42
S2	11.7	0.47	452.2	40
S3	8.28	0.37	452.2	45

Table 11. Wavelength and Absorbance values for complexes VIII-X, for both MMA at all partition compositions

	Concentration (M) x 10^{-4}		Absorbance at λ max		λ max		ε ($L\ mm^{-1}mol^{-1}$)	
Complex XI Mon/Water	**Mon**	**Water**	**Mon**	**Water**	**Mon**	**Water**	**Mon**	**Water**
50/50	5.04	3.7	0.511	0.335	448.2	448.2	102	90
90/10	9.6	5.3	1.96	0.025	444.2	444.2	204	4.71
10/90	67.2	6.16	2.28	0.605	451.2	453.7	34	11
Complex XII Mon/Water								
50/50	15	1.3	1.286	0.15	436	436	85	115
90/10	14.9	55.7	2.43	0.75	439.2	432.8	163	13
10/90	55	1.3	1.537	0.15	435.2	435.2	28	115
Complex XIII Mon/Water								
50/50	15	0.9	1.643	0.04	453.2	453.2	109	44
90/10	11	4	2.46	0.03	453.3	453.2	223	7.5
10/90	75	2.1	2.69	0.09	454.7	460	35	45

4

DX

230453